Chapter 46
Thermal Recovery

Chieh Chu, Getty Oil Co.*

Introduction

Thermal recovery generally refers to processes for recovering oil from underground formations by use of heat. The heat may be supplied externally by injecting a hot fluid such as steam or hot water into the formations, or it may be generated internally by combustion. In combustion, the fuel is supplied by the oil in place and the oxidant is injected into the formations in the form of air or other oxygen-containing fluids. The most commonly used thermal recovery processes are steam injection processes and in-situ combustion.

Two Forms of Steam Injection Processes

In principle, any hot fluid can be injected into the formations to supply the heat. The fluids used most extensively are steam or hot water because of the general availability and abundance of water. Hot water injection has been found to be less efficient than steam injection and will not be discussed here. A schematic view of the steam injection process is shown in Fig. 46.1, together with an approximate temperature distribution inside the formation.[1]

There are two variations of steam injection processes—steam stimulation and steam displacement.

Steam Stimulation

This method has been known as the huff 'n' puff method, since steam is injected intermittently and the reservoir is allowed to produce after each injection. In this process the main driving force for oil displacement is provided by reservoir pressure, gravitational force, rock and fluid expansion, and, possibly, formation compaction. In the steam stimulation process only the part of the reservoir adjacent to the wellbore is affected. After a number of cycles of injection and production, the near-wellbore region in reservoirs having little or no dip becomes so depleted of oil that further injection of steam is futile. In this case, wells must be drilled at very close spacing to obtain a high oil recovery.

*Now with Texaco Inc.

Steam Displacement

This process, usually referred to as steamflood or steamdrive, has a much higher oil recovery than steam stimulation alone. Whereas steam stimulation is a one-well operation, steamflood requires at least two wells, one serving as the injector and the other serving as the producer. The majority of steamflood projects use pattern floods. In many cases, steam stimulation is required at the producers when the oil is too viscous to flow before the heat from the injector arrives. Because of the high oil recovery achievable through steamflooding, many reservoirs that were produced by steam stimulation previously now are being steamflooded.

Three Forms of In-Situ Combustion

In-situ combustion usually is referred to as fireflood. There are three forms of in-situ combustion processes—dry forward combustion, reverse combustion, and wet combustion.

Dry Forward Combustion

In the earlier days, this was the most commonly used form of the combustion processes. It is dry because no water is injected along with air. It is forward because combustion starts at the injector and the combustion front moves in the direction of the air flow.

Fig. 46.2 gives a schematic view of the dry forward combustion process.[2] The upper part of the figure shows a typical temperature distribution along a cross section leading from the injector at the left to the producer at the right. Two things need to be pointed out. First, the region near the producer is cold, at the original temperature of the reservoir. If the unheated oil is highly viscous, it cannot be pushed forward by the heated oil at its back that has been made mobile by the high temperature of the combustion zone. This phenomenon is called "liquid blocking." Second, the temperature of the region in the back of the combustion zone is high, indicating a great amount of heat being stored in the region, not used efficiently.

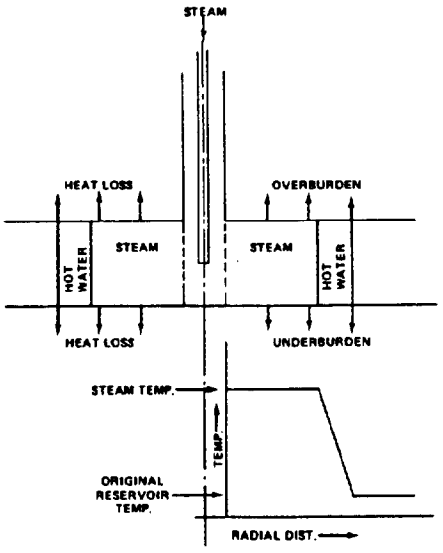

Fig. 46.1—Steam injection processes.

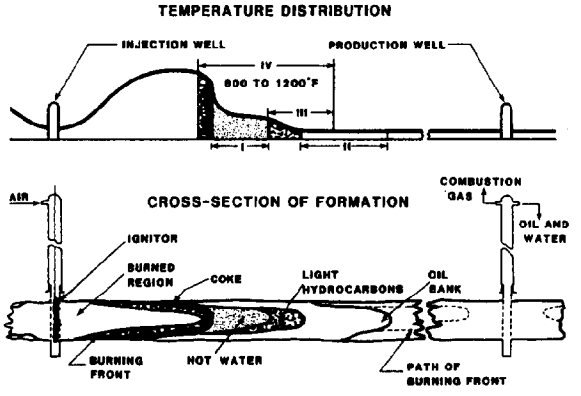

Fig. 46.2—Dry forward combustion.

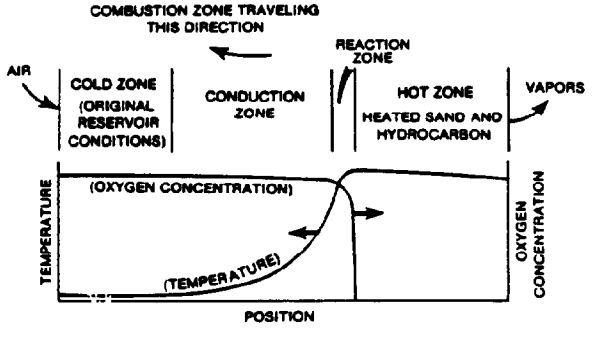

Fig. 46.3—Reverse combustion.

The lower part of Fig. 46.2 shows the fluid saturation distributions inside the formation under the combustion process. One should note the clean sand in the burned-out region. Being able to burn the undesirable fraction of the oil (the heavier portion) is one advantage of the forward combustion process over the reverse combustion process.

Reverse Combustion

Strictly speaking, it should be called dry reverse combustion, because normally only air is injected, no water. A simple example will help to explain how reverse combustion works. In ordinary cigarette smoking, one ignites the tip of the cigarette and inhales. The burning front will travel from the tip of the cigarette toward one's mouth, along with the air. This is forward combustion. The cigarette also can be burned if one exhales. This way, the burning front still moves from the tip of the cigarette toward one's mouth, but the air flow is in the opposite direction. This is, then, reverse combustion.

Fig. 46.3 shows the various zones inside the formation, with the cold zone near the injector at the left and the hot zone near the producer.[3] Since the region around the producer is hot, the problem of liquid blocking mentioned earlier in connection with the dry forward process has been eliminated.

In principle, there is no upper limit for oil viscosity for the application of the reverse combustion process. However, this process is not as efficient as the dry forward combustion because a desirable fraction of the oil (the lighter portion) is burned and an undesirable fraction of the oil (the heavier portion) remains in the region behind the combustion front. Besides, spontaneous ignition could occur at the injector.[4] If this happens, the oxygen will be used up near the injector and will not support combustion near the producer. The process then reverts to forward combustion.

No reverse combustion project has ever reached commercial status. Nevertheless, this process should not be written off because, in spite of the difficulties facing this process, it could offer some hope of recovering extremely viscous oil or tar.

Wet Combustion

The term "wet combustion" actually refers to wet forward combustion. This process was developed to use the heat contained behind the combustion zone. In this process, water is injected either alternately or simultaneously with air. Because of its high heat capacity and latent heat of vaporization, water is capable of moving the heat behind the combustion front forward, and helping to displace the oil in front of the combustion zone.

Fig. 46.4 shows the temperature distributions of the wet combustion process as the water/air ratio (WAR) increases.[5] The curve for WAR=0 refers to dry combustion. With an increase in WAR, the high-temperature zone behind the combustion zone shortens (WAR=moderate). With a further increase in WAR, the combustion will be partially quenched as shown by the curve for WAR=large.

The wet combustion process also is known as the COFCAW process, which is an acronym for "combination of forward combustion and waterflood." This process also can be construed as steamflood with in-situ steam

generation. It should be noted that this method cannot prevent liquid blocking and its application is limited by oil viscosity, as is the dry forward combustion.

Historical Development

The following lists chronologically some of the major events that occurred in the development of the thermal recovery methods.

1931 A steamflood was conducted in Woodson, TX.[6]
1949 A dry forward combustion project was started in Delaware-Childers field, OK.[7]
1952 A dry forward combustion project was conducted in southern Oklahoma.[8]
1955 A reverse combustion project was initiated in Bellamy, MO.[9]
1958 The steam stimulation process was accidentally discovered in Mene Grande Tar Sands, Venezuela.[10]
1960 Steam stimulation was started in Yorba Linda, CA.[11]
1962 Wet combustion phase of a fireflood project was started in Schoonebeek, The Netherlands.[12]

Current Status

U.S. Oil Production by Enhanced Recovery Methods

The significance of the thermal recovery processes can be seen from the April 1982 survey of the *Oil and Gas J.*[13] As shown in Table 46.1, of the daily U.S. oil production with EOR processes, 76.9% comes from steam injection and 2.7% comes from in-situ combustion, totalling 79.6% obtained by thermal recovery processes. The combustion process, although dwarfed by the steam injection processes, accounts for more than double the production of all the chemical floods combined, which amounts to 1.2%.

Geographical Distribution of Thermal Recovery Projects

Table 46.2, based largely on the 1982 survey,[13] shows the geographical distribution of the steam injection projects in the world. Of the daily oil production from steam injection processes, 71.7% comes from the U.S., 15.4% from Indonesia, 7.0% from Venezuela, and 3.0% from Canada. In the U.S., California accounts for nearly all the production, with small percentages coming from Louisiana, Arkansas, Texas, Oklahoma, and Wyoming.

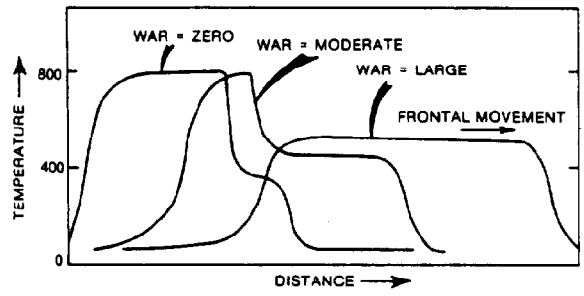

Fig. 46.4—Wet combustion.

The daily oil production by in-situ combustion is shown in Table 46.3. Here, the U.S. accounts for 40.0% of the total production, followed by Romania (26.0%), Canada (22.1%), and Venezuela (10.8%). Of the U.S. production, nearly one-half comes from California, one-third from Louisiana, with the rest from Mississippi, Texas, and Illinois.

Major Thermal Recovery Projects

The major thermal recovery projects, again based largely on the 1982 survey,[13] are listed in Table 46.4.

Reservoirs Amenable to Thermal Recovery

Table 46.5 shows the ranges of reservoir properties in which the technical feasibility of steamflood and fireflood has been proven.[14]

Potential for Incremental Recovery

According to Johnson *et al.*,[15] vast energy resources exist in the tar sands in Venezuela and Colombia (1,000 to 1,800 billion bbl), Canada (900 billion bbl), and the U.S. (30 billion bbl). These tar sands should be a major target

TABLE 46.1—U.S. EOR PRODUCTION (1982)

	B/D	%
Steam	288,396	76.9
Combustion	10,228	2.7
Total thermal	298,624	79.6
Micellar/polymer	902	0.2
Polymer	2,587	0.7
Caustic	580	0.2
Other chemicals	340	0.1
Total chemicals	4,409	1.2
CO_2 miscible	21,953	5.9
Other gases	49,962	13.3
Total	71,915	19.2
Grand Total	374,948	100.0

TABLE 46.2—OIL PRODUCTION BY STEAM INJECTION PROCESSES (1982)

	B/D	%
U.S.	288,396	71.7
Arkansas	800	
California	284,093	
Louisiana	1,600	
Oklahoma	617	
Texas	711	
Wyoming	575	
Canada (Alberta)	12,180	3.0
Brazil	1,920	0.5
Trinidad	3,450	0.9
Venezuela	28,030	7.0
Congo	2,500	0.6
France	360	0.1
Germany	3,264	0.8
Indonesia	62,000	15.4
Total	402,100	100.0

TABLE 46.3—PRODUCTION BY IN-SITU COMBUSTION (1982)

	B/D	%
U.S.	10,228	40.0
California	4,873	
Illinois	179	
Kansas	2	
Louisiana	2,940	
Mississippi	1,300	
Texas	934	
Canada	5,690	22.1
Alberta	150	
Saskatchewan	5,540	
Brazil	284	1.1
Venezuela	2,799	10.8
Romania	6,699	26.0
Total	25,760	100.0

TABLE 46.4—MAJOR THERMAL RECOVERY PROJECTS

	Field, Location (Operator)	Enhanced Oil Production (B/D)
Steamflood	Kern River, CA (Getty)	83,000
	Duri, Indonesia (Caltex)	40,000
	Mount Poso, CA (Shell)	22,800
	San Ardo, CA (Texaco)	22,500
	Tia Juana Este, Venezuela (Maraven)	15,000
Steam stimulation	Lagunillas, Venezuela (Maraven)	40,850
	Duri, Indonesia (Caltex)	22,000
	Cold Lake, Alberta (Esso)	10,000
Fireflood	Suplacu de Barcau, Romania (IFP/IPCCG)	6,552
	Battrum No. 1, Saskatchewan (Mobil)	2,900
	Bellevue, LA (Getty)	2,723
Thermal	Jobo, Venezuela (Lagoven)	13,000

TABLE 46.5—RESERVOIRS AMENABLE TO STEAMFLOOD AND FIREFLOOD

	Steamflood	Fireflood
Depth, ft	160 to 5,000	180 to 11,500
Net pay, ft	10 to 1,050	4 to 150
Dip, degrees	0 to 70	0 to 45
Porosity, %	12 to 39	16 to 39
Permeability, md	70 to 10,000	40 to 10,000
Oil gravity, °API	−2 to 44	9.5 to 40
Oil viscosity at initial temperature, cp	4 to 10^6	0.8 to 10^6
Oil saturation at start, %	15 to 85	30 to 94
OOIP at start, bbl/acre-ft	370 to 2,230	430 to 2,550

for development of thermal recovery methods, since the results will be most rewarding if a percentage of these resources can be tapped economically.

Based on an assumed oil price of $22.00/bbl, Lewin and Assocs. Inc.[16] estimated that the ultimate recovery in the U.S. by thermal recovery methods will amount to 5.6 to 7.9 billion bbl. This includes 4.0 to 6.0 billion bbl by steamfloods and 1.6 to 1.9 billion bbl by firefloods.

Production Mechanisms

The production mechanisms in steam injection processes have been identified by Willman *et al.*[17] as (1) hot waterflood, including viscosity reduction and swelling, (2) gas drive, (3) steam distillation, and (4) solvent extraction effect. The relative importance of these mechanisms on light and heavy oil, represented by 37.0 and 12.2 °API, respectively, is given in Table 46.6.

In firefloods, the above mechanisms are also important. In addition, the breaking up of heavy oil fractions into light oil fractions through cracking should have at least two effects: increase in volume and more drastic reduction in viscosity. The gas drive effect also should be increased because of the large amount of air injected and combustion gas produced.

Theoretical Considerations

Surface Line and Wellbore Heat Losses

In current field practice, downhole steam generators are still in the developmental stage. Surface steam generators are being used in almost all of the steam injection projects. Steam from a generator normally is sent to the injector wellhead through a surface line. Some heat will be lost to the surrounding atmosphere by convection and radiation. As steam travels from the wellhead through the wellbore to the sandface at the pay zone, heat will be lost to the overburden, mainly by conduction. The method of calculating surface line and wellbore heat losses is discussed below.

Surface Line Heat Losses

The steam lines in most of the steam injection projects are insulated. The heat loss from such a line, Btu/hr, is:

$$Q_{rl} = 2\pi r_{in} U_{ti} (T_s - T_{at}) \Delta L, \quad \ldots\ldots\ldots\ldots\ldots (1)$$

where

r_{in} = outside radius of the insulation surface, ft,
T_s = steam temperature, °F,
T_{at} = atmospheric temperature, °F, and
ΔL = pipe length, ft.

In the above, U_{ti} is the overall heat transfer coefficient (based on inside radius of the pipe or tubing), Btu/hr-ft-°F, and can be calculated as follows.

$$U_{ti} = \left[\frac{r_{in} \ln\left(\frac{r_{in}}{r_{to}}\right)}{k_{hin}} + \frac{1}{h+I} \right]^{-1}, \quad \ldots\ldots\ldots\ldots (2)$$

where r_{to} is the outside radius of pipe, ft, and k_{hin} is the thermal conductivity of insulation material, Btu/hr-sq ft-°F.

The convection heat transfer coefficient, h, Btu/hr-sq ft-°F, can be calculated thus[18]:

$$h=0.75v_w^{0.6}/r_{in}^{0.4}, \quad \ldots\ldots\ldots\ldots\ldots\ldots\ldots\ldots (3)$$

where v_w is the wind velocity, mi/hr. The radiation heat transfer coefficient, I, normally can be neglected.

If the pipe is bare, that is, uninsulated, then $r_{to}=r_{in}$ and

$$U_{ti}=h. \quad \ldots\ldots\ldots\ldots\ldots\ldots\ldots\ldots\ldots\ldots\ldots (4)$$

If the steam is superheated, T_s will vary along the line as heat is being lost to the atmosphere. When the pipe is long, it needs to be broken up into segments and the heat loss calculated segment by segment. In each segment,

$$T_{s2}=T_{s1}-Q_{rl}/w_sC_s, \quad \ldots\ldots\ldots\ldots\ldots\ldots\ldots (5)$$

where

T_{s1}, T_{s2} = steam temperatures at the beginning and the end of the segment, °F,
Q_{rl} = heat loss along the segment, Btu/hr,
w_s = mass rate of steam, lbm/hr, and
C_s = heat capacity of steam, Btu/lbm-°F.

If the steam is saturated, the heat loss will cause reduction in steam quality.

$$f_{s2}=f_{s1}-Q_{rl}/w_sL_s, \quad \ldots\ldots\ldots\ldots\ldots\ldots\ldots (6)$$

where f_{s1} and f_{s2} equal the steam quality at the beginning and the end of the pipe segment, fraction, and L_s is the latent heat of steam, Btu/lbm.

Wellbore Heat Losses

In most of the steam injection projects, saturated steam at a certain quality is injected into the formation. Here, we assume a more general case in which the steam first enters the wellbore as superheated steam, becomes saturated with a gradually diminishing quality, and is further cooled after its complete condensation into hot water.

Superheated Steam. Assume that when the depth D is 0, the temperature of the steam is T_s and varies with time. Also assume that a linear geothermal gradient exists so that

$$T_f=g_GD+T_{su}, \quad \ldots\ldots\ldots\ldots\ldots\ldots\ldots\ldots (7)$$

where T_f is the temperature of the formation. Suppose one starts with the temperature of the steam at a depth D_1, and desires to calculate the temperature at depth D_2 with the length of the depth interval $\Delta D=D_2-D_1$. Since the formation temperature at D is $g_GD_1+T_{su}$, Ramey's equation for the gas case[19] becomes

$$T(D_2,t)=g_GD_2+T_{su}-g_GA-AB$$
$$+[T(D_1,t)-g_GD_1-T_{su}+g_GA+AB]e^{-\Delta D/A}. \quad \ldots\ldots\ldots\ldots\ldots\ldots\ldots (8)$$

A is defined as

$$A=\frac{w_sC_s[k_{hf}+r_{ti}U_{ti}f(t)]}{2\pi r_{ti}U_{ti}k_{hf}} \quad \ldots\ldots\ldots\ldots\ldots\ldots (9)$$

and

$$B=\frac{1}{778C_s}, \quad \ldots\ldots\ldots\ldots\ldots\ldots\ldots\ldots\ldots (10)$$

where

k_{hf} = thermal conductivity of the formation, Btu/D-ft-°F,
r_{ti} = inside radius of the tubing, ft,
U_{ti} = overall heat transfer coefficient for the annular space between inside of the tubing and outside of the casing based on r_{ti}, Btu/D-ft-°F,
$f(t)$ = transient heat conduction time function for earth, dimensionless, shown in Fig. 46.5,
C_s = heat capacity of steam, Btu/lbm-°F,
g_G = geothermal gradient, °F/ft, and
T_{su} = surface temperature, °F.

For $t>7$ days,

$$f(t)=\ln\frac{2\sqrt{\alpha t}}{r_{co}}-0.29, \quad \ldots\ldots\ldots\ldots\ldots\ldots (11)$$

where α is the thermal diffusivity, sq ft/D, and r_{co} is the outside radius of casing, ft.

Saturated Steam. When the steam is saturated, the wellbore heat loss will cause changes in the steam quality whereas the steam temperature, T_s, is kept constant. If

TABLE 46.6—MECHANISMS CONTRIBUTING TO STEAM RECOVERY

	Recovery (% Initial Oil in Place)			
	Torpedo Sandstone Core 37°API Crude		Torpedo Sandstone Core 12.2°API Crude	
Steam injection pressure, psig	800 (520°F)	84 (327°F)	800 (520°F)	84 (327°F)
Hot waterflood recovery (includes viscosity reduction and swelling)	71.0	68.7	68.7	66.0
Recovery from gas drive	3.0	3.0	3.0	3.0
Extra recovery from steam distillation	18.9	15.6	9.3	4.9
Recovery improvements from solvent/extraction effects	4.7	4.6	3.0	3.7
Total recovery by steam	97.6	91.9	84.0	77.6

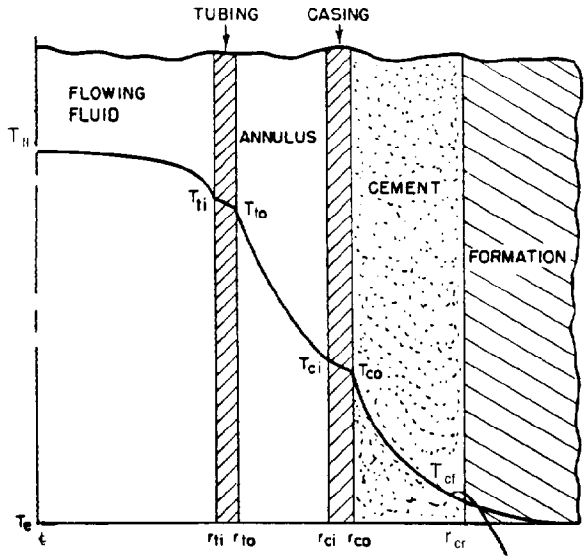

Fig. 46.5—Transient heat conduction in an infinite radial system.

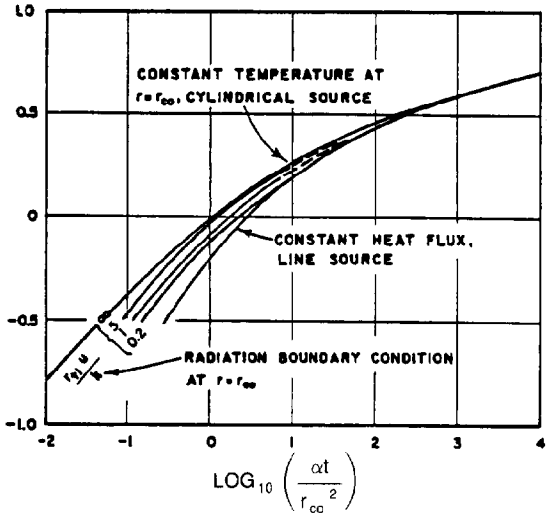

Fig. 46.6—Temperature distribution in an annular completion.

the steam quality at D is $f_s = f_s(D_1, t)$, the steam quality at D_2 can be calculated by Satter's equation[20]:

$$f_s(D_2,t) = f_s(D_1,t) + \frac{A'B' + aD_1 + b - T_s}{A'}\Delta D + \frac{a(\Delta D)^2}{2A'}. \quad \ldots\ldots (12)$$

In Eq. 12,

$$A' = \frac{w_s L_s [k_{hf} + r_{ti} U_{ti} f(t)]}{2\pi r_{ti} U_{ti} k_{hf}} \quad \ldots\ldots (13)$$

and

$$B' = \frac{1}{778 L_s}. \quad \ldots\ldots (14)$$

Hot Water. For cooling of the hot water, Ramey's equation for the liquid phase[19] applies. To advance from depth D_1 to D_2,

$$T(D_2,t) = g_G D_2 + T_{su} - g_G A + [T(D_1,t) - g_G D_1 + T_{su} + g_G A] e^{-\Delta D/A}. \quad \ldots\ldots (15)$$

Overall Heat Transfer Coefficient. The temperature distribution in an annular completion is shown in Fig. 46.6.[21] To evaluate the overall heat transfer coefficient, U_{to}, based on the outside tubing surface, the following procedure developed by Willhite[21] can be used.

1. Select U_{to} based on outside tubing surface.
2. Calculate $f(t)$, as defined previously.
3. Calculate T_{cf} at cement/formation interface.

$$T_{cf} = \frac{T_{fl} f(t) + \frac{k_{hf}}{r_{to} U_{to}} T_f}{f(t) + \frac{k_{hf}}{r_{to} U_{to}}}, \quad \ldots\ldots (16)$$

where T_{fl} = temperature of fluid, °F.

4. Calculate T_{ci} at casing inside surface.

$$T_{ci} = T_{cf} + \left(\frac{\ln \frac{r_{cf}}{r_{co}}}{k_{hce}} + \frac{\ln \frac{r_{co}}{r_{ci}}}{k_{hca}} \right) r_{to} U_{to} (T_{fl} - T_{cf}), \quad \ldots\ldots (17)$$

where

r_{cf} = radius to cement/formation interface, ft,
r_{ci} = inside radius of casing, ft,
k_{hce} = thermal conductivity of the cement, Btu/hr-ft-°F, and
k_{hca} = thermal conductivity of the casing material, Btu/hr-ft-°F.

5. Estimate I for radiation and h for natural convection.
6. Calculate U_{to}.

$$U_{to} = \left(\frac{1}{h+I} + \frac{r_{to} \ln \frac{r_{cf}}{r_{co}}}{k_{hce}} \right)^{-1} \quad \ldots\ldots (18)$$

With commercial insulation of thickness Δr,

$$U_{to} = \left[\frac{r_{to} \ln \frac{r_{in}}{r_{to}}}{k_{hin}} + \frac{r_{to}}{r_{in}(h'+I')} + \frac{r_{to} \ln \frac{r_{cf}}{r_{co}}}{k_{hce}} \right]^{-1}, \quad \ldots\ldots (19)$$

where h' and I' are based on insulation outside surface.

Calculations Including Pressure Changes. A more sophisticated calculation procedure proposed by Earlougher[22] includes the effect of pressure changes inside the wellbore. The wellbore is divided into a sequence

of depth intervals. The conditions at the bottom of each interval are calculated, on the basis of the conditions at the top of that interval. The procedure is as follows.

1. Calculate the pressure at the bottom of the interval, p_2.

$$p_2 = p_1 + 1.687\times10^{-12}(v_{t1}-v_{t2})\frac{{w_s}^2}{{r_{ti}}^4} + 6.944\times10^{-3}\frac{\Delta D}{v_{t1}} - \Delta p, \quad \ldots\ldots\ldots\ldots\ldots (20)$$

where

v_t = specific volume of the total fluid, cu ft/lbm (condition 1 is top of interval and 2 is bottom),
ΔD = length of depth interval, ft, and
Δp = frictional pressure drop over interval, psi.

The Beggs and Brill correlation[23] for two-phase flow can be used to calculate the Δp in the above equation.

2. Calculate the heat loss over the interval.

$$Q_l = \frac{2\pi k_{hf} r_{co} U_{co} \Delta D}{k_{hf} + r_{co} U_{co} f(t)} \times [0.5(T_{s1} + T_{s2}) - 0.5(T_{f1} + T_{f2})], \quad \ldots\ldots\ldots\ldots\ldots\ldots (21)$$

where U_{co} is the overall heat transfer coefficient based on outside casing surface, Btu/hr-sq ft-°F.

3. Calculate the steam quality at the bottom of the interval.

$$f_{s2} = \frac{f_{s1}L_{v1} + H_{w1} - H_{w2} - Q_{rl}/w_s}{L_{v2}}, \quad \ldots\ldots\ldots (22)$$

where H_{w1} and H_{w2} are the enthalpy of liquid water at top and bottom of the interval, Btu/lbm, and L_{v1} and L_{v2} are the latent heat of vaporization at top and bottom of the interval, Btu/lbm.

More Recent Developments. A new model has been developed by Farouq Ali[24] that treats wellbore heat losses rigorously by using a grid system to represent the surrounding formation. In addition, the pressure calculation accounts for slip and the prevailing flow regime, based on well-accepted correlations.

Analytical Models for Steam Injection

For predicting reservoir performance under steam injection processes, the usual practice is to use three-dimensional (3D), three-phase numerical simulators. Where the simulators are unavailable or a quick estimate of the performance is needed, one can resort to simple analytical methods. Usually these methods take into account the thermal aspects of the process only, without regard to the fluid flow aspects.

Front Displacement Models

Marx-Langenheim Method.[25] Consider that heat is injected into a pay zone bounded by two neighboring formations. The heat-carrying fluid is supposed to advance with a sharp front perpendicular to the boundaries of the formation (Fig. 46.7). The heat balance gives: heat injected into the pay zone equals heat loss to the overburden and underlying stratum plus heat contained in the pay zone.

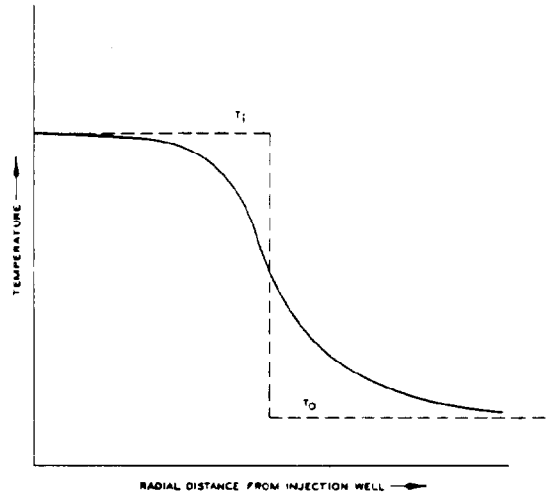

Fig. 46.7—Temperature distribution in Marx-Langenheim model.

The heated area at any time t can be calculated

$$A = \frac{Q_{ri}Mh\alpha_o}{4{k_{ho}}^2\Delta T}\left(e^{t_D}\operatorname{erfc}\sqrt{t_D} + 2\sqrt{\frac{t_D}{\pi}} - 1\right), \quad \ldots (23)$$

where

A = heated area at time t, sq ft,
t = time since injection, hr,
Q_{ri} = heat injection rate, Btu/hr,
M = volumetric heat capacity of the solid matrix containing oil and water, Btu/cu ft-°F

$$= (1-\phi)\rho_r C_r + S_{wi}\phi\rho_w C_w + S_{oi}\phi\rho_o C_o, \quad \ldots\ldots\ldots\ldots\ldots\ldots\ldots (24)$$

ϕ = porosity, fraction,
ρ_r, ρ_o, ρ_w = density of rock grain, oil, water, lbm/cu ft,
C_r, C_o, C_w = heat capacity of rock, oil, water, Btu/lbm-°F,
S_{oi}, S_{wi} = initial saturation of oil, water, fraction,
h = pay thickness, ft,
α_o = overburden thermal diffusivity, sq ft/hr,
k_{ho} = overburden thermal conductivity, Btu/hr-ft-°F,
$\Delta T = T_{inj} - T_{fi}$, °F,
T_{inj} = injection temperature, °F,
T_{fi} = initial formation temperature, °F,
t_D = dimensionless time

$$= \left(\frac{4{k_{ho}}^2}{M^2h^2\alpha_o}\right)t, \quad \ldots\ldots\ldots\ldots (25)$$

and

$$\sqrt{t_D} = \left(\frac{2k_{ho}}{Mh\sqrt{\alpha_o}}\right) t^{1/2}. \quad \ldots\ldots\ldots\ldots\ldots\ldots (26)$$

The complementary error function is:

$$\text{erfc } x = 1 - \text{erf } x = 1 - \frac{2}{\pi}\int_o^x e^{-\beta^2}\, d\beta, \quad \ldots\ldots\ldots\ldots (27)$$

where β is a dummy variable.

To evaluate $e^{t_D}\text{erfc}\sqrt{t_D}$, one can use the following approximation.[26]

$$\text{Let } y = \frac{1}{1+0.3275911\sqrt{t_D}}, \quad \ldots\ldots\ldots\ldots\ldots\ldots (28)$$

$$e^{t_D}\text{erfc}\sqrt{t_D} = 0.254829592y - 0.284496736y^2 + 1.42143741y^3 - 1.453152027y^4 + 1.061405429y^5. \quad \ldots\ldots\ldots\ldots\ldots\ldots\ldots\ldots (29)$$

Assume that all the movable oil is displaced in the heated area. If we assume that all the displaced oil is produced, we can calcuate the cumulative steam/oil ratio (SOR):

$$F_{so}{}^* = \frac{i_s t}{4.275Ah\phi(S_{oi} - S_{io})}, \quad \ldots\ldots\ldots\ldots\ldots\ldots (30)$$

where

i_s = steam injection rate, B/D, cold water equivalent,
S_{oi} = initial oil saturation, and
S_{io} = irreducible oil saturation.

Differentiation of the expression for A with t gives the rate of expansion of the heated area. The oil displacement rate, q_{od}, in B/D, is

$$q_{od} = 4.275\left[\frac{Q_{ri}\phi(S_{oi} - S_{or})}{M\Delta T}\right] e^{t_D}\text{erfc}\sqrt{t_D}. \quad \ldots (31)$$

From this one can calculate the instantaneous SOR:

$$F_{so} = \frac{i_s}{q_{od}}. \quad \ldots\ldots\ldots\ldots\ldots\ldots\ldots\ldots (32)$$

The thermal (heat) efficiency, E_h, is defined as

$$E_h = \frac{Q_{hz}}{Q_{it}}, \quad \ldots\ldots\ldots\ldots\ldots\ldots\ldots\ldots (33)$$

where

Q_{hz} = heat remaining in the heated zone, Btu,
Q_{it} = total heat injection, Btu, and

$$E_h = \frac{AhM\Delta T}{Q_{ri}T}. \quad \ldots\ldots\ldots\ldots\ldots\ldots (34)$$

It can easily be shown that

$$E_h = \frac{1}{t_D}\left(e^{t_D}\text{erfc}\sqrt{t_D} + 2\sqrt{\frac{t_D}{\pi}} - 1\right). \quad \ldots\ldots\ldots (35)$$

Ramey's Generalization of the Marx-Langenheim Method.[27] The Marx-Langenheim method can be extended to the case where a series of constant injection rates is maintained over various time periods. If the heat injection rate is $(Q_{ri})_i$ over the period $0 < t < t_1$, and $(Q_{ri})_n$ over the period $t_{n-1} < t < t_n$,

$$A = \frac{Mh\alpha_o}{4k_{ho}{}^2\Delta T}\left\{(Q_{ri})_n F(t_{Dn}) + \sum_{i=1}^{i=n-1}[(Q_{ri})_i - (Q_{ri})_{i+1}]F(t_{Di})\right\}, \quad \ldots\ldots\ldots (36)$$

where

$$F(t_{Di}) = e^{t_{Di}}\text{erfc}\sqrt{t_{Di}} + 2\sqrt{\frac{t_{Di}}{\pi}} - 1 \quad \ldots\ldots\ldots (37)$$

and $F(t_{Dn}) = F(t_{Di})$ with $i = n$. The oil displacement rate at t_i depends on the heat injection rate at that time, independent of the previous heat injection rates.

Mandl-Volek's Refinement of the Marx-Langenheim Method.[28] Mandl and Volek observed that the heated area measured in laboratory experiments tends to be lower than that predicted by the Marx-Langenheim method after a certain critical time, t_c. For $t \geq t_c$,

$$A = \frac{Q_{ri}Mh\alpha_o}{4k_{ho}{}^2\Delta T}\left[e^{t_D}\text{erfc}\sqrt{t_D} + 2\sqrt{\frac{t_D}{\pi}} - 1 - \sqrt{\frac{t_D - t_{cD}}{\pi}} \times \left(\frac{1}{1 + \frac{L_s f_s}{C_w\Delta T}} + \frac{t_D - t_{cD}}{3}{}^{-3} e^{t_D}\text{erfc}\sqrt{t_D} - \frac{t_D - t_{cD}}{3\sqrt{\pi t_D}}\right)\right]. \quad \ldots\ldots\ldots\ldots\ldots\ldots (38)$$

t_c is determined by this equation:

$$e^{t_{cD}}\text{erfc}\sqrt{t_{cD}} = \frac{1}{1 + \frac{L_s f_s}{C_w\Delta T}}. \quad \ldots\ldots\ldots\ldots (39)$$

The relationship between t_c and t_{cD} is again

$$t_{cD} = \left(\frac{4k_{ho}{}^2}{M^2h^2\alpha_o}\right) t_c. \quad \ldots\ldots\ldots\ldots\ldots (40)$$

Myhill and Stegemeier[29] used a slightly different version of the Mandl-Volek model and calculated oil/steam ratio (OSR) for 11 field projects. They found that the actual OSR's range from 70 to 100% of the calculated ratios.

Steam Chest Models

In contrast to the front displacement models discussed previously, Neuman[30] visualized that steam rises to the top and grows both horizontally outward and vertically downward. Doscher and Ghassemi[31] took a view even more drastic than Neuman's. They theorized that steam rises to the top instantly and the only direction of the steam zone movement is vertically downward. Vogel[32] followed the same reasoning and developed the following simple equation for thermal efficiency:

$$E_h = \frac{1}{1+\sqrt{\frac{4}{\pi}t_D}} \quad \ldots\ldots\ldots\ldots\ldots\ldots\ldots\ldots (41)$$

Table 46.7 compares the thermal efficiencies calculated by the Marx-Langenheim method and the Vogel method. This table shows that the Vogel method predicts a thermal efficiency that lies between 80 and 100% of that calculated by the Marx-Langenheim method.

Steam Stimulation

Steam stimulation usually is carried out in a number of cycles. Each cycle consists of three stages: steam injection, soaking, and production. The basic concept of this process follows.

Without stimulation, the oil production rate is

$$q_{oc} = \frac{0.00708 k k_{ro} h}{\mu_{oc} \ln\frac{r_e}{r_w}}(p_e - p_w), \quad \ldots\ldots\ldots\ldots (42)$$

where

q_{oc} = cold oil production rate, B/D,
k = absolute permeability, md,
k_{ro} = relative permeability to oil, fraction,
μ_{oc} = cold oil viscosity, cp,
p_e = static formation pressure at external radius r_e, psia, and
p_w = bottomhole pressure, psia.

After steam injection, the oil inside the heated region, $r_w < r < r_h$, will have a lower viscosity, μ_{oh}. The hot oil production, q_{oh}, is:

$$q_{oh} = \frac{0.00708 k k_{ro} h}{\mu_{oh} \ln\frac{r_h}{r_w} + \mu_{oc} \ln\frac{r_e}{r_h}}(p_e - p_w), \quad \ldots\ldots (43)$$

TABLE 46.7—COMPARISON BETWEEN MARX-LANGENHEIM AND VOGEL METHODS

	Thermal Efficiency		Ratio
t_D	Marx-Langenheim	Vogel	Vogel/ML
0.01	0.930	0.900	0.967
0.1	0.804	0.737	0.917
1.0	0.556	0.470	0.845
10.0	0.274	0.219	0.799
100.0	0.103	0.081	0.787

where r_h equals the radius of the heated region, ft. The ratio between q_{oh} and q_{oc} is

$$\frac{q_{oh}}{q_{oc}} = \frac{1}{\frac{\mu_{oh}}{\mu_{oc}}\frac{\ln\frac{r_h}{r_w}}{\ln\frac{r_e}{r_w}} + \frac{\ln\frac{r_e}{r_h}}{\ln\frac{r_e}{r_w}}}. \quad \ldots\ldots\ldots\ldots\ldots (44)$$

As the reservoir fluids are produced, energy associated with the fluids are removed from the reservoir. This causes a reduction in r_h and a reduction in temperature, which increases μ_{oh}.

Several methods have been developed for calculating reservoir performance under steam stimulation. One of the methods, which has enjoyed wide acceptance, is the Boberg and Lantz method.[33] This method assumes a constant r_h, with a changing $\bar{T}$ inside the heated zone. The method consists of the following steps.

1. Calculate the size of the heated region using the Marx-Langenheim method.
2. Calculate the average temperature in this region.
3. Calculate the oil production rate, taking into account the reduced oil viscosity in this region.
4. Repeat Steps 1 through 3 for succeeding cycles, by including the residual heat left from preceding cycles.

The average temperature of the heated region is calculated by

$$\bar{T} = T_R + (T_s - T_R)[\bar{V}_r \bar{V}_z (1-\delta) - \delta], \quad \ldots\ldots\ldots\ldots (45)$$

where

$\bar{T}$ = average temperature of the heated region, $r_w < r < r_h$, at any time t, °F,
T_R = original reservoir temperature, °F,
T_s = steam temperature at sandface injection pressure, °F,
$\bar{V}_r, \bar{V}_z$ = average values of V_r, V_z for $0 < r < r_h$ and all h_j,*
V_r, V_z = unit solution for the component conduction problems in the r and z directions, and
δ = energy removed with the produced fluids, dimensionless.

The quantities $\bar{V}_r$ and $\bar{V}_z$ can be obtained from Fig. 46.8 as functions of dimensionless time, t_D. For $\bar{V}_r$,

$$t_D = \frac{\alpha_o (t - t_i)}{r_h^2}, \quad \ldots\ldots\ldots\ldots\ldots\ldots\ldots (46)$$

*These symbols have no physical connotation. They are simply mathematical symbols.

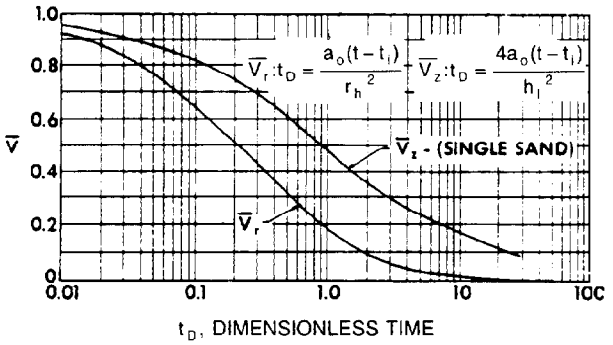

Fig. 46.8—Solutions for V_r and V_s, single sand.

where

α_o = overburden thermal diffusivity, sq ft/D,
t = time since start of injection for the current cycle, D,
t_i = time of injection for the current cycle, D, and
r_h = radius of region originally heated, ft.

For $\bar{V}_z$,

$$t_D = \frac{\alpha_o(t-t_i)}{\bar{H}_1^{\,2}}, \quad \ldots\ldots\ldots\ldots\ldots\ldots\ldots\ldots (47)$$

where

$$\bar{H}_1 = \frac{m_{sit}(f_s L_s + H_{ws} - H_{wR})}{\pi(r_h^{\,2} M)(T_s - T_R)N_s}, \quad \ldots\ldots\ldots\ldots (48)$$

and

m_{sit} = total mass of steam injected, lbm,
N_s = number of sands,
H_{ws}, H_{wR} = enthalpy, Btu/lbm, of water at steam and reservoir temperatures, °F, and
M = volumetric heat capacity, Btu/cu ft-°F.

The energy removed with produced fluids, δ, can be calculated thus:

$$\delta = \frac{1}{2}\int_{t_i}^{t} \frac{Q_{rt}\, dt}{h_t \pi r_h^{\,2} M(T_s - T_R)}, \quad \ldots\ldots\ldots\ldots\ldots (49)$$

where

h_t = total thickness of all sands, ft,
Q_{rt} = heat removal rate at time t, Btu/D,

$$Q_{rt} = q_{oh}(H_{og} + H_w), \quad \ldots\ldots\ldots\ldots\ldots (50)$$

$$H_{og} = (5.6146 M_o + R_t C_g)(\bar{T} - T_R), \quad \ldots\ldots\ldots (51)$$

and

$$H_w = 5.6146 \rho_w [F_{wot}(h_f - H_{wR}) + R_t L_s], \quad \ldots\ldots (52)$$

where h_f is the enthalpy of liquid water at T above 32°F (see steam tables), Btu/lbm, H_{og} is the enthalpy of oil and gas based on a STB of oil, Btu/STB oil, and H_w is the enthalpy of water carried by oil based on a STB of oil, Btu/STB oil. Also, L_s is h_{fg} in the steam tables.

If $p_w > p_s$ and $F_{so} < F_{wot}$

$$F_{so} = 0.0001356\left(\frac{p_s}{p_w - p_s}\right)R_t, \quad \ldots\ldots\ldots\ldots\ldots (53)$$

bbl liquid water at 60°F/STB oil.

If F_{so} (calculated) $> F_{wot}$,

$$F_{so} = F_{wot}. \quad \ldots\ldots\ldots\ldots\ldots\ldots\ldots\ldots\ldots (54)$$

In the above,

R_t = total produced GOR, scf/STB,
F_{wot} = total produced WOR, STB/STB,
F_{so} = steam/oil ratio, STB/STB,
p_w = producing bottomhole pressure, psia, and
p_s = saturated vapor pressure of water at $\bar{T}$, psia.

The rate of hot oil production can be calculated thus:

$$q_{oh} = F_J J_c \Delta p, \quad \ldots\ldots\ldots\ldots\ldots\ldots\ldots (55)$$

where F_J is the ratio of stimulated to unstimulated productivity indexes, dimensionless,

$$F_J = \frac{1}{\frac{\mu_{oh}}{\mu_{oc}}C_1 + C_2}, \quad \ldots\ldots\ldots\ldots\ldots\ldots (56)$$

and J_c is the unstimulated (cold) productivity index, STB/D/psi,

$$J_c = \frac{0.000708 k k_{ro} h}{\mu_{oc} \ln\frac{r_e}{r_w}}. \quad \ldots\ldots\ldots\ldots\ldots (57)$$

If p_e is constant,

$$C_1 = \frac{\ln\frac{r_h}{r_w}}{\ln\frac{r_e}{r_w}} \quad \ldots\ldots\ldots\ldots\ldots\ldots\ldots (58)$$

and

$$C_2 = \frac{\ln\frac{r_e}{r_h}}{\ln\frac{r_e}{r_w}}. \quad \ldots\ldots\ldots\ldots\ldots\ldots\ldots (59)$$

Thus Eq. 55 is identical with Eq. 43 in this case. If p_e is declining,

$$C_1 = \frac{\ln\frac{r_h}{r_w} - \frac{r_h^2}{2r_e^{\,2}}}{\ln\frac{r_e}{r_w} - \frac{1}{2}} \quad \ldots\ldots\ldots\ldots\ldots\ldots (60)$$

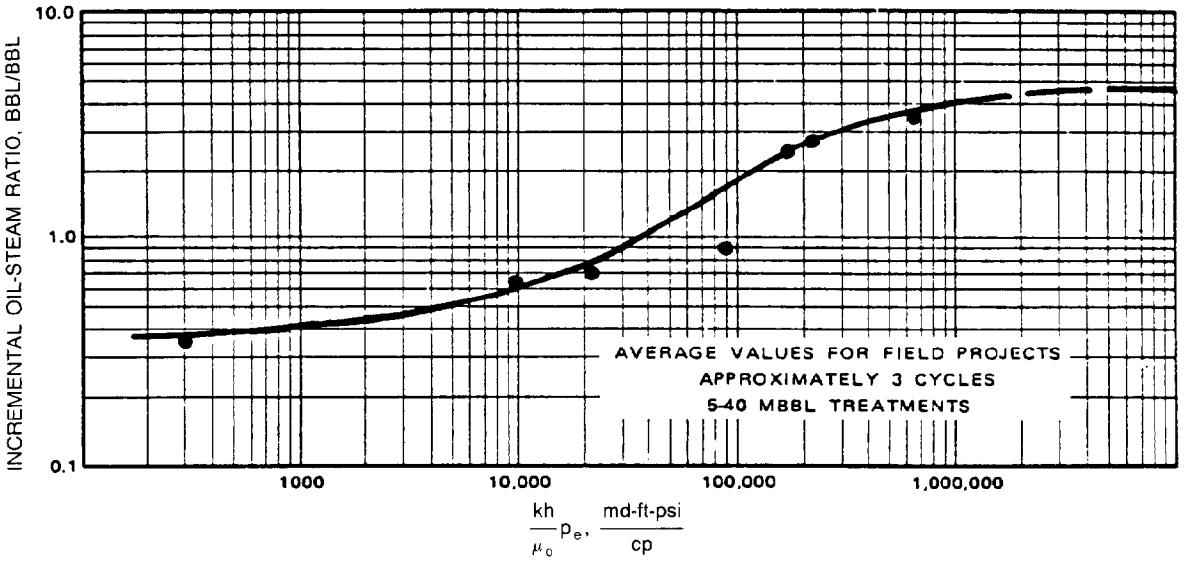

Fig. 46.9—Correlation of steam stimulation results.

and

$$C_2 = \frac{\ln\frac{r_e}{r_h} - \frac{1}{2} + \frac{r_h^2}{2r_e^2}}{\ln\frac{r_e}{r_w} - \frac{1}{2}} \quad \ldots\ldots\ldots\ldots\ldots\ldots (61)$$

This method of calculating oil production rate is probably the weakest part of the Boberg-Lantz method.

1. It assumes a monotone decline between p_e and p_w. Actually, because the injected steam is at a high pressure, there could be a high pressure p_s near r_h and the pressure declines toward both p_w and p_e.

2. Only the change in μ_o is accounted for in changing from cold oil productivity to hot oil productivity. Left unaccounted for is the change in k_{ro}, which should change with changing S_o.

Based on the Boberg-Lantz method, a correlation was developed by Boberg and West[34] that allows one to estimate incremental OSR with known reservoir properties (Fig. 46.9).

Numerical Simulation

The analytical models for thermal recovery processes usually are concerned with the thermal aspects of the processes only. The fluid flow aspects are neglected. To account adequately for the fluid flow inside porous media under a thermal recovery process, numerical simulators will be needed. In these simulators, the reservoir is divided into a number of blocks arranged in one, two, or three dimensions. A detailed study is made of the reservoir by applying fundamental equations for flow in porous media to each one of the blocks.

Numerical reservoir simulators are no substitute for field pilots. They have several advantages, however, over field pilots. Field conditions are irreversible. It took millions of years for the field to develop to the present state. Once disturbed, it cannot revert to the original conditions and start over again. Furthermore, it takes a long time, in terms of months or even years, before the pilot results can be evaluated. The cost for pilots is, of course, enormous. In comparison, a simulated reservoir can be produced many times, each time starting at the existing state. This can be done within a short period of time, in terms of seconds, once the reservoir model is properly set up. The cost for reservoir simulation is much less than that of a pilot. However, simulated reservoirs may never duplicate field performance. Modern practice is to use reservoir simulation to help design a pilot before launching a large-scale field development.

Numerical models and physical models are complementary to each other. As will be detailed later, physical models can be classified into two types: elemental models and partially scaled models. In an elemental model, experiments are conducted with actual reservoir rock and fluids. The results can help explain various fluid flow and heat transfer mechanisms as well as chemical reaction kinetics. In a partially scaled model, reservoir dimensions, fluid properties, and rock properties are scaled for the laboratory model so that the ratios of various forces in the reservoir and the physical model are nearly the same. One can only build partially scaled models because fully scaled models are difficult or impossible to construct. One of the advantages of a numerical model over a physical model is that there is no scaling problem in numerical simulation. However, in many cases, a numerical model needs physical models to validate the formulation or to provide necessary input data for the simulation.

Steam Injection Model

Numerical simulation models for steam injection processes have been developed by Coats *et al.*[35] and Coats.[36,37] A steam injection model consists of a number of conservation equations.

1. *Mass balance of H_2O.* Both water and steam are included.

2. *Mass balances of hydrocarbons.* Only one equation will be necessary for nonvolatile oil. For volatile oil, two or more pseudocomponents will be needed to describe the vaporization/condensation phenomenon of the oil and two or more equations will be needed.

3. *Energy balance.* The energy balance accounts for heat conduction, convection, vaporization/condensation phenomenon, and heat loss from the pay zone to its adjacent formations. The need to include an energy balance in the model sets the thermal recovery processes apart from isothermal processes for oil recovery.

In addition to the conservation equations, the model needs to include the following auxiliary equations.

1. If both water and steam coexist, temperature is the saturated steam temperature for a given pressure. An equation is needed to describe this relationship between temperature and pressure.
2. The sum of saturations for the oil, water, and gas phases equals unity.
3. The mol fractions of hydrocarbon components in the liquid and gas phases are related through equilibrium vaporization constants (*K*-values).
4. The sum of gas-phase mol fractions equals unity. This includes steam and any volatile components of hydrocarbons.
5. The sum of liquid-phase mol fractions for hydrocarbons equals unity.

In-Situ Combustion Model

Numerical simulation models have been developed by Crookston *et al.*,[38] Youngren,[39] Coats,[40] and Grabowski *et al.*[41] The in-situ combustion model is more complicated than the model for steam injection. The conservation equations are as follows.

1. *Mass balance of H_2O.* This equation includes the water produced from combustion.
2. *Mass balances of hydrocarbons.* This includes consumption of certain hydrocarbons through cracking and combustion. It also may include the production of certain other components through cracking.
3. *Mass balance of oxygen.* This accounts for the consumption of oxygen by combustion.
4. *Mass balance of inert gas.* If air is used, the conservation of nitrogen should be accounted for. CO_2 produced from combustion may be included in the equation for the inert gas or be treated separately.
5. *Mass balance of coke.* This includes the formation and burning of coke.
6. *Energy balance.* This equation now includes the heat of reaction for the reactions involved in the in-situ combustion process. These reactions may include low-temperature oxidation of hydrocarbons, high-temperature oxidation or burning of hydrocarbons, thermal cracking (which produces coke and other products), and combustion of coke.

This model also needs a number of auxiliary equations, which include (1) steam/water equilibrium, (2) vaporization equilibrium of hydrocarbons, (3) phase saturation constraints, (4) mol fraction constraints, and (5) chemical stoichiometry. An example is:

$$\text{Oil} + a\ O_2 \rightarrow b\ CO_2 + c\ H_2O.$$

This says that one mol of oil reacts with a mols of oxygen to form b mols of CO_2 and c mols of H_2O.

This model also requires a chemical reaction kinetics equation. For each reaction involved in the process, an equation can be written to denote that the reaction rate varies as a function of temperature and concentrations of the various reactants. One possible form of the reaction rate equation is the following Arrhenius equation:

$$w = k'(C_o)^m (C_{O_2})^n \exp\left(-\frac{E}{RT}\right). \quad \ldots\ldots\ldots\ldots (62)$$

This equation says that the reaction rate, w, is proportional to the concentration of oil, C_o, raised to the mth power times the concentration of oxygen, C_{O_2}, raised to the nth power. The temperature dependence of the reaction rate is in the given exponential form, where E is the activation energy, the energy barrier the reactants need to overcome before being converted to the products, R is the gas constant, and T is the absolute temperature. The proportionality constant, k', usually is called the pre-exponential factor.

The models developed so far are believed to be adequate as far as the formulation of the process mechanisms is concerned. However, problems abound.

1. Artificial breakdown of the crude oil into two components may not be sufficient to describe faithfully the vaporization/condensation phenomena and the chemical reactions involved in the combustion process. More components mean more equations to be solved and hence higher computer costs.
2. The grid size problem could be severe. A grid size large enough for economic computation could greatly distort the temperature distributions in the simulated reservoir. This would lead to erroneous predictions of the chemical reaction rates and thus of reservoir performance under combustion.

Laboratory Experimentation

The thermal numerical models have been used widely for screening thermal prospects, designing field projects, and formulating production strategies. Still, we cannot completely dispense with laboratory experiments for several reasons. First, the numerical models need data that can be measured only experimentally. These data include relative permeabilities, chemical kinetics, adsorption of chemicals on rocks, etc. Second, the numerical models are valid only when all the pertinent mechanisms are accounted for. The currently available models cannot handle adequately situations such as injection of chemicals along with steam, swelling of clays, which reduces the permeability, etc.

As previously mentioned, physical models for thermal recovery processes may be classified into two types, namely, elemental models and partially scaled models. The elemental models are used to study the physico-chemical changes inside a rock-fluid system under certain sets of operating conditions and are normally zero-dimensional (0D) or one-dimensional (1D). The partially scaled models are used to simulate the performance of a reservoir under thermal recovery operations and are normally 3D. Although the intent is to scale every physico-chemical change that takes place in the processes, the models usually are partially scaled because of the extreme difficulty in achieving full scaling.

Elemental Models

Elemental models used for steamflooding can be exemplified by those used by Willman *et al.*[17] In their classic work, they used glass bead packs and natural cores

of different lengths to study the recovery of oil under hot waterflood and steamflood at different temperatures. The oils used included crudes of different gravities and oil fractions.

Fireflood pots and combustion tubes are also elemental models. In another classic work, Alexander *et al.*[42] used fireflood pots (0D) to study fuel laydown and air requirement, as affected by crude oil characteristics, porous medium type, oil saturation, air flux, and time-temperature relationships. The combustion tube (1D) used by Showalter[43] enabled him to delineate the temperature profiles at various times, thus giving the combustion front velocity. More recently, combustion tubes were used to study the use of water along with air[44-46] and the use of oxygen-enriched air in combustion.[47]

Partially Scaled Models

Partially scaled models have been used to simulate steamfloods in ⅛ of a five-spot pattern, ¼ of a five-spot pattern, etc.[48-53] Similar attempts have also been made for firefloods.[54] However, it is certainly much more difficult to include chemical kinetics along with the fluid flow and heat transfer aspects of the combustion process.

Partially scaled models for steamfloods fall into two types, namely, high-pressure models and vacuum or low-pressure models.

High-Pressure Models. All experimental studies on steamflooding had used high-pressure models until vacuum models came along and offered an alternative approach. The scaling laws of Pujol and Boberg[55] normally were followed in the design. If the dimensions are scaled down by a factor of F in the model, the steam injection rate will be scaled down by the same factor and so will the pressure drop between the injector and the producer. The permeability will be scaled up by a factor of F, and the model time will be scaled down by a factor of F^2. Because of the necessity of increasing the permeability in the model to a great extent, reservoir rock material cannot be used. Nevertheless, the experiments will be conducted with the actual crude. Also, the steam pressure and steam quality to be employed in the field will be used in the model.

Vacuum Models. In a small-scale physical model, the thickness is reduced greatly as compared with that in the field. To obtain the same gravitational effects as in the field, the pressure drop from the injector to the producer also must be reduced greatly. The vaporization/condensation phenomenon of water and hydrocarbons is governed by the Clausius-Clapeyron equation, which involves $d \ln p$, or dp/p. Thus, a decrease in the pressure drop (dp) necessitates a corresponding decrease in the pressure (p) itself. This is the rationale behind the vacuum-model approach developed by the Shell group as reported by Stegemeier *et al.*[56]

To see the differences between a high-pressure model and the vacuum model, Table 46.8 has been prepared for using both models to simulate a hypothetical field element with a hypothetical oil. The entries for the high-pressure models were based on the scaling laws of Pujol and Boberg[55] and the entries for the vacuum model were based on the work of Stegemeier *et al.*[56]

TABLE 46.8—COMPARISON OF HIGH-PRESSURE AND VACUUM MODELS FOR STEAMFLOODS

	Field	High-Pressure Model	Vacuum Model
Length, ft	229	1	1
Permeability, darcies	2	458	1,527
Time	5 yrs	50 min	120 min
Steam rate	300 B/D	144.7 cm^3/min	263.1 cm^3/min
Pressure 1, psia	400	400	2.70
Steam quality	0.80	0.80	0.082
Oil viscosity, cp	3.0	3.0	23.6
Temperature, °F	445	445	137.5
Pressure 2, psia	100	100	1.24
Steam quality	0.80	0.80	0.108
Oil viscosity, cp	6.3	6.3	38.2
Temperature, °F	328	328	108.9

The following observations can be made on the high-pressure and vacuum models.

1. Neither the high-pressure model nor the vacuum model can accurately simulate the capillary forces and the relative permeability curves of the actual rock/fluid system because, to obtain a very high permeability, actual rock material is not being used.
2. The high-pressure model does not observe the Clausius-Clapeyron equation, whereas the vacuum model follows it to a large extent but not exactly.
3. To use the vacuum model, an oil has to be reconstituted to obtain the required oil viscosity/temperature relationship. This is completely different from the actual crude in many physicochemical aspects, including its vaporization/condensation behavior and chemical kinetics. In contrast, a high-pressure model normally uses actual crudes.

Field Projects

Screening Guides

In dealing with oil prospects, the first step is to find out whether the field in question can be produced by certain recovery methods. Screening guides are useful for this purpose. Screening guides for steamflood and fireflood processes have been proposed by various authors including Farouq Ali,[57] Geffen,[58] Lewin *et al.*,[59] Iyoho,[60] Chu,[61-63] and Poettmann.[64] These screening guides are listed in Table 46.9.

A perusal of the various screening guides listed in Table 46.9 shows that some of the earlier screening guides were quite restrictive in selecting oil prospects. Such a guide tends to minimize the error of the second kind, that is, the risk of excluding some undesirable prospects. In so doing, it tends to increase the error of the first kind, that is, the risk of missing some desirable prospects. Recent changes in the price structure of the crude oil and improved technology helped to widen the range of applicability for the steamflood and fireflood processes. This is reflected in the less restrictive screening guides developed in more recent years. However, in minimizing the error of the first kind (erroneous rejection), the newer guides may possibly increase the error of the second kind (erroneous acceptance). This should be borne in mind when applying these guides to oil prospects.

TABLE 46.9—SCREENING GUIDES FOR STEAMFLOOD AND FIREFLOOD PROJECTS

References	Year	h	D	ϕ	k	p	S_o	°API	μ	kh/μ	ϕS_o	y^*	Remarks
Steamfloods													
Farouq Ali[57]	1973	≥30	<3,000	0.30	~1,000			12 to 15	<1,000		0.15 to 0.22		
Geffen[58]	1973	>20	<4,000					>10		>20	>0.10		
Lewin and Assocs.[59]	1976	>20	<5,000				>0.50	>10		>100	>0.065		
Iyoho[60]	1979	30 to 400	2,500 to 5,000	>0.30	>1,000		>0.50	10 to 20	200 to 1,000	>50	>0.065		
Chu[61]	1983	>10	>400	>0.20			>0.40	<36			>0.08		
Firefloods													
Poettmann[64]	1964			>0.20	>100						>0.10		
Geffen[58]	1973	>10	>500			>250		<45		>100	>0.05		for COFCAW only
Lewin and Assocs.[59]	1976	>10	>500				>0.50	10 to 45		>20	>0.05		
Chu[62]	1977			≥0.22			≥0.50	≤24	<1,000		>0.13		confidence limits approach
	1977											>0.27	regression analysis approach
Iyoho[60]	1978	5 to 50	200 to 4,500	≥0.20	>300		>0.50	10 to 40	<1,000	>20	>0.077 (>600 B/AF)		for dry combustion (well spacing ≤ 40 acres)
	1978	10 to 120		≥0.20			>0.50	<10	no upper limit				for reverse combustion
	1978	>10	>500	≥0.25			>0.50	<45	<1,000		>0.064		for wet combustion
Chu[63]	1982			>0.16	>100		>0.35	<40		>10	>0.10		

*$y = -0.12 + 0.00262h + 0.000114k + 2.23S_o + 0.000242kh/\mu - 0.000189D - 0.0000652\mu$.

Reservoir Performance

Performance Indicators Common to Both Steamfloods and Firefloods.

Sweep Efficiency. The areal and vertical sweep of the steam front or burning front has pronounced influence on the economics of the steamflood or fireflood projects. Some reported sweep efficiencies of the steamflood and fireflood projects are given in Table 46.10.[65-81] Whereas the volumetric sweep of steamfloods varies from 24 to 99%, that of firefloods appears to be lower, ranging from 14 to 60%.

TABLE 46.10—SWEEP EFFICIENCY OF STEAMFLOOD AND FIREFLOOD PROJECTS

Field, Location (Operator)	Areal	Vertical	Volumetric
Steamfloods			
Inglewood, CA[65] (Chevron-Socal)	60.0	50.0	30.0
Kern River, CA[66,67] (Chevron)	—	—	80.0
Kern River, CA[68-70] (Getty)	~100.0		62.8 to 98.8
Midway Sunset, CA[71,72] (Tenneco)	—	—	60.0 to 70.0
El Dorado, KA[73] (Cities)	—	—	<50.0
Deerfield, MO[74] (Esso-Humble)	85.0	40.0	34.0
Schoonebeek, The Netherlands[75] (Nederlandse)	—	—	24.3 to 41.9
Firefloods			
South Belridge, CA[76] (General Petroleum)			
Within Pattern Area (2.75 acres)	100	59.6	59.6
Within Total Burned Area (7.90 acres)	100	50.4	50.4
Sloss, NE[77-79] (Amoco)	50	28	14
South Oklahoma[80] (Magnolia)	85	—	26
Shannon Pool, WY[81] (Pan American/Casper)	43	100	43

Oil Recovery. Table 46.11 lists some of the reported oil recoveries of steamflood and fireflood projects.[82-121]

For the estimation of the oil recovery obtainable in a steam injection project, the analytical methods discussed previously can be used. As steam injection continues, the thermal efficiency will gradually diminish and the instantaneous SOR will increase gradually. When this ratio reaches a certain limit, further injection of steam will become uneconomical and needs to be stopped. The cumulative oil production at that time divided by the original oil in place (OOIP) will give the oil recovery.

The oil recovery from a fireflood project can be calculated with the recognition that oil production comes from both the burned and unburned regions (Nelson and McNeil[122]). Let E_{vb} equal the volumetric sweep efficiency of the burning front and E_{Ru} equal the recovery efficiency in the unburned region. The overall oil recovery is:

$$E_R = \left(1 - \frac{C_m}{62.4\phi S_o}\right) E_{vb} + (1 - E_{vb}) E_{Ru}, \quad \ldots\ldots (63)$$

where C_m is the fuel content, lbm/cu ft. In this equation, the fuel consumed is taken to be a 10°API oil with a density of 62.4 lbm/cu ft.

The equation developed by Satman *et al.*[123] can be used to calculate the oil recovery from a dry combustion project.

$$Y = 47.0\left[0.427S_o - 0.00135h - 2.196\left(\frac{1}{\mu_o}\right)^{0.25}\right]X, \quad \ldots\ldots (64)$$

where

$$Y = \frac{\Delta N_p + V_{fb}}{N} \times 100 \quad \ldots\ldots (65)$$

and

$$X = \frac{i_{at} E_{O_2}}{[N_{sp}/(\phi S_o)](1-\phi)}. \quad \ldots\ldots (66)$$

TABLE 46.11—OIL RECOVERY OF STEAMFLOOD AND FIREFLOOD PROJECTS

Field, Location (Operator)	Thermal Oil Recovery (% OOIP)
Steamfloods	
Smackover, AR (Phillips)[82,83]	25.7*
Kern River, CA (Chevron)[84]	69.9*
Kern River, CA (Getty)[68-70]	46.6 to 72.6
Midway Sunset, CA (CWOD)[85]	63.0*
Mount Poso, CA (Shell)[86,87]	34.6*
San Ardo, CA (Texaco)[88]	47.5, 51.2
Slocum, TX (Shell)[89,90]	55.8*
Winkleman Dome, WY (Amoco)[91,92]	28.1*
Tia Juana Estes, Venezuela (Maraven)[93-95]	26.3*
Firefloods	
Brea-Olinda, CA (Union)[96,97]	25.1*
Midway Sunset, CA (Mobil)[98]	20.0
Midway Sunset, CA (CWOD)[99]	52.8
South Belridge, CA (General Petroleum)[76]	56.7
South Belridge, CA (Mobil)[100]	14.5
Robinson, IL (Marathon)[101-106]	31.9
Bellevue, LA (Cities)[107,108]	41.5*
Bellevue, LA (Getty)[109-112]	44.6*
May Libby, LA (Sun)[113]	68.0
Heidelberg, MS (Gulf)[114,115]	22.4*
Sloss, NE (Amoco)[77-79]	14.3
Glen Hummel, TX (Sun)[116,117]	31.0
Gloriana, TX (Sun)[116,118]	29.7
North Tisdale, WY (Continental)[119]	23.0
Suplacu de Barcau, Romania (IFP/ICPPG)[120]	47.5
Miga, Venezuela (Gulf)[121]	11.6

*Anticipated.

In the above equation,

ΔN_p = cumulative incremental oil production, bbl,
V_{fb} = fuel burned, bbl,
N = OOIP, bbl,
i_{at} = cumulative air injection, 10^3 scf,
E_{O_2} = oxygen utilization efficiency, fraction, and
N_{sp} = oil in place at start of project, bbl.

Gates and Ramey[124] developed a correlation between oil recovery and PV burned at various initial gas saturation, on the basis of field data taken from the South Belridge fireflood project[76] and laboratory combustion-tube data. This correlation, shown in Fig. 46.10, should be useful in predicting current oil recovery as the fireflood proceeds.

Changes in Oil Property. At the temperatures and pressures prevailing in steamfloods, no changes in the oil property are expected to occur because of any chemical reactions. However, the properties of the recovered oil could have been changed as a result of steam distillation. In firefloods, of course, oil properties change considerably because of thermal cracking and combustion, as well as steam distillation. Changes in oil property in some of the reported steamfloods and firefloods are shown in Table 46.12.[125-130]

Performance Indicator Pertaining to Steamfloods Only. ***Steam Oil Ratio (SOR).*** The SOR, F_{so}, is the most important factor characterizing the success or failure of a steamflood project. Its reciprocal, the OSR, F_{os}, also is used commonly. In projects where oil is used as fuel

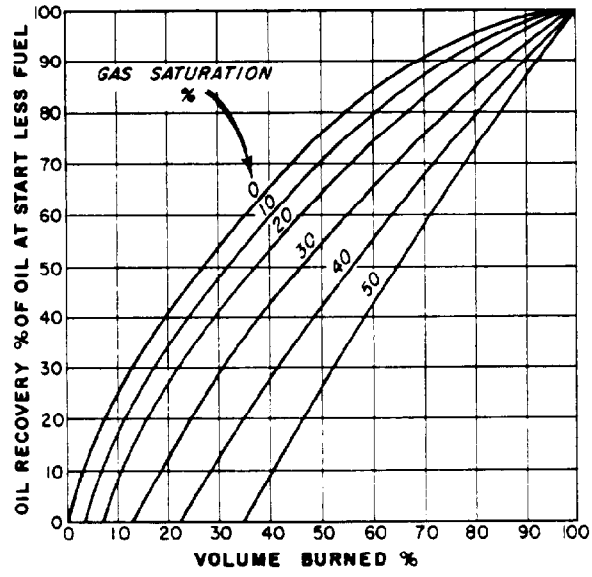

Fig. 46.10—Estimated oil recovery vs. volume burned.

for steam generation, 1 bbl of oil normally can generate 13 to 14 bbl (cold-water equivalent) of steam. Thus, the highest SOR that is tolerable without burning more oil than that produced is 13 to 14. For steamflood operation, there are other costs than fuel alone. Because of this, steam injection is normally terminated when the instantaneous SOR reaches the level of eight or so. Ideally the overall SOR should be around four. This corresponds to 3 to 4 bbl of oil produced per barrel of oil burned.[131] This ideal case is, unfortunately, not normally achievable. The SOR of the majority of the steamflood field projects falls into the range of 5 to 7.

The following set of regression equations developed by Chu[62] can be used to estimate the SOR with known reservoir and crude properties.

1. For $F_{so} > 5.0$ ($F_{os} < 0.20$),

$$F_{so} = 1/(-0.011253 + 0.00002779D + 0.0001579h - 0.001357\Theta + 0.000007232\mu_o + 0.00001043kh/\mu_o + 0.5120\phi S_o). \quad \ldots\ldots\ldots\ldots\ldots\ldots\ldots\ldots (67)$$

2. For $F_{so} \le 5.0$ ($F_{os} \ge 0.20$),

$$F_{so} = 18.744 + 0.001453D - 0.05088h - 0.0008864k - 0.0005915\mu_o - 14.79S_o - 0.0002938kh/\mu_o, \quad \ldots (68)$$

where

D = depth, ft,
h = reservoir thickness, ft,
Θ = dip angle, degrees,
μ_o = oil viscosity, cp,
k = permeability, md, and
S_o = oil saturation at start, fraction.

Another method of estimating F_{so} has been given by Myhill and Stegemeier,[29] based on the Mandl-Volek model.

TABLE 46.12—CHANGES IN OIL PROPERTY IN STEAMFLOOD AND FIREFLOOD PROJECTS

Field, Location (Operator)	°API		Temperature (°F)	Viscosity (cp)	
	Before	After		Before	After
Steamflood					
Brea, CA[125] (Shell)*	23.5	25.9	—	—	—
Fireflood					
South Belridge, CA[76] (General Petroleum)	12.9	14.2	87	2,700	800
			120	540	200
			160	120	54
West Newport, CA[126,127] (General Crude)	15.2	20.0	60	4,585	269
			100	777	71
			210	32	10
East Venezuela[128] (Mene Grande)	9.5 then 10.5	12.2			
Kyrock, KY[129] (Gulf)	10.4	14.5	60	90,000	2,000
			210	120	27
South Oklahoma[80] (Magnolia)	15.4	20.4	66	5,000 after a month	800 5,000
Asphalt Ridge, UT[130] (U.S. DOE)**	14.2	20.3			

*Changes in % $C_4 - C_{12}$: before—21, after—28.

**Changes in other properties:

	Before	After
Pour point, °F	140	25
Residue boiling above 1,000°F, wt%	62	35

Performance Indicators Pertaining to Firefloods Only.

Fuel Content. Fuel content (lbm/cu ft of burned volume) is the amount of coke available for combustion that is deposited on the rock as a result of distillation and thermal cracking. It is the most important factor influencing the success of a fireflood project. If the fuel content is too low, combustion cannot be self-sustained. A high fuel content, however, means high air requirement and power cost. Besides, oil production also may suffer.

Fuel content can be determined by laboratory tube runs. Gates and Ramey[124] presented a comparison of the estimated fuel content by use of various methods including laboratory experiments and field project data from the South Belridge project.[76] Their comparison shows that fuel content determined from the tube runs can provide reasonably good estimation of the fuel content obtainable in the field.

In the absence of experimental data, the correlation of Showalter[43] relating the fuel content to API gravity can be used. Fig. 46.11 shows a comparison of the Showalter data and field project data.[63] In addition, the following regression equation developed by Chu[62] based on data from 17 field projects can be used to calculate the fuel content:

$$C_m = -0.12 + 0.00262h + 0.000114k + 2.23S_o + 0.000242kh/\mu_o - 0.000189D - 0.0000652\mu_o, \quad \ldots\ldots\ldots\ldots\ldots\ldots\ldots\ldots\ldots\ldots (69)$$

where C_m is the fuel content, lbm/cu ft.

Both laboratory experiments and field projects indicate that, for a specific reservoir, fuel content decreases as WAR increases. However, no statistically significant correlation was found to exist between fuel content and WAR in the presence of widely varying reservoir properties.[63]

Air Requirement. As pointed out by Benham and Poettmann,[132] air requirement, a, in 10^6 scf/acre-ft of burned volume, can be calculated on the basis of stoichiometric considerations:

$$a = \frac{\left(\frac{2F_{cc}+1}{F_{cc}+1} + \frac{F_{HC}}{2}\right) C_m}{0.001109(12+F_{HC})E_{O_2}} \times 0.04356, \quad \ldots\ldots\ldots (70)$$

where F_{cc} is the CO_2/CO ratio in produced gas and F_{HC} is the atomic H/C ratio. In the absence of necessary data for Eq. 70, the Showalter correlation[43] relating air requirement to API gravity can be used. A comparison of the Showalter data and field project data is given in Fig. 46.12.[63] It can be seen that all the field points fall on the upper side of the Showalter curve. Air requirement in the fields can exceed laboratory values because of air channeling and migration. In addition, the following regression equation developed by Chu[63] can be used:

$$a = 4.72 + 0.03656h + 9.996S_o + 0.000691k. \quad \ldots\ldots (71)$$

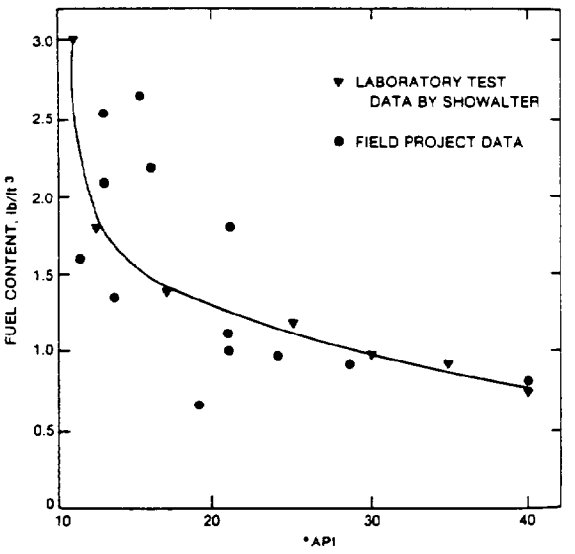

Fig. 46.11—Effect of oil gravity on fuel content.

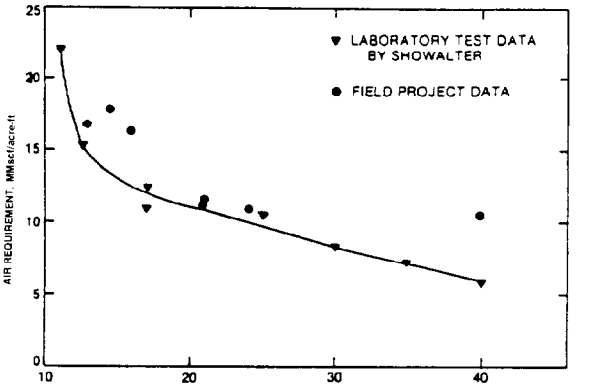

Fig. 46.12—Effect of oil gravity on air requirement.

Air-Oil Ratio (AOR). This important ratio relates air injection to oil production and usually is expressed in terms of 10^3 scf/bbl. Oil recovery comes from both the burned and unburned regions. The AOR can be calculated thus[122]:

$$F_{ao} = \frac{a}{\left[\left(\frac{\phi S_o}{5.6146} - \frac{C_m}{350}\right)E_{vb} + \frac{\phi S_o}{5.6146}(1-E_{vb})E_{Ru}\right]43.56} \quad \ldots\ldots\ldots\ldots\ldots\ldots\ldots\ldots\ldots\ldots (72)$$

In the absence of E_{vb} and E_{Ru}, the following regression equation developed by Chu[62] based on 17 field projects can be used.

$$F_{ao} = 21.45 + 0.0222h + 0.001065k + 0.002645\mu_o - 76.76\phi S_o. \quad \ldots\ldots\ldots\ldots\ldots\ldots (73)$$

Besides, the correlation between oil recovery and PV burned developed by Gates and Ramey[124] can be used for estimating the current AOR as the fireflood proceeds.

Both laboratory experiments and field projects indicate that, for a specific reservoir, AOR decreases as WAR increases. No statistically significant correlation, however, has been found between AOR and WAR in the presence of widely varying reservoir properties.[63]

Project Design

Design Features Common to Both Steamfloods and Firefloods

Pattern Selection. For any oil recovery process with fluid injection, a cardinal rule of pattern selection is that, to achieve a balance between fluid injection and production, the ratio of the number of producers to the number of injectors should be equal to the ratio of well injectivity to well productivity (Caudle *et al.*[133]). Because of the high mobility of air or steam compared to that of the oil, the injectivity/productivity ratio is high, favoring a high producer/injector ratio. This rule generally has been followed by the various reported steamflood and fireflood projects. The use of inverted 13-spot, 9-spot, 7-spot, and 6-spot patterns, unconfined five-spot patterns, down-the-center line of injectors, and single well injection has been reported.

Aside from the injectivity/productivity ratios, other factors also should enter into consideration in pattern selection. These factors include: heat loss considerations, utilization of existing wells, reservoir dip, difficulty in producing hot wells, etc. Based on these and other considerations, repeated five-spot patterns, updip and crest injections and line drive also were used. The choice of pattern or nonpattern floods in the various steamflood and fireflood projects is shown in Table 46.13.[134-138]

Completion Intervals. In most of the steamflood and fireflood projects, the producers usually are completed for the entire sand interval to maximize production. The injectors usually are completed at the lower third or lower half of the interval, to minimize the override of the steam or air. In wet combustion projects, it is advisable to complete the lower part for air injection and upper part for water injection. This is to minimize the underflow of water as well.

Producer Bottomhole Pressure (BHP). In their study for a steamflood, Gomaa *et al.*[139] found that decreasing the producer BHP lowers the average reservoir pressure, increases steam volume, and increases predicted oil recovery. It is, therefore, important to keep the producers pumped off all the time. Without any reason to believe otherwise, keeping the producers pumped off should benefit a fireflood as well as a steamflood.

TABLE 46.13—PATTERN TYPES OF STEAMFLOODS AND FIREFLOODS

Pattern Types	Steamfloods	Firefloods
Inverted 13-spot	Slocum, TX[89,90] (Shell)	
Inverted 9-spot	San Ardo, CA[88] (Texaco) Yorba Linda, CA[11] (Shell)	Bellevue, LA[107,108] (Cities Service) Bellevue, LA[109-112] (Getty)
Inverted 7-spot	Kern River, CA[84] (Chevron) Slocum, TX[89,90] (Shell) Tia Juana, Venezuela[135] (Shell)	Silverdale, Alta.[134] (General Crude)
Unconfined inverted 5-spot		West Newport, CA[126,127] (General Crude)
Down-the-center-line of injectors		Trix-Liz, TX[116,136] (Sun) Glen Hummel, TX[116,117] (Sun)
Single well injection		Miga, Venezuela[121] (Gulf)
Repeated 5-spot	East Coalinga, CA[137] (Shell) Kern River, CA[84] (Chevron) Kern River, CA[68-70] (Getty) Winkleman Dome, WY[91,92] (Pan American)	Sloss, NE[77-79] (Amoco)
Updip or crest injection	Brea, CA[125] (Shell) Midway Sunset, CA[71,72] (Tenneco)	Midway Sunset, CA[98] (Mobil) Heidelberg, MS[114,115] (Gulf)
Downdip injection	South Belridge, CA[138] (Mobil)	
Updip and downdip injection	Mount Poso, CA[86,87] (Shell)	
Line drive		Suplacu de Barcau, Romania (IPF/ICPPG)[120]

Design Features Pertaining to Steamfloods Only

Steam Injection Rate. According to Chu and Trimble,[140] the optimal choice of a constant steam injection rate is relatively independent of sand thickness. As sand thickness decreases, the total oil content in the reservoir decreases. This calls for a lower steam rate. At the same time, a higher steam rate is needed to compensate for the increased percentage heat loss with a decrease in thickness. These two counteracting factors result in only a small variation in the optimal steam rate as thickness is changed from 90 to 30 ft.

The same study with five-spot patterns shows that the optimal choice of a constant steam rate is proportional to the pattern size. Furthermore, varying steam rates appear to be preferable to constant steam rates. An optimal steam rate schedule calls for a high steam rate in the initial stage and a decrease in the steam rate with time.

Steam Quality. Steam quality refers to the mass fraction of water existing in vapor form. Gomaa *et al.*[139] reported that increasing steam quality increases oil recovery vs. time but had little effect on recovery vs. Btu's injected. This indicates that heat injection is the important parameter in determining steamflood performance.

Just as with steam injection rates, the optimal choice of steam quality should be studied. High-quality steam could cause excessive steam override. This may be remedied by using lower-quality steam at one stage of a steamflood.

Design Features Pertaining to Fireflood Only

Dry vs. Wet Combustion. The choice between dry combustion and wet combustion is an important decision to be made in conducting a field project. Laboratory experiments indicated that the use of water either simultaneously

or alternately with air does reduce the AOR, although the oil recovery may not be improved significantly. As was mentioned previously, a correlation between AOR and WAR, based on data from 21 field projects, was found to be statistically insignificant in the presence of widely varying reservoir properties.[63]

Cities Service conducted a field comparison test of dry and wet combustion in the Bellevue field, LA,[141] in which possible interference by variations in reservoir properties was essentially circumvented by using two contiguous patterns, one with dry combustion and another with wet combustion. This test found that, with wet combustion, the volumetric sweep was improved to a great extent. This indirectly implies an increase in oil recovery. Furthermore, the air requirement for a specific volume of reservoir was reduced. This reduced the operating cost and improved the economics. Because of these encouraging results, the possible advantages of using wet combustion should be explored.

Air Injection Rate. According to Nelson and McNeil,[122] the air injection rate depends on the desired rate of advance of the burning front. A satisfactory burning rate was stated to be 0.125 to 0.5 ft/D. In the design method proposed by these authors, a maximum air rate is first determined, based on the minimum burning rate of 0.125 ft/D. They recommended a time schedule such that the air rate would be increased gradually to the maximum rate, held at this rate for a definite period, and then reduced gradually to zero. The Midway Sunset, CA, project of Chanslor-Western[99] used a burning rate of 1 in./D (0.08 ft/D). Gates and Ramey[124] found that the air rate should provide a minimum rate of burning front advance of 0.15 ft/D or an air flux of at least 2.15 scf/hr-sq ft at the burning front.

WAR. The reported WAR in various field projects ranged from 0 (for dry combustion) to 2.8 bbl/10^3 scf. The choice of WAR depends on water availability, quality of the water available, well injectivity, and economic considerations. Combustion tube experiments, properly designed and executed, should be helpful.

Well Completion

Special well completions are needed for injectors and producers to withstand the high temperatures in steamfloods, and to withstand the corrosive environment as well in firefloods.

According to Gates and Holmes,[142] wells used in steam operations should be completed with due consideration of heat loss with thermal stresses. In deep wells, tubular goods with high qualities, such as the normalized and tempered P-105 tubing and P-110 casing, should be used if the tubing and casing are not free to expand. Thermal stress can be minimized by the proper use of expansion joints. Thermal packers should be used on steam injection wells and deep wells undergoing cyclic steaming. The cement should include a thermal strength stabilizing agent, an insulating additive and a bounding additive.

For firefloods, Gates and Holmes[142] felt that steel casing and tubing such as J-55 is suitable for injectors. These wells can be completed with normal Portland cement, with high-temperature cement placed opposite and about 100 ft above the pay zone. The high-temperature cement recommended for the injectors is calcium aluminate cement (with or without silica flour), pozzolan cement, or API Class G cement (with 30% silica flour). If spontaneous ignition occurs, the use of cemented and perforated liners is required to prevent well damage resulting from burnback into the borehole. The producers should be completed to withstand relatively high temperatures and severe corrosion and abrasion. These authors recommended the use of gravel-flow pack, and stainless steel 316 for both liner and tubing opposite the pay zone.

The well completion methods for injectors and producers in the various steamflood and fireflood projects, detailed by Chu[61,63] previously, are given in Table 46.14.

Field Facilities

Steamflood Facilities

Steam Generation and Injection. Most of the steam injection projects use surface steam generators. The major difference between oilfield steam generators and industrial multitube boilers is the ability to produce steam from saline feedwater with minimum treatment. Other features include unattended operation, portability, weatherproof construction, and ready accessibility for repairs. The ability to use a wide variety of fuels including lease crude is also an important requirement. The capacity of steam generators used in steamflood projects usually ranges from 12 to 50×10^6 Btu/hr, with 50×10^6 Btu/hr becoming the industry standard in California.

With surface steam generators, the steam goes from the generators to the injection wells through surface lines. Most surface steam lines are insulated with a standard insulation with aluminum housings. The steam is split into individual injectors through a header system using chokes to reach critical flow. This procedure requires that the steam achieve sonic velocity, which, under one field condition,[68] calls for a pressure drop of about 55% across the choke. The chokes are sized to each other to give the desired flow rate into each injector. As long as the pressure drop is greater than 55%, the flow rate will be independent of the actual wellhead injection pressure.

A recent development is the use of downhole steam generators to eliminate wellbore heat losses in deep wells. There are two basic designs, which differ on the method of transferring heat from the hot combustion gases to produce steam.[143] In one design, the combustion gas mixes directly with feed water and the resulting gas/steam mixture is injected into the reservoir. Because of this, the combustion process takes place at the injection pressure. In another design, there is no direct contact between the combustion gas and water, just as in the surface generators. The combustion gas returns to the surface to be released after giving up much of the heat to generate steam. A lower pressure than injection pressure can be used in this case.

Still another new development is cogeneration of steam and electricity.[144] The effluent gas from a combustor is used in a gas turbine, which drives an electrical generator. The exhaust gas from the turbine is then used in steam generators to produce steam for thermal recovery purposes.

TABLE 46.14—WELL COMPLETION FOR STEAMFLOODS AND FIREFLOODS

	Steamfloods	Firefloods
Injectors		
Casing	Grades: J-55, K-55, and N-80 Sizes: 4½, 5½, 6⅝, 7, and 9⅝ in. Tensile prestressing of casing in deep wells	Grades: J-55 and K-55 Sizes: 4½, 5½, 7, and 8½ in. across the pay zone
Openhole or perforated completions	Both openhole completions with slotted liners and solid-string completion with jet perforations have been reported. Liner sizes: 4½, 5½, or 7 in. Perforations: ¼ or ½ in., one or two per foot, or one-half per foot Some with stainless steel wire-wrapped screens.	Perforated completion more prevalent than openhole completion with or without liners. Liner sizes: 3½ or 5½ in. Perforations: ¼ or ½ in. (two or four per foot)
Cement	Class A, G, and H cement with silica flour (30 to 60% of dry cement).	Use of high-temperature cement prevalent.
Gravel packing	Use not prevalent.	Use not prevalent.
Tubing	Tubing insulations used in deep wells: asbestos with calcium silicate, plus aluminum radiation sheld; or jacketed tubing with calcium silicate.	Tubing used for air injection or as a thermowell. In wet combustion, various ways have been used for injection of air and water.
Producers		
Casing	Grade: K-55 Sizes: 4½, 5½, 6⅝, 7, and 8⅝ in. Tensile prestressing of casing in deep wells	Grades: H-40, J-55, and K-55 Sizes: 5½, 7, 8⅝, and 9⅝ in.
Openhole or perforated completions	Both openhole completion with slotted liners and solid-string completion with jet perforations have been reported. Liner sizes: 4½, 4¾, or 6⅝ in. Slot sizes: 40, 60, or 60/180 mesh Perforations: ½ in., four per foot Some with stainless steel wire-wrapped screens.	Openhole completion with or without slotted liners and perforated completion are equally prevalent. Liner sizes: 4¾, 5½, or 6⅝ in. Slot sizes: 60-mesh, 0.05, 0.07, or 0.08 in. Perforations: ½ in. (two or four per foot)
Cement	Class G and H cement with silica flour (30 to 60% of dry cement).	Use of high-temperature cement was reported.
Gravel packing	Use more prevalent than in injectors. Gravel size: 6/9 mesh flow-packed.	Use more prevalent than in injectors. Gravel sizes: 20/40 or 6/9 mesh, flow- or pressure-packed.
Tubing	Tubing for rod pump.	Tubing for rod pump, to serve as a thermowell, or for cooling water injection.

Water Treatment. The feedwater treatment for steam generation consists mainly of softening, usually through zeolite ion exchange. Some feedwaters may require filtration and deaeration to remove iron. Still others may need to use KCl for control of clay swelling and chlorine to combat bacteria. Facilities for oil removal also will be needed if the produced water is to be reused as feedwater for steam generation.

Fireflood Facilities

Ignition Devices. In many fields, the reservoir temperature is so high that spontaneous ignition would occur only a few days after starting air injection. In some projects, steam, reactive crude, or other fuels will be added to help ignition.

Many other fields need artificial ignition devices, which include electrical heaters, gas burners, and catalytic ignition systems. The various ignition methods, including equipment and operational data, have been discussed by Strange.[145]

Air Compressors. The air compressors can be gas engine or electrical motor driven. Depending on the total injection rate the compressor needs to supply and the output pressure needed, the capacity of the compressors can range from 1.0 to 20.0×10^6 scf/D, and the power rating can range from 300 to 3,500 hp.

Monitoring and Coring Programs

Monitoring Programs

A thermal recovery project could be a complete failure economically and still be considered a success if it could provide useful information on the reservoir performance under steamflood or fireflood. A properly designed monitoring program carried out during the project and coring programs during and after the project are important in providing the information necessary for evaluating steamflood or fireflood performance.

The Sample, Control, and Alarm Network (SCAN) automation system installed by Getty in the Kern River field[146] illustrates how a large steam injection operation can be monitored. This system consists of a devoted central computer that monitors 96 field sites. At these sites, the production rates of more than 2,600 producers and the operating rates of 129 steam generators are gathered. The SCAN performs several functions.

1. It automatically schedules and controls well production tests at each site.
2. It monitors results of well production tests, steam generator operating rates, flow status, and injection status of producers, valve positions during well tests, and various status contact checks.
3. It sounds the alarm upon any malfunctioning at a field site or a steam generator.
4. It reports necessary operating information routinely on a daily, weekly, or monthly basis, and other special reports on demand from the operator.

The Silverdale, Alta., fireflood project of General Crude[134] also uses an automatic data collection system. Differential pressure transducers, thermocouple-amplifier transducers, pressure transducers, and motor load transducers are used to measure and record data at each well. These data are transmitted to a central system, which can be interrogated and can indicate any alarm situation when pressures, temperatures, or flow rates fall outside certain specified ranges.

Not all thermal projects call for elaborate automatic monitoring programs. The following program used in the Bodcau, LA, fireflood project of Cities Service-DOE[147] typifies one needed for a small-scale pilot.

1. Gas production rates, useful for mass balance calculations, were measured monthly. Monthly analysis of the produced gas gave data for the calculation of the oxygen utilization efficiency.
2. Oil and water production rates were measured at least twice each month.
3. Flow line temperatures were measured daily. These temperatures, in conjunction with the gas production rates, were useful in determining the amount of quench water needed at the producers.
4. Downhole temperature profiles were taken monthly at the observation wells. These profiles helped to delineate the development of the burned volume.

Coring Program

Drilling core holes could be very expensive, depending on the depths of the pay zones. However, a judiciously designed and properly executed coring program, either during a thermal project or afterward, could provide valuable information on the project performance. Such a program can give the following information: (1) residual oil saturation (ROS) after steamflood or fireflood, (2) vertical sweep of the injected steam or burned volume, (3) areal sweep of the steam front or burning front, (4) maximum temperature distribution, both areally and vertically, and (5) effective permeability of the rock, and whether any deposits formed during the process could have reduced the flow capacity.

A typical coring program, used for postmortem evaluation in the Sloss, NE, fireflood project,[79] is summarized next.

Core Analyses. Porosity, permeability, and oil saturations were measured on each foot of the recovered cores. Oil saturations were determined by the routine Dean-Stark extraction and weight loss method, and the infrared absorption method.

Log Analyses. Compensated formation density and dual-induction laterolog logs were run in the core holes to determine porosity and oil saturation.

Photographs and Visual Examination. Whereas black-and-white photographs were found to be rather useless, ultraviolet photographs gave an excellent picture as to where the oil was removed by the burning process. The absence of oil also could be seen by visual examination. In some intervals, the reddish color of the core indicated that the core had been subjected to a temperature high enough for iron oxidation.

Mineral Analyses of the Cores. Various minerals, including glauconite, illite, chlorite, and kaolinite, underwent permanent changes with the temperature increase. The maximum temperature to which the core samples had been exposed could be determined from the form and color of these minerals.

Microscopic Studies. The scanning electron microscope was used to study anhydrite formation and clay alteration in the core samples, which had been subjected to high temperatures.

Tracers

The use of tracers helped to monitor fluid movement and interpret areal coverage in individual steamflood patterns. According to Wagner,[148] preferred aqueous-phase or gaseous-phase tracers include radioisotopes, salts with detectable cations and anions, fluorescent dyes, and water-soluble alcohols. Radioactive tracers include tritium, tritiated water, and krypton-85. Other tracers include ammonia, air, sodium nitrite, sodium bromide, and sodium chloride.

Operational Problems and Remedies

Operational problems plaguing steamflood and fireflood projects and their remedies, previously detailed by Chu,[61,63] are summarized next.

Problems Common to Steamfloods and Firefloods

Well Productivity. Production of the highly viscous crude may be extremely low before the arrival of the steam front or burning front. The production rate can be improved by injecting light oil as a diluent, hot oil treatment, cyclic steam injection, or burning at the producers.

When producer temperature exceeds 250°F, pump efficiency decreases to a great extent because of hot produced fluids flashing to steam or direct breakthrough of the injected steam or flue gas. The best remedy is to plug off the hot zone and redirect the steam or flue gas to the oil section before entering the wellbore.

Sanding. Sanding can be severe even in steamflood projects. The remedies include the Hyperclean™ technique, foamed-in tight-hole slotted liners, a sodium aluminate sand consolidation technique, and the use of phenolic-resin gravel packing.

In firefloods, sanding is particularly severe if the sand is extremely unconsolidated. The erosion can be aggravated further by coke particles and high gas rates. Sandblasting could require frequent pulling of wells and replacement of pumps.

Emulsions. In steamfloods, emulsions sometimes can be broken easily by chemical treatment. The problem could

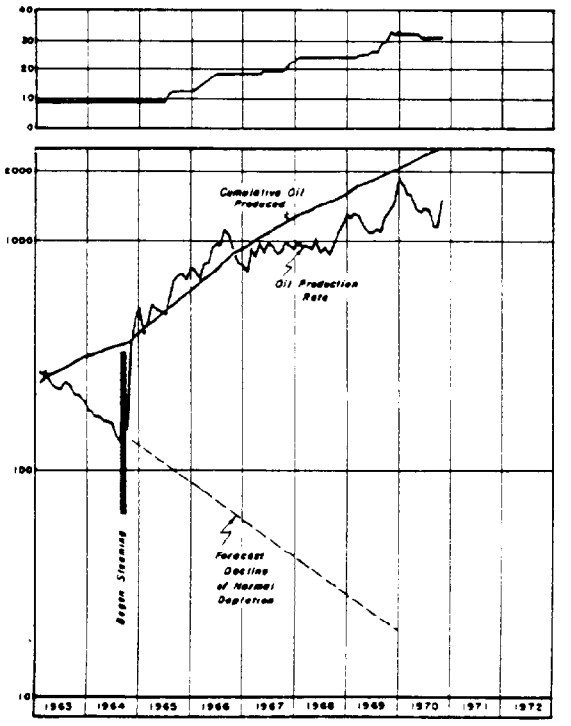

Fig. 46.13—Production history of cyclic steam stimulation, TM sand, Huntington Beach offshore field, CA.

become severe if the emulsion is complicated with the solids produced and with the continuously changing nature of the produced fluids.

Emulsions found in fireflood projects are formed of heavy oil, cracked light ends, quench and formation water, solids, and possibly, corrosion products. They can become a continual and major problem in some projects, and require expensive emulsion breakers.

Problems Plaguing Steamfloods Only

Steam Placement. The lack of control of steam placement during steam stimulation is a major problem in producers with liner completions. The use of solid string completions will help reduce the problem.

Steam Splitting. The uneven splitting of steam in a two-phase regime can cause significant differences in steam quality into different injectors. This can be corrected by modifying the layout of the steam line branching system.

TABLE 46.15—RESERVOIR ROCK AND FLUID PROPERTY DATA, TM SAND, HUNTINGTON BEACH OFFSHORE FIELD, CA

Depth, ft	2,000 to 2,300
Thickness, ft	
Gross	115
Net	40 to 58
Porosity, %	35
Permeability, md	400 to 800
Oil gravity, °API	12 to 15
Reservoir temperature, °F	125
Reservoir pressure at start, psig	600 to 800
Oil viscosity at 125°F, cp	682
Oil saturation at start, %	75

Problems Plaguing Firefloods Only

Poor Injectivity. Various substances can cause losses in injectivity for the air injectors. If identifiable, these problems can be remedied by appropriate means. Injector plugging by iron oxide can be reduced by injecting air into the casing and bleeding it through the tubing. Asphaltene buildup can be reduced by squeeze washing with asphaltene solvent. Emulsion formed in situ can be reduced by emulsion breakers. Scale formation caused by barium and strontium sulfate can be reduced by an organic phosphate. The injection of NuTri™ (trichloromethylene) and acidizing are useful in improving the injectivity.

Corrosion. Corrosion can be mild or serious and is caused by simultaneous injection of air and water, production of acids, sulfur, oxygen, and CO_2. Corrosion inhibitors are needed regularly.

Exploration Hazards. To minimize explosion hazards in the air injection system, an explosion-proof lubricant should be used. Flushing of the interstage piping with a nitrox solution is necessary.

Case Histories

Many thermal recovery projects have been reported in the literature. The following describes a number of selected projects and gives the reasons for their selection.

Steam Stimulation Operations

Huntington Beach, CA (Signal)[149]—Typical Operation. The steam stimulation project was conducted in the TM sand, in the Huntington Beach offshore field, Orange County, CA. This project typifies the behavior of a heavy-oil reservoir under cyclic steam stimulation. The reservoir properties are given in Table 46.15.

Steam injection was started in nine producers in Sept. 1964, resulting in a large increase in oil production. This early success prompted the expansion of the project by drilling wells on 5-acre spacing. The number of wells increased from 9 in 1964 to 35 in 1969. The performance of the steam stimulation project during the 1964–70 period is shown in Fig. 46.13. With steam stimulation and with the almost quadrupling of the number of wells, the oil rate increased more than 10-fold, from 125 B/D oil in 1964 to about 1,500 B/D oil in 1970.

The performance of steam stimulation normally deteriorates as the number of cycles increases. As shown in Table 46.16, the OSR changed from the range of 3 to 3.8 bbl/bbl for the first two cycles to the range of 2.4 to 2.5 bbl/bbl for the third and fourth cycles.

Fig. 46.14 shows how oil production in one well decreases during a cycle and how it varies from one cycle to another.

Paris Valley, CA (Husky)[150]—Co-Injection of Gas and Steam. A wet combustion project was initiated at Paris Valley, which is located in Monterey County, CA. Before the arrival of the heat front, the producers were stimulated with steam. A special feature that made this project interesting was the co-injection of air and steam in three of the stimulation cycles. The reservoir properties are given in Table 46.17.

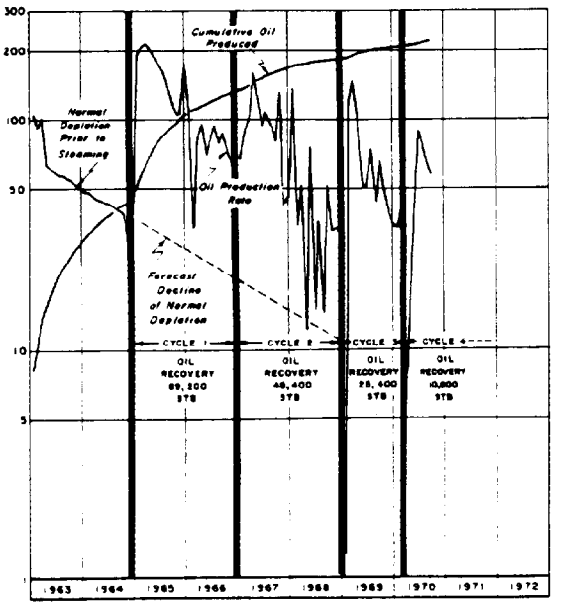

Fig. 46.14—Oil production rate, Well J-128, Huntington Beach offshore field.

In Table 46.18, Cycles 3 and 5 of Well 20 and Cycle 7 of Well 3 used air-steam injection. For Well 20, oil production in Cycle 3 was 4,701 bbl while that in Cycle 2 was 2,449 bbl. Thus, with air-steam injection, oil production increased by 92%. A similar increase was noticeable for Cycle 5 of Well 20 and Cycle 7 of Well 3 when compared with their respective preceding cycles, which used steam only.

Steamflood Projects

Kern River, CA (Getty)[68-70]—Largest Steamflood. The Kern River field is located northeast of Bakersfield, CA, in the southeastern part of the San Joaquin Valley. Getty Oil Co.'s steam displacement operation in this field is the largest in the world, based on a 1982 survey.[13] According to this survey, the thermal oil production rate was 83,000 B/D in an area of 5,070 acres.

The Kern River formation consists of a sequence of alternating sand and shale members. The reservoir properties are given in Table 46.19.

The Kern River field was discovered in the late 1890's. In the mid-1950's, bottomhole heaters were used to improve the oil productivity. In Aug. 1962, a 2.5-acre normal five-spot hot waterflood was started. Results showed that this process was technically feasible but economically unattractive. In June 1964, the hot waterflood pilot was converted to a steam displacement test and the number of injectors was increased from the original 4 wells to 47 wells. Continued expansion through the years has increased the number of injectors to 1,788 wells, with 2,556 producers by 1982. The original Kern project and some later expansions are shown in Fig. 46.15. The steam displacement operation was in general conducted in 2.5-acre five-spot patterns.

Getty Oil Co.'s steam displacement operation includes many projects. For illustration purposes, the Kern project is presented here with a map showing the well patterns (Fig. 46.16) and a figure showing the injection and

TABLE 46.16—SUMMARY OF PERFORMANCE THROUGH FOUR "HUFF 'N' PUFF" CYCLES AS OF OCTOBER 1, 1970; TM SAND, HUNTINGTON BEACH OFFSHORE FIELD, CA

	Cycle 1	Cycle 2	Cycle 3	Cycle 4
Number of wells	24	18	11	4
Average cycle length, months	14	18	15.3	14.5
Average oil recovery per well, STB	28,900	30,900	24,650	29,225
Average quality of steam injected, %	71.4	69.3	75.1	78.5
Average volume of steam injected, bbl	9,590	8,130	10,190	11,760
Ratio of oil recovered to steam injected, STB/bbl	3	3.8	2.4	2.5

TABLE 46.17—RESERVOIR ROCK AND FLUID PROPERTY DATA, ANSBERRY RESERVOIR, PARIS VALLEY FIELD, CA

Depth, ft	800
Net thickness, ft	50
Dip, degrees	15
Porosity, %	32
Permeability, md	3,750
Oil gravity, °API	10.5
Reservoir temperature, °F	87
Initial pressure, psig	220
Saturation at start, %	
Oil	64
Water	36

Oil viscosity, cp

	Upper Lobe	Lower Lobe
87°F	227,000	23,000
100°F	94,000	11,000
200°F	340	120

TABLE 46.18—RESPONSE TO CYCLIC AIR/STEAM

	Well 20				Well 3	
	Cycle 2	Cycle 3	Cycle 4	Cycle 5	Cycle 6	Cycle 7
Steam volume, 10^3 bbl	13.2	16.2	15.7	10.4	8.2	9.2
Air volume, 10^6 scf	0	1.5	0	3.7	0	3.6
Air/steam ratio, scf/bbl	0	91	0	355	0	394
Comparable producing days	161	161	90	90	97	97
Oil produced, bbl	2,449	4,701	270	503	2,375	4,203
Steam/oil ratio, bbl/bbl	5.4	3.4	58	21	3.5	2.2
Oil/steam ratio, bbl/bbl	0.19	0.29	0.02	0.05	0.29	0.45
Peak oil production test, B/D	51	81	24	38	60	141

TABLE 46.19—RESERVOIR ROCK AND FLUID PROPERTY DATA, KERN RIVER FIELD, CA

Depth, ft	500 to 1,300
Thickness, ft	30 to 90
Dip, degrees	4
Porosity, %	28 to 33
Permeability, md	1,000 to 5,000
Oil gravity, °API	12.0 to 16.5
Reservoir temperature, °F	90
Reservoir pressure at start, psig	100
Oil viscosity, cp	
90°F	4,000
250°F	15
Oil saturation at start, %	35 to 52

production history of the four-pattern pilot (Fig. 46.17). In this project, the cumulative SOR was 3.8 bbl/bbl and the production rate reached 100 B/D of oil per pattern. Core hole data before and after the steamflood showed an oil recovery of 72% and also a very high areal sweep efficiency.

Brea, CA (Shell)[125]—Steam Distillation Drive, Deep Reservoir, Steeply Dipping. A steam distillation drive was initiated in 1964 in the Brea field, which is located about 25 miles east of Los Angeles. This project is interesting because the oil is relatively light with low viscosity, and the reservoir is steeply dipping at a great depth. The reservoir properties are summarized in Table 46.20.

The dipping reservoir is seen clearly in Fig. 46.18. The injectors are located updip, as shown in Fig. 46.19. Because of the depth, insulated tubing was used for the injectors. This figure also shows the area of temperature response and production response. The injection and production rates are given in Table 46.20. As of Dec. 1971, the steam rate was 1,010 B/D water and the oil rate was 230 B/D, giving an estimated SOR of 4.4 bbl/bbl.

Smackover, AR (Phillips)[82,83]—Reservoir With Gas Cap. The Smackover field is located in Ouachita County, AR. The steamflood pilot, conducted in the Nacatoch sand, is worth mentioning because the reservoir has a gas cap thicker than the oil sand itself. This gas cap can be seen readily in the log and coregraph of Sidum Well W-35 (Fig. 46.21). The reservoir properties are given in Table 46.21.

TABLE 46.20—RESERVOIR ROCK AND FLUID PROPERTY DATA, BREA FIELD, CA

Depth, ft	4,600 to 5,000
Gross stratigraphic thickness, ft	300 to 800
Ratio of net to gross sand, %	63
Dip, degrees	66
Porosity, %	22
Permeability, md	77
Oil gravity, °API	24
Reservoir temperature, °F	175
Reservoir pressure at start, psi	110
Oil viscosity at 175°F, cp	6
Saturation at start, %	
Oil	49
Gas	18

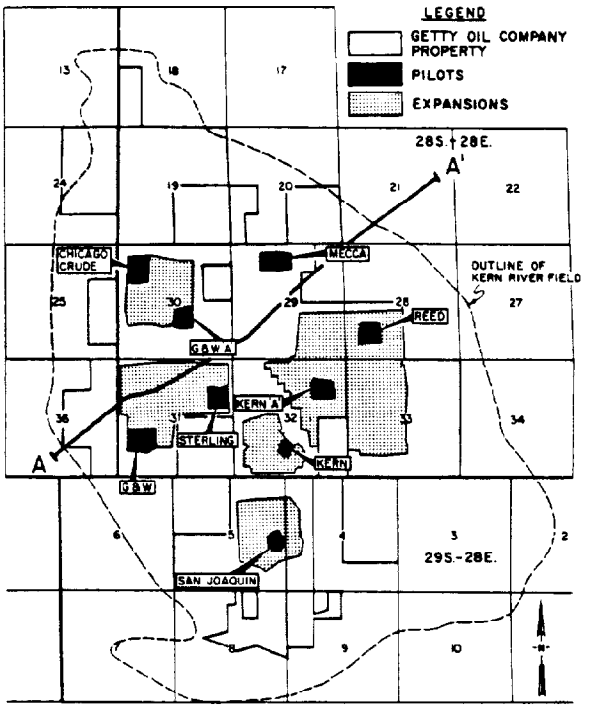

Fig. 46.15—Kern River field, CA.

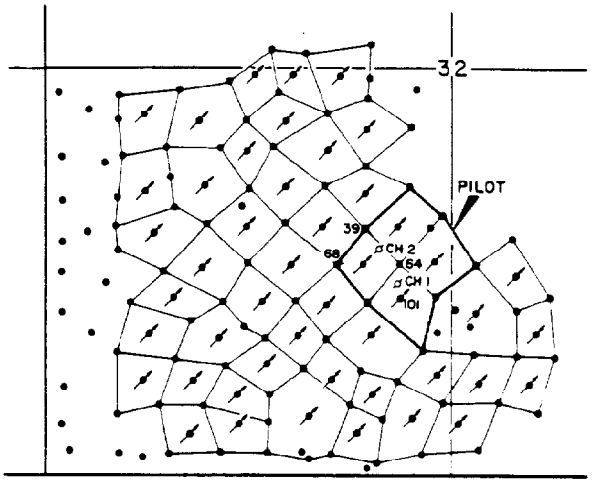

Fig. 46.16—Kern steam displacement project, Kern River field.

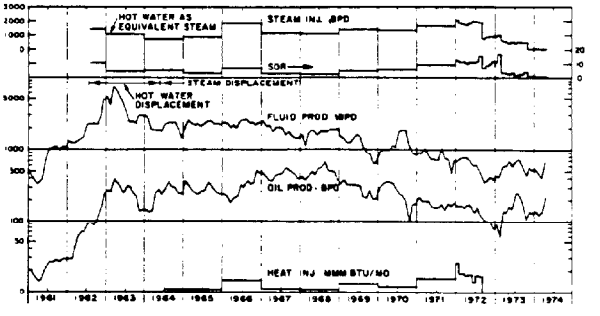

Fig. 46.17—Injection and production history, Kern hot water and steam displacement project (four patterns) Kern River field.

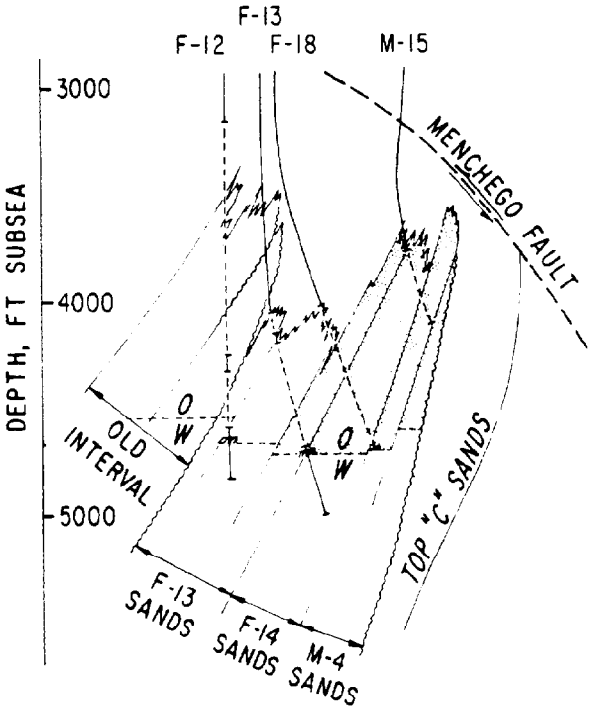

Fig. 46.18—Cross section through the lower "B" sands, Brea field.

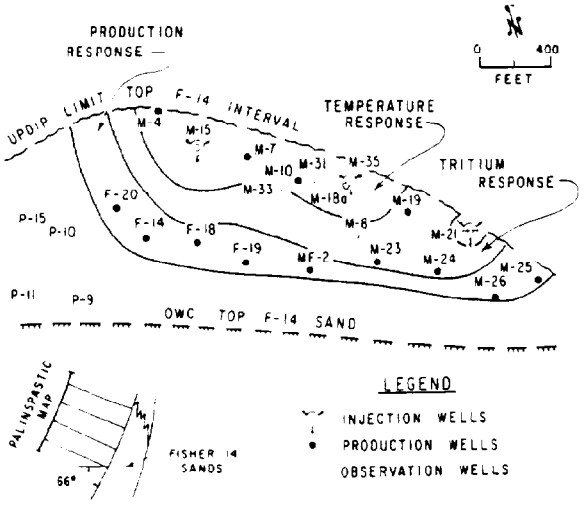

Fig. 46.19—Well locations and area of temperature, tritium, and production responses, Brea field, CA.

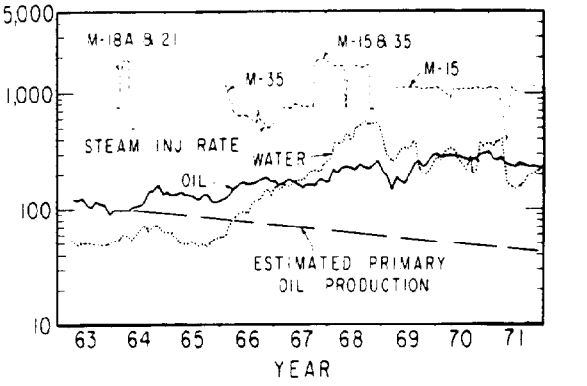

Fig. 46.20—Injection and production history, Brea steam distillation pilot.

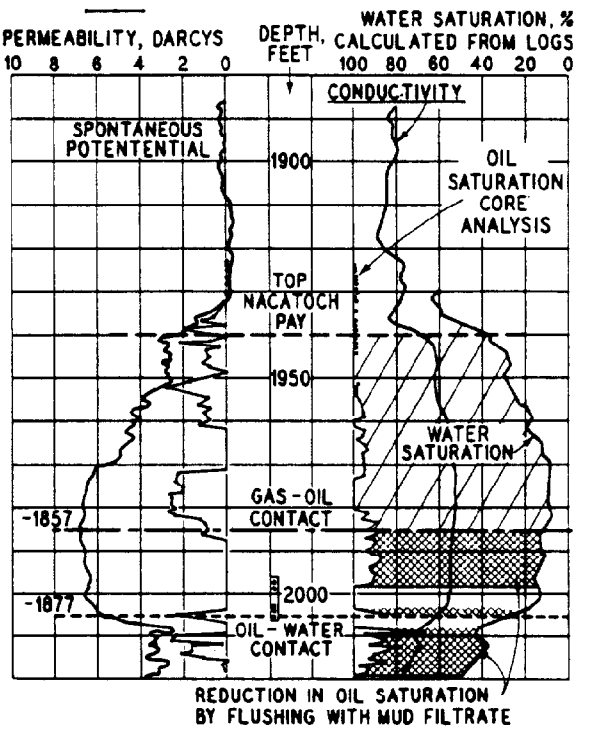

Fig. 46.21—Log and coregraph, Sidum Well W-35, Smackover field, AR.

Fig. 46.22 is a map of the 10-acre five-spot pilot, which was later expanded to a 22-acre nine-spot pattern by adding four more producers. As shown in Fig. 46.23, steam injection started in Nov. 1964 and stopped in Oct. 1965. The oil production continued long after steam injection stopped. As of Aug. 1970, the additional oil produced by steamflood was 207,000 bbl. With total steam injection of 860,000 bbl, the cumulative SOR was 4.14 bbl/bbl.

The temperature log in Fig. 46.24 shows that steam goes to the gas cap. It can be concluded that the increase in oil production was not caused by frontal displacement. Rather, the oil zone temperature increased because of conduction and convection from the gas cap, thus reducing the oil viscosity and increasing the oil production.

TABLE 46.21—RESERVOIR ROCK AND FLUID PROPERTY DATA, SMACKOVER FIELD, AR

Depth, ft	1,920
Thickness, ft	
Gross	130
Net	25
Dip, degrees	0 to 5
Porosity, %	35
Permeability, md	2,000
Oil gravity, °API	20
Reservoir temperature, °F	110
Reservoir pressure at start, psia	5
Oil viscosity, cp	
60°F	180
110°F	75
Saturation at start, %	
Oil	50
Water	50

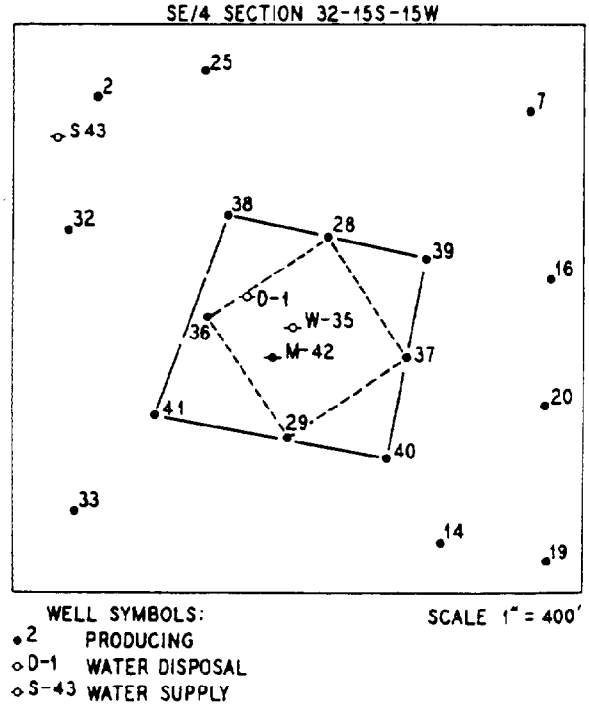

Fig. 46.22—Sidum steam injection pilot, Smackover field.

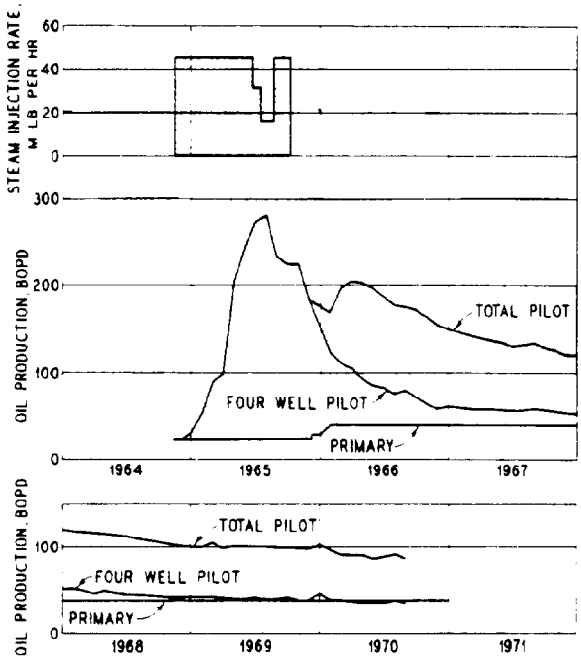

Fig. 46.23—Injection and production history, Sidum steam injection pilot, Smackover field.

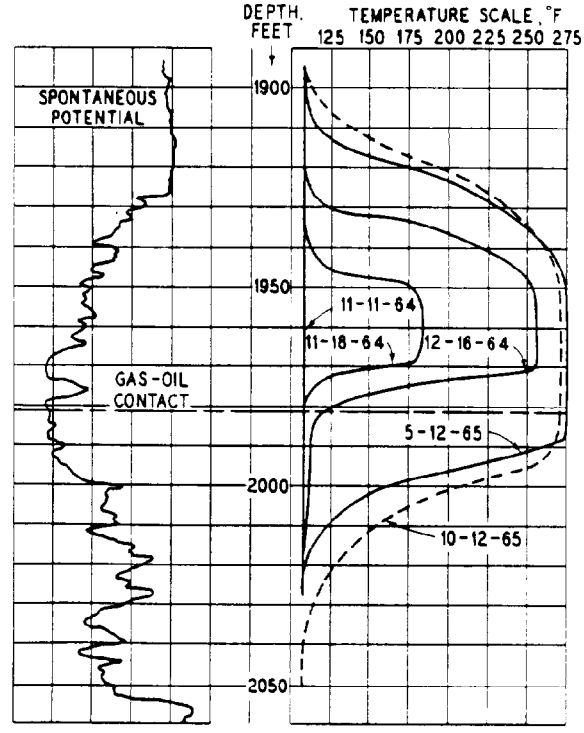

Fig. 46.24—Temperature log, Sidum Well W-42, Smackover field.

Slocum, TX (Shell)[89,90]—Reservoir With Water Sand. The Slocum field is located in southern Anderson County in northeast Texas. The steamflood project interests us since it is conducted in an oil reservoir underlain by a water sand, as shown in the type log (Fig. 46.25). The reservoir properties are given in Table 46.22.

The field was discovered in 1955. Only about 1% of OOIP was produced by primary operation. A small steamflood pilot using a ¼-acre normal five-spot pattern showed encouraging results. A full-scale seven-pattern project was initiated in 1966–67, with 5.65-acre, 13-spot patterns (Fig. 46.26).

Both injectors and producers were completed a few feet into the water sand. Steam moves horizontally through the water layer, rises vertically into the oil layer, and displaces oil that had been heated and mobilized. The oil then falls down and subsequently is swept toward the producers. The injection and production history is shown in Fig. 46.27.

Street Ranch, TX (Conoco)[151]—Extremely Viscous Tar, Fracture-Assisted Steamflood. The Street Ranch pilot was conducted in the San Miguel-4 tar sand reservoir located in Maverick County, TX. This pilot proved the technical feasibility of the fracture-assisted steamflood technology (FAST) in recovering extremely viscous heavy oils and tars. The reservoir properties are given in Table 46.23. The pilot used a 5-acre inverted five-spot pattern. The four producers were fractured horizontally with cold water, steam stimulated, perforated, and resteamed. The injector then was fractured horizontally to establish communication with the producers. The pilot consisted of three

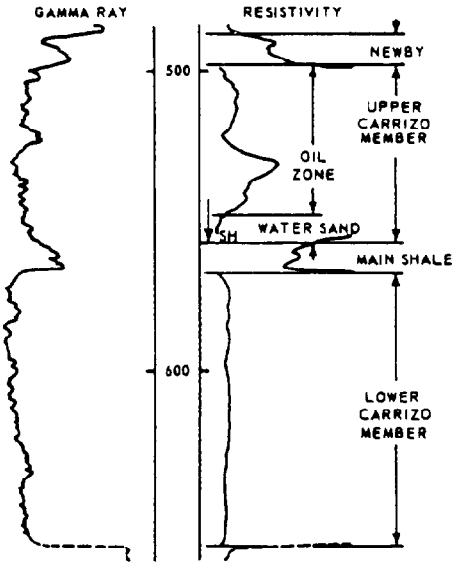

Fig. 46.25—Type log, Slocum field, TX.

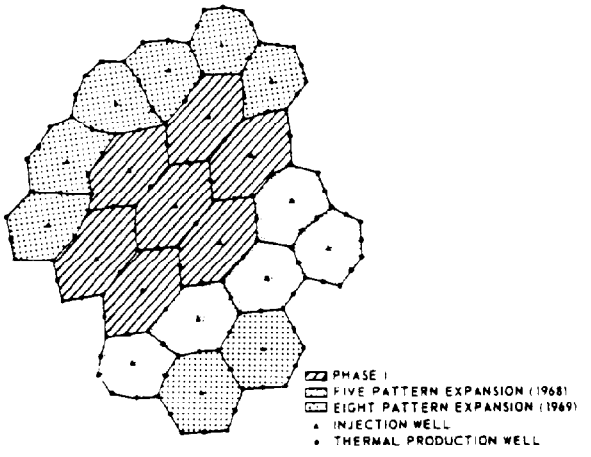

Fig. 46.26—Slocum thermal recovery project.

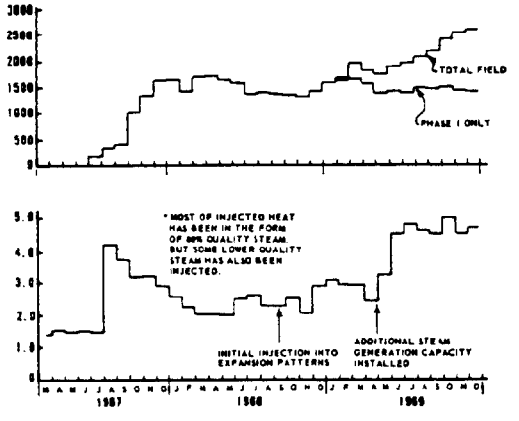

Fig. 46.27—Injection and production history, Slocum thermal recovery project.

TABLE 46.22—RESERVOIR ROCK AND FLUID PROPERTY DATA, SLOCUM FIELD, TX

Depth, ft	520
Thickness, ft	
Gross	34
Net	32
Dip, degrees	0 to 5
Porosity, %	34
Permeability, md	>2,000
Oil gravity, °API	18 to 19
Reservoir temperature, °F	80
Initial reservoir pressure, psig	110
Oil viscosity, cp	
60°F	1,000 to 3,000
400°F	3 to 7
Oil saturation at start, %	68

phases: (1) fracture preheat, (2) matrix steam injection, and (3) heat scavenging with water injection. The tar production and steam/tar ratio during the 31-month history are shown in Figs. 46.28 and 46.29, respectively. The average tar production rate was 185 B/D and the cumulative steam/tar ratio was 10.9 bbl/bbl. Postpilot core holes showed residual tar saturations as low as 8% and an average recovery efficiency of 66%.

Lacq Supérieur, France (Elf Aquitaine)[152]—Carbonate Reservoir. The Lacq Supérieur field is on the north side of the Pyrenees Mts. in southwest France. The steamflood pilot is unique because it was conducted in a carbonated, dolomitized, and highly fractured reservoir. The reservoir properties are given in Table 46.24.

The pilot was located in the central part of the fractured limestone zone, near the top of an anticline. The pattern area is 35 acres, defined by six old producers, as shown in Fig. 46.30. The injector was the only one drilled for the pilot. Steam injection started in Oct. 1977. Oil production started to increase, only 3 months after steam injection began. The production history is shown in Fig. 46.31. By June 1980, incremental oil production amounted to 176,000 bbl with a cumulative steam injection of 926,000 bbl. The cumulative SOR is 5.26 bbl/bbl. This

TABLE 46.23—RESERVOIR ROCK AND FLUID PROPERTY DATA, STREET RANCH PILOT, TX

Depth, ft	1,500
Thickness, ft	
Gross	52
Net	40.5
Dip, degrees	2
Porosity, %	26.5 and 27.5
Permeability, md	250 to 1,000
Tar gravity, °API	−2.0
Reservoir temperature, °F	95
Tar viscosity at 95°F, cp (est.)	20,000,000
Tar kinematic viscosity, cSt	
175°F	520,000
200°F	61,000
250°F	2,900
300°F	870
Pour point, °F	170 to 180
Total sulfur, wt%	9.5 to 11.0
Initial boiling point, °F	500
Tar saturation at start, %	54.7 and 38.9

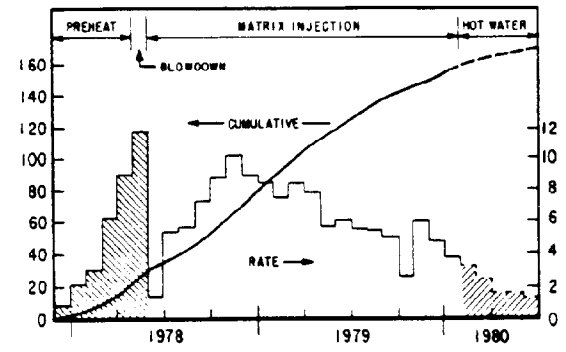

Fig. 46.28—Tar production history, Street Ranch pilot, TX.

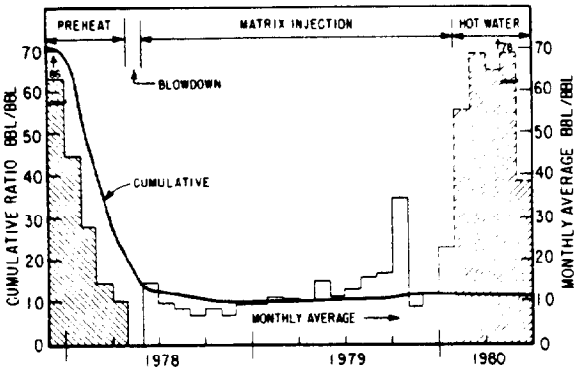

Fig. 46.29—Steam/tar ratios, Street Ranch pilot.

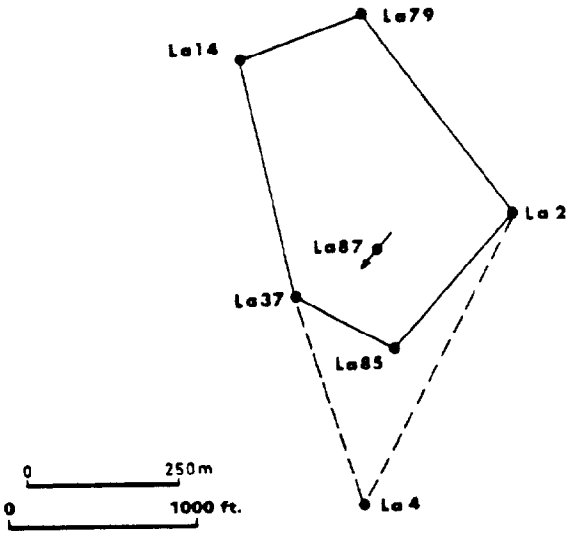

Fig. 46.30—Pilot area, Lacq Supérieur field, France.

TABLE 46.24—RESERVOIR ROCK AND FLUID PROPERTY DATA, LACQ SUPERIEUR FIELD, FRANCE

Depth, ft	1,970 to 2,300
Thickness, ft	400
Oil gravity, °API	21.5
Reservoir temperature, °F	140
Reservoir pressure, psi	870
Oil viscosity at 140°F, cp	17.5

	Matrix Blocks	Fissure Network
Porosity, %	12	0.5
Permeability, md	1	5,000 to 10,000
Water saturation at start, %	60	100

pilot showed that a strongly fissured reservoir can be exploited efficiently by the steamflood process, as if it were a homogeneous reservoir. The dissociation of the carbonate rocks by steam apparently produced no unfavorable effects. Rather, the CO_2 evolved might have some positive effect on the process efficiency.

Fireflood Projects

Suplacu de Barcau, Romania (IFP-ICPP)[120]—Largest Fireflood. The Suplacu de Barcau field lies in northwestern Romania. This is reportedly the largest fireflood project in the world, producing nearly 6,563 B/D of 15.9°API oil. The reservoir properties are given in Table 46.25.

The project started with a pilot in 1964 using a 1.24-acre inverted five-spot pattern that was later expanded into a 4.94-acre inverted nine-spot pattern. This was followed by a semicommercial operation in the period 1967–71 with eight 9.88-acre inverted nine-spot patterns. This operation further expanded into full commercial operation, first retaining the nine-spot patterns with the same spacing, and later changing to linedrive operation. The original pilot and later expansions are shown in Fig. 46.32. Injection wells numbered 38 in 1979 with 20 using alternate air and water injection and the balance using straight air. The production history is given in Fig. 46.33. The WAR was 0.089 to 0.178 bbl/10^3 scf. As of 1979, the air injection rate was $63{,}600\times10^3$ scf/D. With an oil rate of 6,563 B/D, the AOR was estimated to be 9.7×10^3 scf/bbl.

West Heidelberg, MS (Gulf)[114,115]—Deepest Fireflood. The West Heidelberg field is located in Jasper County in eastern Mississippi. With a depth exceeding 2 miles, it is the deepest fireflood project, or the deepest thermal project, for that matter. The Cotton Valley formation has eight sands. The fireflood was conducted in Sand No. 5. The reservoir properties are given in Table 46.26.

As shown in the structure map of Sand No. 5 (Fig. 46.34), only one injector was used, near the top of the structure, with seven producers located downdip. The injection and production history is given in Fig. 46.35. It can be estimated from this figure that, during the period 1973–76, the average air injection rate was about 900×10^3 scf/D whereas the average oil production rate was about 400 B/D. This gives an AOR of only 2.25×10^3 scf/bbl.

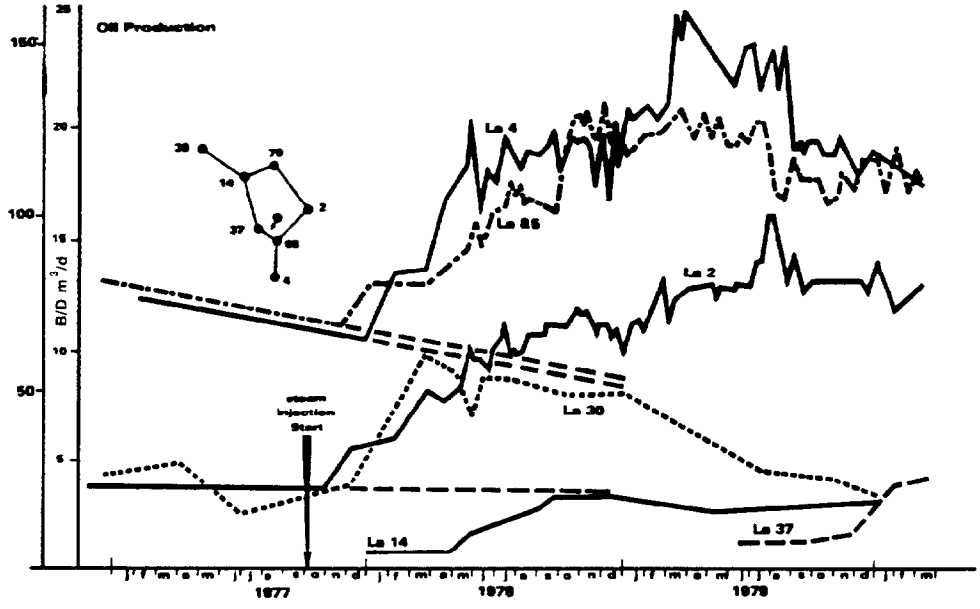

Fig. 46.31—Production history, Lacq Supérieur field.

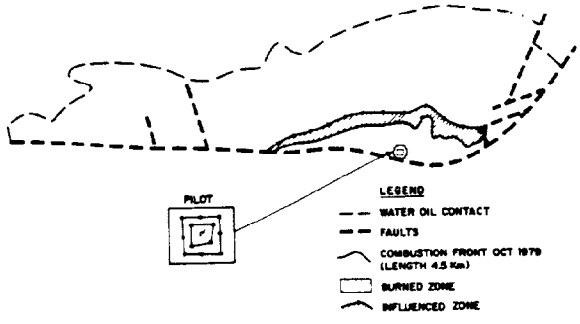

Fig. 46.32—Suplacu de Barcau field, Romania.

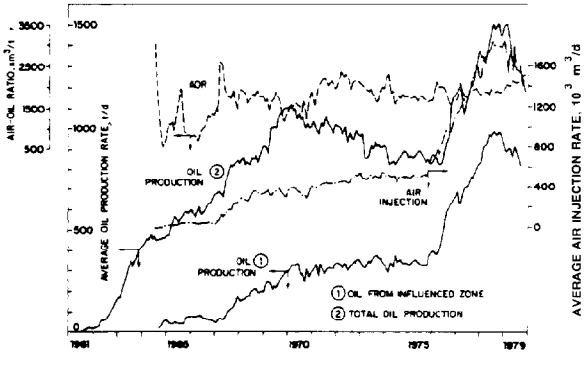

Fig. 46.33—Injection and production history, Suplacu de Barcau field.

TABLE 46.25—RESERVOIR ROCK AND FLUID PROPERTY DATA, SUPLACU DE BARCAU FIELD, ROMANIA

Depth, ft	164 to 656
Net thickness, ft	32.8
Porosity, %	32
Permeability, md	1,722
Oil gravity, °API	15.9
Reservoir temperature, °F	64
Oil viscosity at 64°F, cp	2,000
Oil saturation at start, %	85

TABLE 46.26—RESERVOIR ROCK AND FLUID PROPERTY DATA, WEST HEIDELBERG FIELD, MS

Depth, ft	11,500
Thickness, ft	
Gross	20 to 40
Net	30
Dip, degrees	5 to 15
Porosity, %	16.4
Permeability, md	39
Oil gravity, °API	24
Reservoir temperature, °F	221
Oil viscosity at 221°F, cp	4.5
Oil saturation at start, %	77.8

Gloriana, TX (Sun)[116,118]—Thinnest Reservoir Produced by a Fireflood. The Gloriana field is in Wilson County, TX. The fireflood took place in the Poth "A" Sand. It is possibly the thinnest reservoir that has ever been produced by a fireflood. The reservoir properties are given in Table 46.27.

The field originally was developed on 40-acre spacing. A new well, Well 2-8, was ignited in May 1969. Well 2-5, a producer, burned out and was converted to air injection in May 1971. These wells, along with other wells,

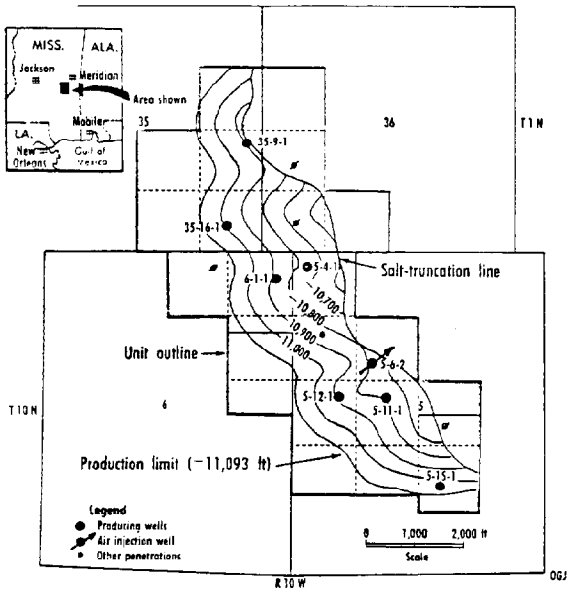

Fig. 46.34—Structure map of Sand No. 5, West Heidelberg field, MS.

are shown in the isopachous map in Fig. 46.36. The injection and production histories are given in Figs. 46.37 and 46.38, respectively. Air injection stopped in Dec. 1974 when the oil production rate declined to the economic limit.

Sloss, NE (Amoco)[77-79]—Wet Combustion, Tertiary Recovery. The Sloss field is located in Kimball County, NE. The pilot used a wet combustion process in a previously waterflooded reservoir. Here, the pay is thin and deep, the oil is light, the viscosity is low, and the oil saturation at the start of the flood was low. The reservoir properties are given in Table 46.28.

TABLE 46.27—RESERVOIR ROCK AND FLUID PROPERTY DATA, GLORIANA FIELD, TX

Depth, ft	1,600
Thickness, ft	
Gross	10
Net	4
Dip, degrees	0 to 5
Porosity, %	35
Permeability, md	1,000
Oil gravity, °API	20.8
Reservoir temperature, °F	112
Oil viscosity, cp	
112°F	70 to 150
80°F	250 to 500
Oil saturation at start, %	58.5

The fireflood started in 1967 with six 80-acre five-spots. Additional wells were included so that it covered 960 acres in its final stage. The pilot area is shown in Fig. 46.39. The injection and production data in the 4½-year period of its operation are given in Figs. 46.40 and 46.41, respectively. Between Feb. 1967 and July 1971, total air injected was $13,754\times10^6$ scf and water injected was $10,818\times10^3$ bbl, giving a WAR of 0.79 bbl/10^3 scf. The total oil production was 646,776 bbl. This gives an AOR of 21.3×10^3 scf/bbl. The areal sweep by the greater-than-350°F zone was 50%. Combining with a vertical sweep of 28%, the volumetric sweep was only 14%.

Asphalt Ridge, UT (DOE)[130]—Extremely Viscous Tar, Combination Reverse/Forward Combustion. The Northwest Asphalt Ridge deposit is located in northeast Utah, near the city of Vernal. The fireflood conducted

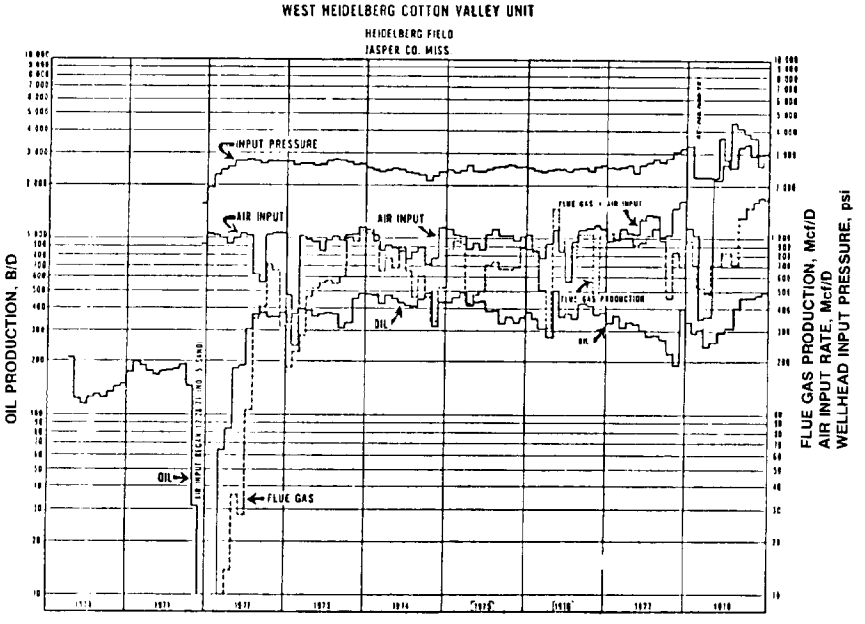

Fig. 46.35—Injection and production history, West Heidelberg field.

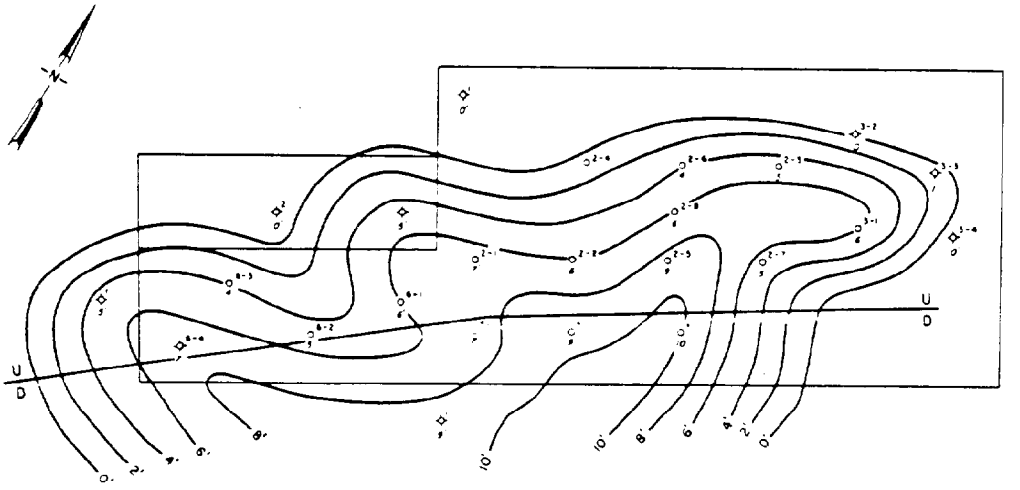

Fig. 46.36—Isopachous map, net oil, Poth "A" sand, Gloriana field, TX.

in this deposit is interesting because it attempted to use a combination of reverse and forward combustion for the recovery of oil from tar sands. The reservoir properties are given in Table 46.29.

The U.S. DOE conducted two fireflood tests in the Asphalt Ridge area. The first, conducted in 1975, demonstrated the feasibility of using reverse combustion to recover oil in the tar sand. The second tested a combination of reverse combustion and forward combustion during the period from Aug. 1977 to Feb. 1978. The location of the test sites and well arrangements are shown in Fig. 46.42. In both tests, the line drive was on a small area of 120×40 ft, covering only 0.11 acres. In the second test, several echoings of reverse and forward combustion phases were noticed in the northwest area, as seen from the temperature variations at observation Well 203 (Fig. 46.43). The reverse combustion phase had an areal sweep of 95% and vertical sweep of 91%, giving a volumetric sweep of 86%. The echoing forward combustion phase had an areal sweep of 75% and vertical sweep of 44%, giving a volumetric sweep of only 33%. The produced oil was of better quality than the original bitumen, with the pour point reduced from 140 to 25°F and the amount of residue lowered from 62 to 35 wt%.

Forest Hill, TX (Air Products-Greenwich)[153]—Oxygen-Enriched Air. The Forest Hill field is located in Wood County, TX. The significance of the field test lies in the use of oxygen-enriched air for the fireflood. The reservoir properties are given in Table 46.30.

The field was on primary production in 1964. Air injection started in 1976. One of the air injectors was switched to oxygen-enriched air in 1980. The test site is shown in Fig. 46.44. As seen in Fig. 46.45, during a 2-year period, the oxygen concentration in the injected gas ranged from 21 to 90%. The test showed that essentially pure oxygen can be handled and injected safely in a typical oilfield environment. Short of any definitive comparison, the test only hinted that using enriched air might produce oil faster than using air only.

Thermal Properties

Only some selected thermal properties of the rock/fluid systems encountered in the thermal recovery projects will be presented briefly. A more complete compilation of tables and figures has been included in Appendix B of Ref. 154.

Oil Viscosities

The viscosity-temperature relationships for representative heavy-oil deposits are shown in Fig.46.46. Oil viscosities should be measured experimentally. In the absence of experimental data, the viscosities can be estimated by charts (Fig. 46.47 to 46.49)[155-157] and equations.[158]

Beggs and Robinson[158] suggested the following equations for estimating viscosities of live oils. Dead-oil viscosity is first calculated:

$$\mu_{od}=10^{X}-1, \quad \ldots\ldots\ldots\ldots\ldots\ldots\ldots\ldots\ldots\ldots (74)$$

where μ_{od} equals the viscosity of dead oil (gas-free oil) at T, cp.

$$X=YT^{-1.163}, \quad \ldots\ldots\ldots\ldots\ldots\ldots\ldots\ldots\ldots\ldots (75)$$

$$Y=10^{Z}, \quad \ldots\ldots\ldots\ldots\ldots\ldots\ldots\ldots\ldots\ldots (76)$$

and

$$Z=3.0324-0.02023\ \gamma_o, \quad \ldots\ldots\ldots\ldots\ldots\ldots\ldots (77)$$

where γ_o equals the oil gravity, °API, and T is the temperature, °F. Live-oil viscosity is calculated next.

$$\mu=A\mu_{od}B, \quad \ldots\ldots\ldots\ldots\ldots\ldots\ldots\ldots\ldots\ldots (78)$$

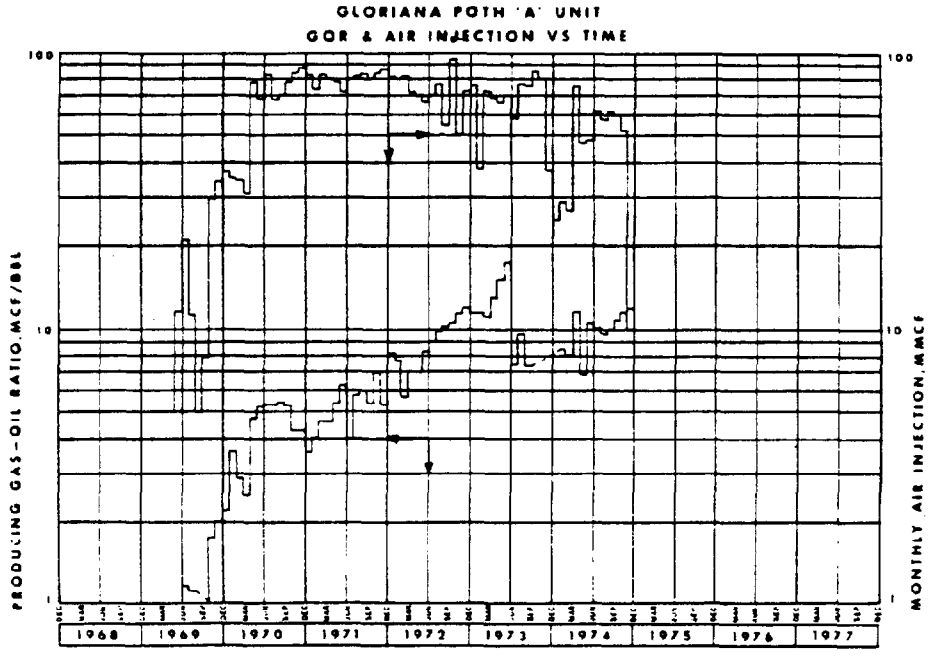

Fig. 46.37—GOR and air injection history, Gloriana field.

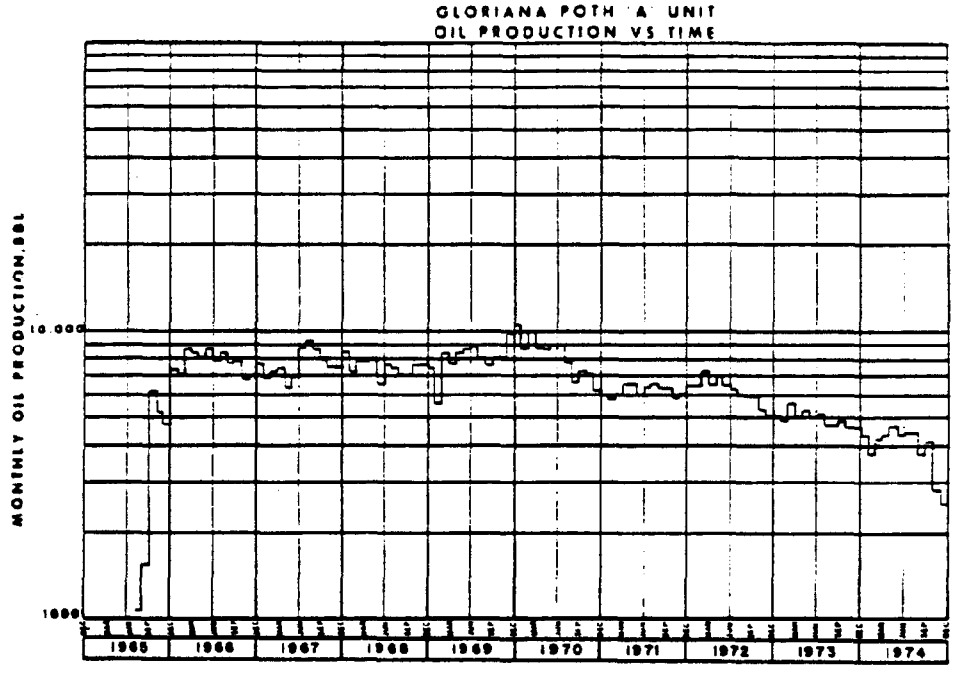

Fig. 46.38—Oil production history, Gloriana field.

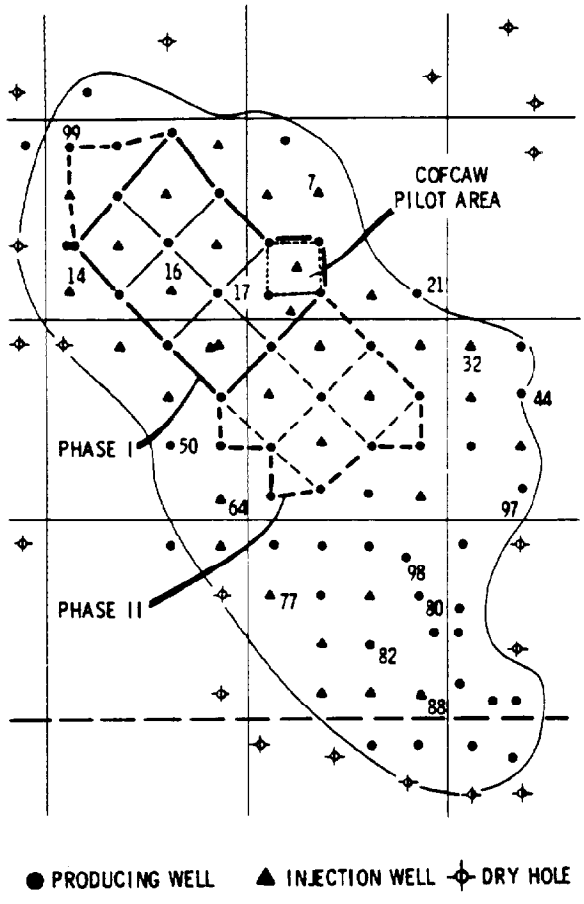

Fig. 46.39—Sloss unit, NE.

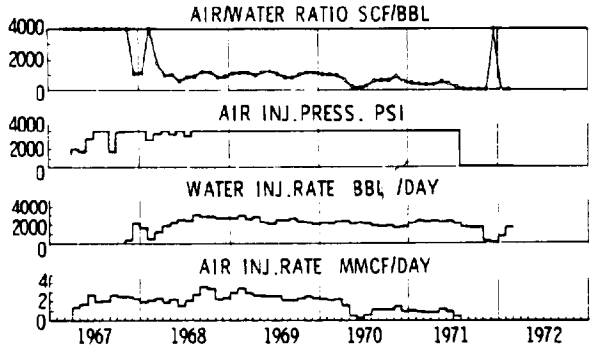

Fig. 46.40—Injection history, Sloss field COFCAW pilot.

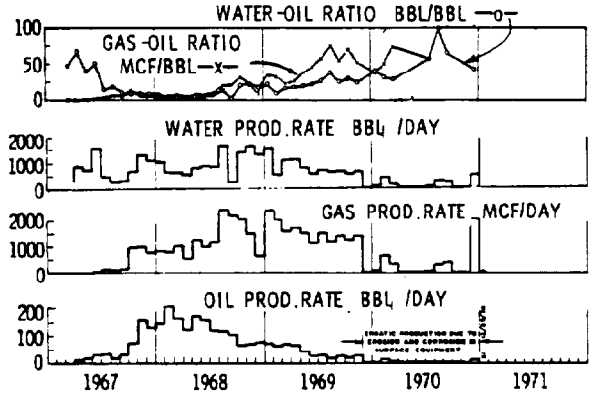

Fig. 46.41—Production history, Sloss field COFCAW pilot.

TABLE 46.28—RESERVOIR ROCK AND FLUID PROPERTY DATA, SLOSS FIELD, NE

Depth, ft	6,200
Net thickness, ft	14.3
Porosity, %	19.3
Permeability, md	191
Oil gravity, °API	38.8
Reservoir temperature, °F	200
Reservoir pressure, psig	2,274
Oil viscosity at 200°F, cp	0.8
Oil saturation at start, %	20 to 40

TABLE 46.29—RESERVOIR ROCK AND FLUID PROPERTY DATA, ASPHALT RIDGE FIELD, UT

Depth, ft	350
Net thickness, ft	13.1
Porosity, %	31.1
Permeability, md	
Saturated	85
Extracted	675
Oil gravity, °API	14
Reservoir temperature, °F	52
Oil viscosity at 60°F, cp	>1,000,000
Pour point, °F	140
Saturations at start, %	
Oil	65
Water	2.4

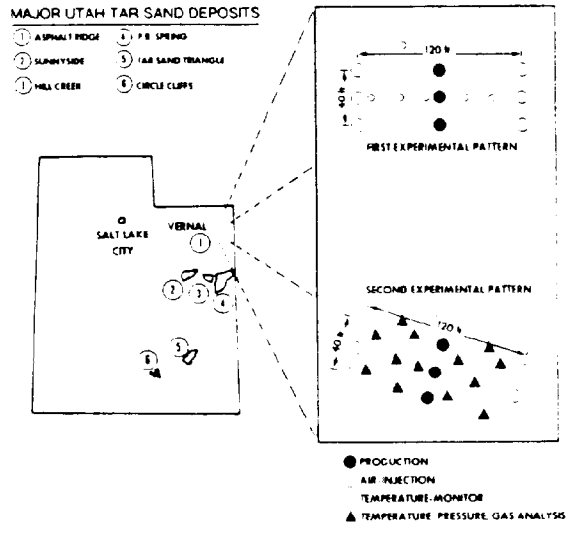

Fig. 46.42—LETC field site, Asphalt Ridge deposit, UT.

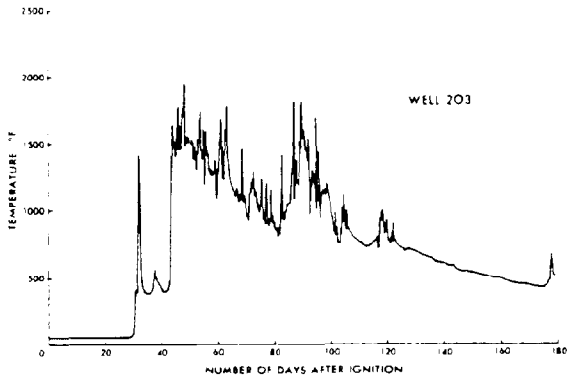

Fig. 46.43—Maximum temperature vs. time, Well 203, Asphalt Ridge deposit.

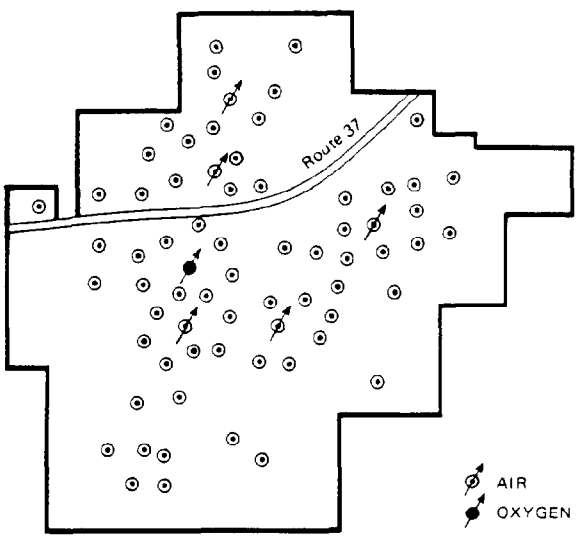

Fig. 46.44—Forest Hill field, TX.

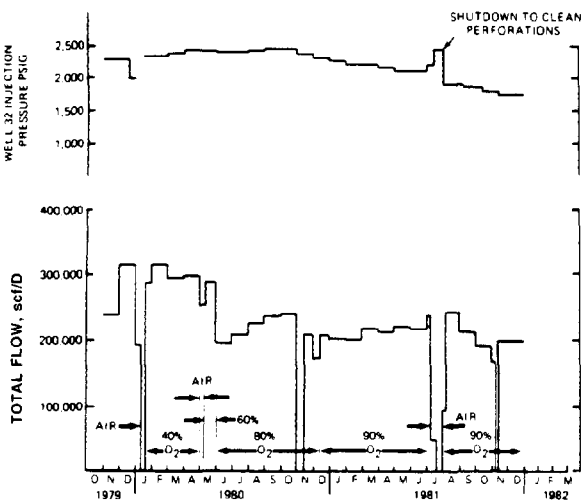

Fig. 46.45—Injection history, Well 32, Forest Hill field.

TABLE 46.30—RESERVOIR ROCK AND FLUID PROPERTY DATA, FOREST HILL FIELD, TX

Depth, ft	4,800
Net thickness, ft	15
Porosity, %	27.7
Permeability, md	626
Oil gravity, °API	10
Reservoir temperature, °F	185
Oil viscosity at 185°F, cp	1,002
Saturations at start, %	
Oil	64
Water	36

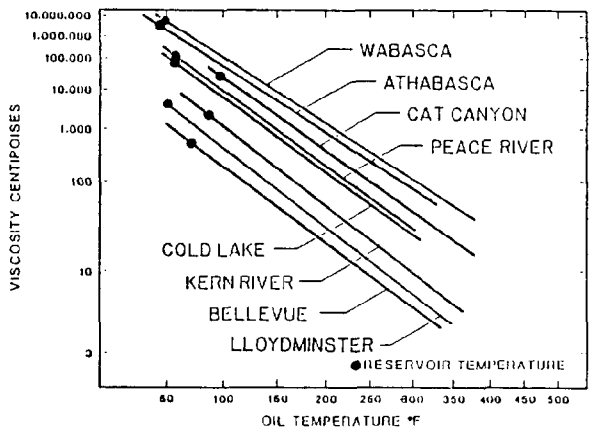

Fig. 46.46—Viscosity/temperature relationships for representative heavy oil deposits.

where

$$A=10.715(R_s+100)^{-0.515}, \quad \ldots\ldots\ldots\ldots\ldots (79)$$

$$B=5.44(R_s+150)^{-0.338}, \quad \ldots\ldots\ldots\ldots\ldots (80)$$

and R_s is the solution gas/oil ratio, scf/STB.

Relative Permeability Curves

Relative permeability data should be determined experimentally. In the absence of experimental data, the following equations may be used for rough estimation. According to Brooks and Corey,[159]

$$k_{rw}=(S_w^*)^5, \quad \ldots\ldots\ldots\ldots\ldots\ldots\ldots\ldots (81)$$

$$k_{ro}=(1-S_w^*)^2(1-S_w^{*2}), \quad \ldots\ldots\ldots\ldots\ldots\ldots (82)$$

and

$$S_w^*=\frac{S_w-S_{iw}}{1-S_{iw}}, \quad \ldots\ldots\ldots\ldots\ldots\ldots\ldots (83)$$

where S_{iw} is the irreducible water saturation, percent.

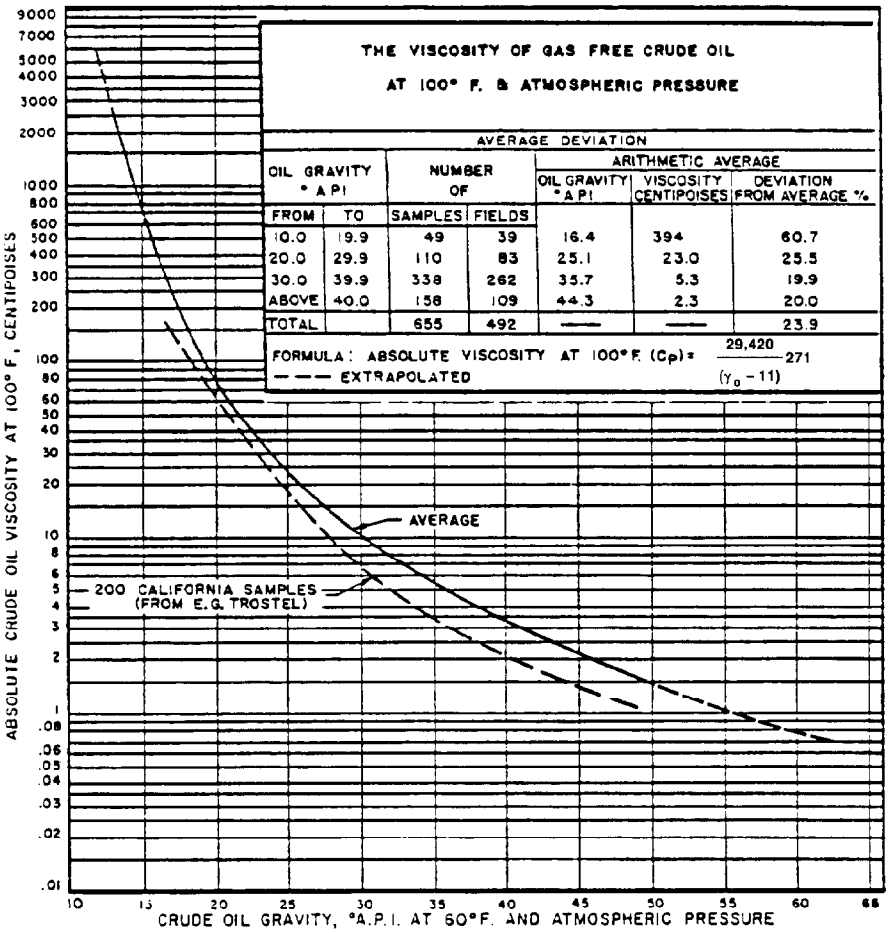

Fig. 46.47—Dead oil viscosity.

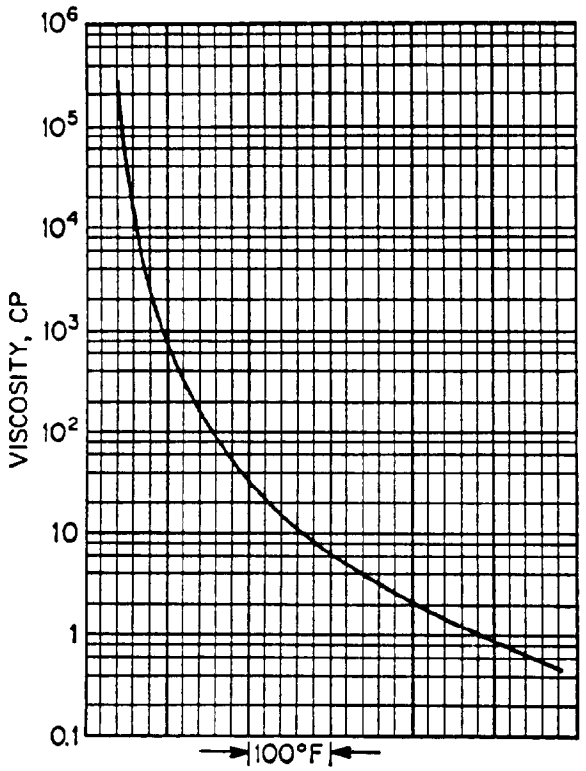

Fig. 46.48—Universal temperature/viscosity chart.

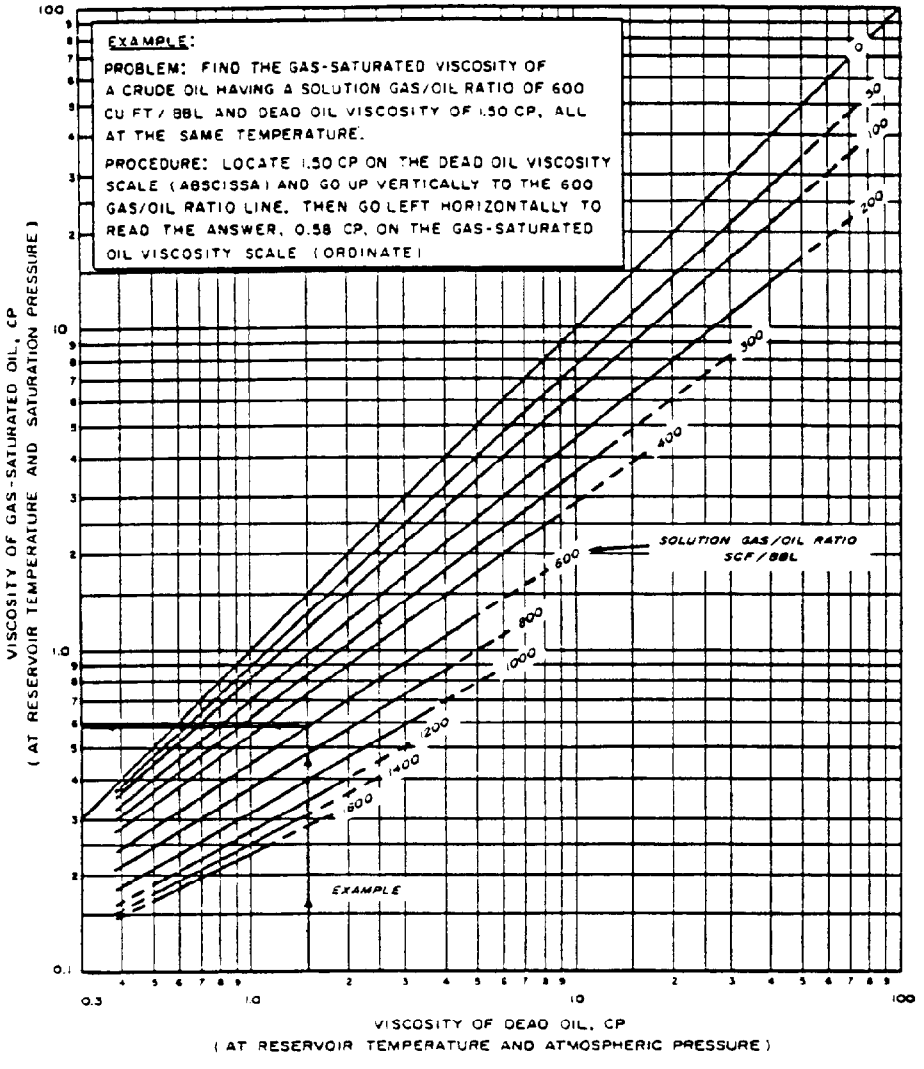

Fig. 46.49—Live oil viscosity.

According to Somerton,[160] for unconsolidated sand,

$$S_{iw}=0.211+2.0\times10^{-4}T+1.1\times10^{-6}T^2, \quad \ldots\ldots(84)$$

where T is the temperature, °F.

The effect of temperature on irreducible water saturation and relative permeability of unconsolidated sands has been studied by Poston *et al.*[161] Some of their results are given in Figs. 46.50 through 46.52. The effect of temperature on relative and absolute permeabilities of consolidated sandstones has been studied by Weinbrandt *et al.*[162] Some of their results are given in Figs. 46.53 through 46.56.

PV Compressibility

The compressibility of unconsolidated, Arkosic sands was measured by Sawabini *et al.*[163] Fig. 46.57 shows that the effective PV compressibility lies in the range between 10^{-4} and 10^{-3} psi^{-1}, about 2 to 3 orders of magnitude higher than the normally accepted figure of 10^{-6} psi^{-1} for consolidated sandstones. In Fig. 46.57, p_{to} is the total overburden pressure, psi, and p_p is the pore pressure, psi.

Thermal Conductivity

Thermal behavior of unconsolidated oil sands was studied by Somerton *et al.*[164] Fig. 46.58 shows how thermal conductivity of Kern River oil sands varies with brine saturation.

Vaporization Equilibrium

Vaporization equilibrium of an oil fraction is described by the equilibrium vaporization constant, K, which is defined as

$$K=\frac{y}{x}, \quad \ldots\ldots(85)$$

where y is the mol fraction in vapor phase and x is the mol fraction in liquid phase.

Poettmann and Mayland[165] in 1949 published a series of charts on equilibrium constants of various oil fractions with normal boiling points of 300°F, 400°F, etc., up to 1,000°F. To illustrate how K values vary with temperature and pressure, the figure for normal boiling point=500°F is shown in Fig. 46.59.

More recently, Lee *et al.*[166] presented equilibrium constants of oil fractions with 100°F boiling ranges. For example, Fraction 1 has the boiling range up to 300°F, Fraction 2 boiling between 300 and 400°F, and Fraction 6 boiling above 700°F. Figs. 46.60 and 46.61 show the effects of pressure and temperature, respectively, on the K values for these oil fractions as well as N_2, CH_4, and CO_2.

Chemical Kinetics

Chemical reactions taking place in an in-situ combustion process are considered to fall into three types: (1) low-temperature oxidation, (2) fuel deposition or coke formation, and (3) combustion. The kinetic data of these three types of reactions reported by various authors have been summarized in the paper by Fassihi *et al.*[167] and will not be reproduced here.

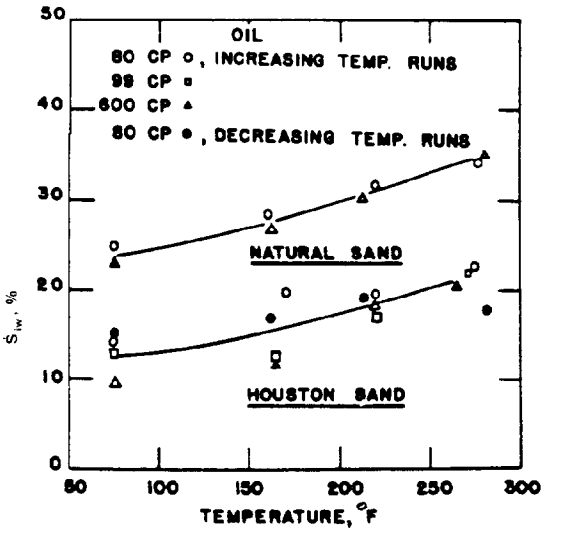

Fig. 46.50—Effect of temperature on irreducible water saturation, Houston sand, and natural sand.

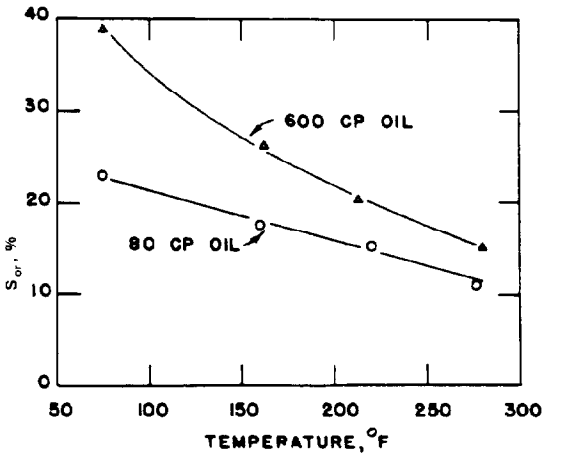

Fig. 46.51—Effect of temperature on ROS, natural sand.

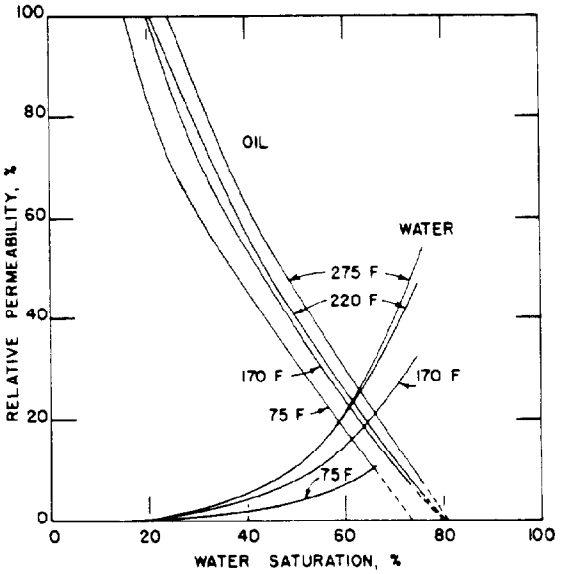

Fig. 46.52—Water and oil relative permeability at four temperatures, Houston sand, 80-cp oil.

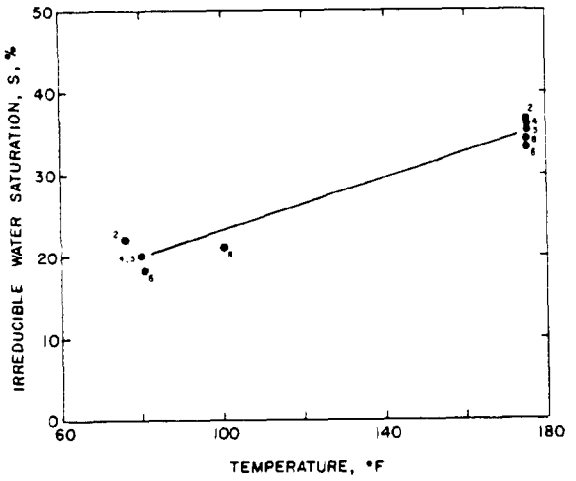

Fig. 46.53—Effect of temperature on irreducible water saturation, sandstone cores.

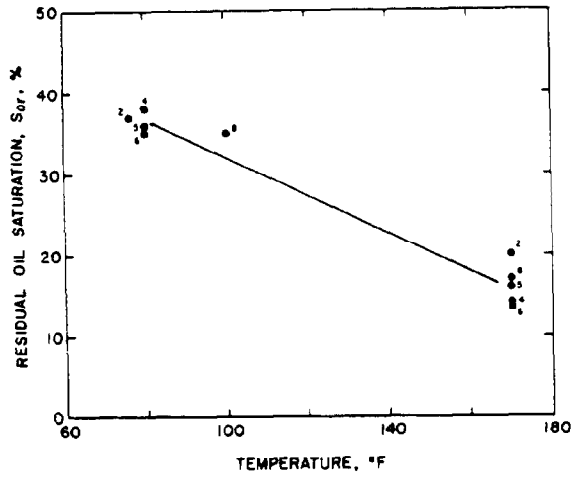

Fig. 46.54—Effect of temperature on ROS, sandstone cores.

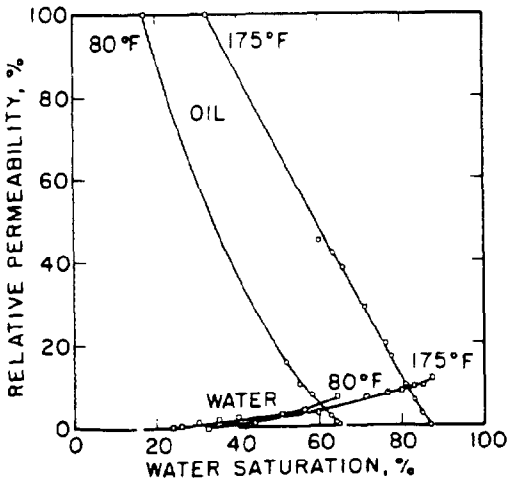

Fig. 46.55—Water and oil relative permeability at two temperatures, Core 4, Boise sandstone.

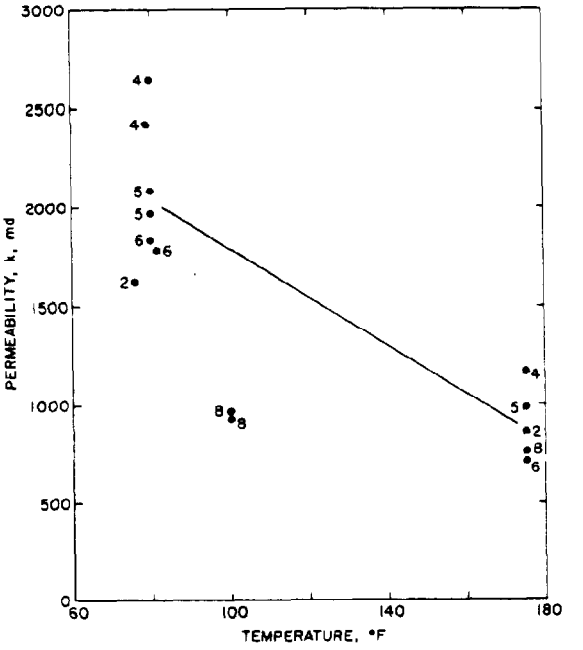

Fig. 46.56—Effect of temperature on absolute permeability, sandstone cores.

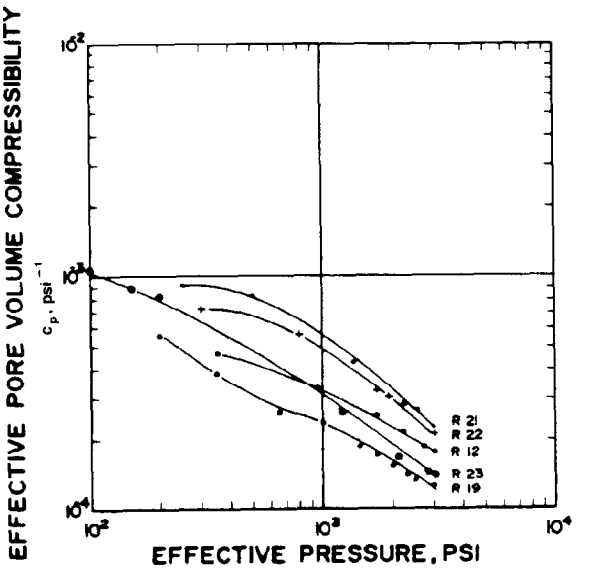

Fig. 46.57—Effective PV compressibility, unconsolidated Arkosic oil sand.

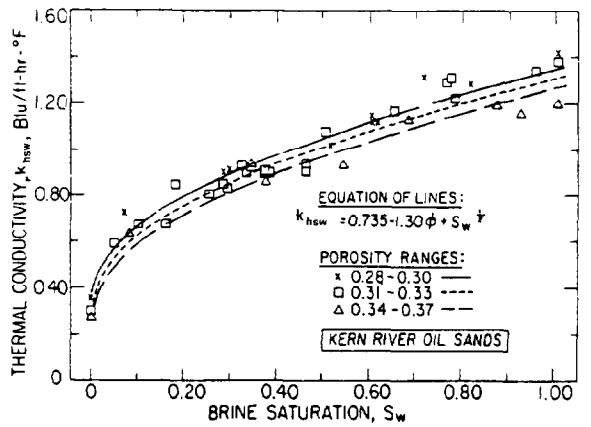

Fig. 46.58—Thermal conductivity of Kern River oil sands.

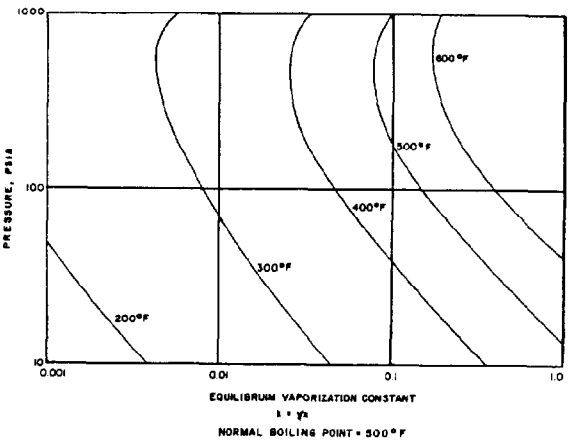

Fig. 46.59—Equilibrium vaporization constant, normal boiling point—500°F.

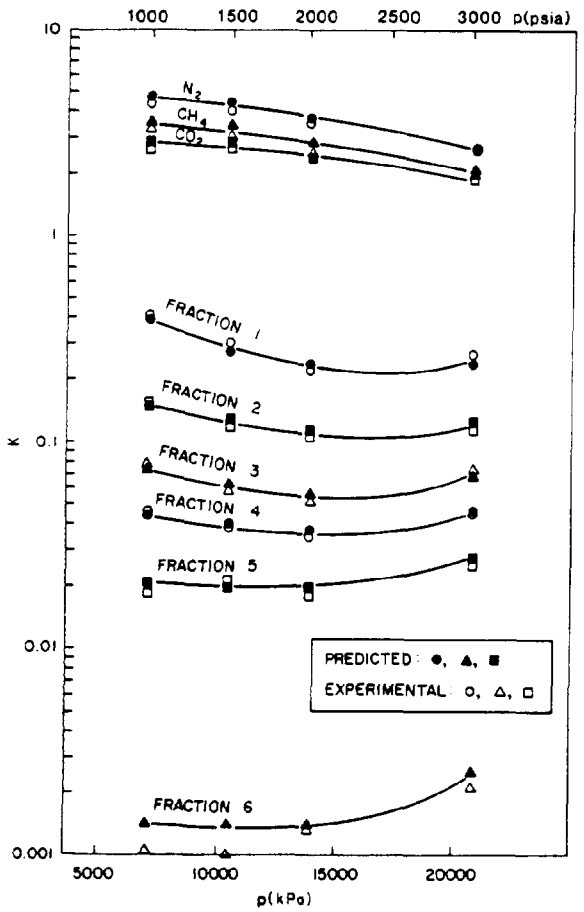

Fig. 46.60—Effect of pressure on equilibrium K values for Crude A at 260°C.

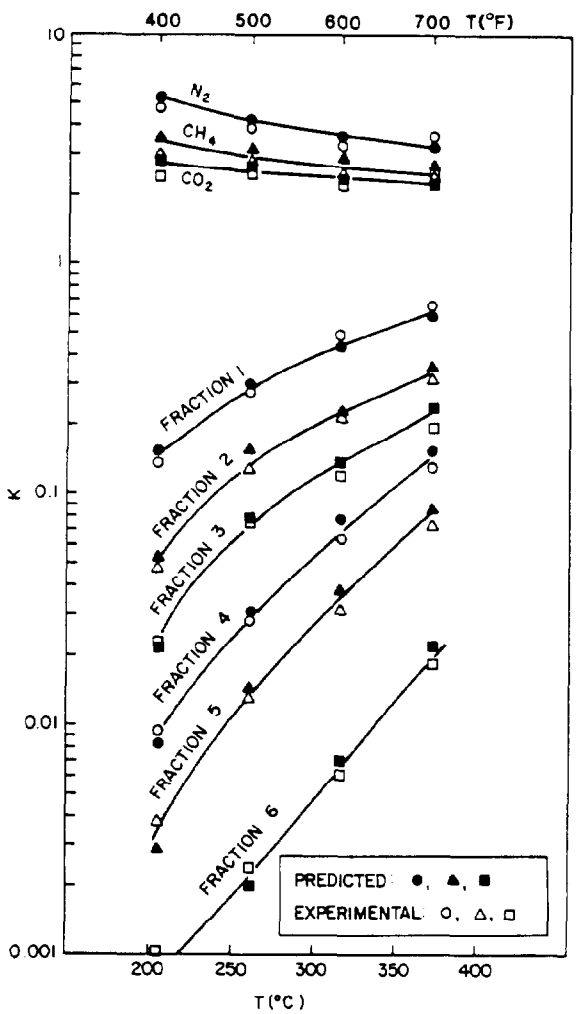

Fig. 46.61—Effect of temperature on equilibrium K values of Crude B at 1,514.7 psia.

TABLE 46.31—SATURATED STEAM TABLE

Absolute Pressure, p (psia)	Temperature T (°F)	Specific Volume, cu ft/lbm			Enthalpy, Btu/lbm		
		Saturated Liquid, v_L	Evaporate, v_{fg}	Saturated Vapor, v_g	Saturated Liquid, H_L	Evaporate, L_s	Saturated Vapor, H_g
0.08865	32.018	0.016022	3,302.4	3,302.4	0.0003	1,075.5	1,075.5
14.696	212.00	0.016719	26.782	26.799	180.17	970.3	1,150.5
50.0	281.02	0.017274	8.4967	8.5140	250.2	923.9	1,174.1
100.0	327.82	0.017740	4.4133	4.4310	298.5	888.6	1,187.2
150.0	358.43	0.01809	2.9958	3.0139	330.6	863.4	1,194.1
200.0	381.80	0.01839	2.2689	2.2873	355.5	842.8	1,198.3
250.0	400.97	0.01865	1.82452	1,84317	376.1	825.0	1,201.1
300.0	417.35	0.01889	1.52384	1.54274	394.0	808.9	1,202.9
400.0	444.60	0.01934	1.14162	1.16095	424.2	780.4	1,204.6
500.0	467.01	0.01975	0.90787	0.92762	449.5	755.1	1,204.7
600.0	486.20	0.02013	0.74962	0.76975	471.7	732.0	1,203.7
700.0	503.08	0.02050	0.63505	0.65556	491.6	710.2	1,201.8
800.0	518.21	0.02087	0.54809	0.56896	509.8	689.6	1,199.4
900.0	531.95	0.02123	0.47968	0.50091	526.7	669.7	1,196.4
1,000.0	544.58	0.02159	0.42436	0.44596	542.6	650.4	1,192.9
1,200.0	567.19	0.02232	0.34013	0.36245	571.9	613.0	1,184.8
1,400.0	587.07	0.02307	0.27871	0.30178	598.8	576.5	1,175.3
1,600.0	604.87	0.02387	0.23159	0.25545	624.2	540.3	1,164.5
1,800.0	621.02	0.02472	0.19390	0.21861	648.5	503.8	1,152.3
2,000.0	635.80	0.02565	0.16266	0.18831	672.1	466.2	1,138.3
2,200.0	649.45	0.02669	0.13603	0.16272	695.5	426.7	1,122.2
2,400.0	662.11	0.02790	0.11287	0.14076	719.0	384.8	1,103.7
2,600.0	673.91	0.02938	0.09172	0.12110	744.5	337.6	1,082.0
2,800.0	684.96	0.03134	0.07171	0.10305	770.7	285.1	1,055.8
3,000.0	695.33	0.03428	0.05073	0.08500	801.8	218.4	1,020.3
3,208.2*	705.47	0.05078	0.00000	0.05078	906.0	0.0	906.0

Steam Properties

An abbreviated steam table[168] is given in Table 46.31.

Nomenclature

a = air requirement, 10^6, scf/acre-ft
A = heated area at time t, sq ft, or quantities defined by Eqs. 9 and 79
A' = quantity defined by Eq. 13
B = quantities defined by Eqs. 10 and 80
B' = quantity defined by Eq. 14
C_m = fuel content, lbm/cu ft
C_o = heat capacity of oil, Btu/lbm-°F, or concentration of oil, lbm mol/cu ft
C_r = heat capacity of rock, Btu/lbm-°F
C_s = heat capacity of steam, Btu/lbm-°F
C_w = heat capacity of water, Btu/lbm-°F
C_{O2} = concentration of oxygen, lbm mol/cu ft
C_1 = quantity defined by Eqs. 58 and 60
C_2 = quantity defined by Eqs. 59 and 61
D = depth, ft
E = activation energy, Btu/lbm mol
E_h = thermal (heat) efficiency, fraction
E_{O2} = oxygen utilization efficiency, fraction
E_r = overall oil recovery
E_{Ru} = recovery efficiency in the unburned region, fraction
E_{vb} = volumetric sweep efficiency of the burning front, fraction
f_{s1} = steam quality at the beginning of the pipe segment, fraction
f_{s2} = steam quality at the end of the pipe segment, fraction
$f(t)$ = transient heat conduction time function for earth, dimensionless
F_{ao} = AOR
F_{cc} = CO_2/CO ratio in produced gas
F_{HC} = atomic H/C ratio
F_J = ratio of stimulated to unstimulated productivity indices, dimensionless
F_{so} = steam/oil ratio, STB/STB
F_{wor} = total produced WOR, STB/STB
h = pay thickness, ft, or convection heat transfer coefficient, Btu/hr-sq ft-°F
h' = convection heat transfer coefficient based on insulation outside surface, Btu/hr-sq ft-°F
h_f = enthalpy of liquid water at T above 32°F, Btu/lbm
h_t = total thickness of all sands, ft
H_{og} = enthalpy of oil and gas Btu/lbm
H_w = enthalpy of water carried by oil based on a STB of oil, Btu/STB oil
H_{wR} = enthalpy of water at reservoir temperature, Btu/lbm
H_{ws} = enthalpy of water at steam temperature, Btu/lbm
i_{at} = cumulative air injection, 10^3 scf
i_s = steam injection rate, B/D
I = radiation heat transfer coefficient, Btu/hr-sq ft-°F

I' = radiation heat transfer coefficient based on insulation outside surface, Btu/hr-sq ft-°F
J_c = unstimulated (cold) productivity index, STB/D-psi
k = absolute permeability, md
k' = pre-exponential factor
k_{hca} = thermal conductivity of the casing material, Btu/hr-sq ft-°F
k_{hce} = thermal conductivity of the cement, Btu/hr-ft-°F
k_{hf} = thermal conductivity of the formation, Btu/D-ft-°F
k_{hin} = thermal conductivity of insulation material, Btu/hr-ft-°F
k_{ho} = overburden thermal conducitivity, Btu/hr-ft-°F
k_{ro} = relative permeability to oil, fraction
k_{rw} = relative permeability to water, fraction
K = equilibrium vaporization constant
L = pipe length, ft
L_s = latent heat of steam, Btu/lbm
L_{v1} = latent heat of vaporization at top of interval, Btu/lbm
L_{v2} = latent heat of vaporization at bottom of interval, Btu/lbm
m_{stt} = total mass of steam injected, lbm
M = volumetric heat capacity, Btu/cu ft-°F
N = OOIP, bbl
N_s = number of sands
N_{sp} = oil in place at start of project, bbl
ΔN_{sp} = cumulative incremental oil production, bbl
p_e = static formation pressure at external radius, psia
p_p = pore pressure, psi
p_s = saturated vapor pressure of water at $\bar{T}$, psia
p_{to} = total overburden pressure, psi
p_w = bottomhole pressure, psia
p_1 = pressure at top of interval, psia
p_2 = pressure at bottom of interval, psia
Δp = frictional pressure drop over interval, psia
q_o = oil displacement rate, B/D
q_{oc} = cold oil production rate, B/D
q_{oh} = hot oil production rate, B/D
Q_{hz} = heat remaining in heated zone, Btu
Q_{it} = total heat injection, Btu
Q_{ri} = heat injection rate, Btu/hr
Q_{rl} = heat loss along the segment, Btu/hr
Q_{rt} = heat removal rate at time t, Btu/D
r_{cf} = radius to cement/formation interface, ft
r_{ci} = inside radius of casing, ft
r_{co} = outside radius of casing, ft
r_e = external radius, ft
r_h = radius of region originally heated, ft
r_{in} = outside radius of insulation surface, ft
r_{ti} = inside radius of tubing, ft
r_{to} = outside radius of pipe, ft
r_w = well radius, ft
R = gas constant
R_s = solution GOR, scf/STB
R_t = total produced GOR, scf/STB
S_g = gas saturation, fraction
S_{io} = irreducible oil saturation, fraction
S_{iw} = irreducible water saturation, percent
S_o = oil saturation at start, fraction
S_{oi} = initial oil saturation, fraction
S_{wi} = initial water saturation, fraction
S_w^* = normalized water saturation, fraction
t = time since injection, hours
t_c = critical time, hours
t_D = dimensionless time
t_i = time of injection for the current cycle, days
$\bar{T}$ = average temperature of the heated region, $r_w < r < r_h$, at any time t, °F
T_{at} = atmospheric temperature, °F
T_{cf} = temperature at cement/formation interface, °F
T_{ci} = temperature at casing inside surface, °F
T_{fi} = initial formation temperature, °F
T_{fl} = temperature of fluid, °F
T_{inj} = injection temperature, °F
T_R = original reservoir temperature, °F
T_s = steam temperature, °F
T_{su} = formation temperature at ground surface, °F
U_{co} = overall heat transfer coefficient based on outside casing surface, Btu/hr-sq ft-°F
U_{ti} = overall heat transfer coefficient based on inside radius of pipe or tubing, Btu/hr-sq ft-°F
U_{to} = overall heat transfer coefficient based on outside tubing surface, Btu/D-sq ft-°F
v_t = specific volume of total fluid, cu ft/lbm
v_w = wind velocity, mile/hr
V_{fb} = fuel burned, bbl
V_r, V_z = unit solution for component conduction problems in the r and z directions*
$\bar{V}_r, \bar{V}_z$ = average values of V_r and V_z for $0 < r < r_h$
w = Arrhenius reaction rate
w_s = mass rate of steam, lbm/hr
x = mole fraction in liquid phase
X = quantity defined by Eq. 66
y = mole fraction in vapor phase
Y = quantity defined by Eq. 65
α = thermal diffusivity, sq ft/D
α_o = overburnden thermal diffusivity, sq ft/D

*These symbols have no physical connotation. They are simply mathematical symbols.

β = dummy variable in Eq. 27
δ = energy removed with the produced fluids, dimensionless
Θ = dip angle, degrees
μ_o = oil viscosity, cp
μ_{oc} = cold oil viscosity, cp
μ_{od} = viscosity of dead oil (gas-free oil) at T, cp
μ_{oh} = hot oil viscosity, cp
ρ_o, ρ_r, ρ_w = density of oil, rock grain, and water, lbm/cu ft
ϕ = porosity, fraction

Key Equations in SI Units

$$h = 7.165 v_w^{0.6} / r_{in}^{0.4}. \quad \ldots\ldots\ldots\ldots\ldots\ldots (3)$$

$$p_2 = p_1 + 7.816 \times 10^{-12} (v_{t1} - v_{t2}) \frac{w_s^2}{r_{ti}^4} + 9.806 \times 10^{-3} \frac{\Delta D}{v_{t1}} - \Delta p. \quad \ldots\ldots\ldots\ldots\ldots\ldots (20)$$

$$F_{so}^* = \frac{Q_s t}{Ah\phi(S_{oi} - S_{io})}. \quad \ldots\ldots\ldots\ldots\ldots\ldots (30)$$

$$q_{oc} = \frac{0.0005427 k k_{ro} h}{\mu_{oc} \ln \frac{r_e}{r_w}} (p_e - p_w). \quad \ldots\ldots\ldots\ldots\ldots\ldots (42)$$

$$Y = 0.2639 \left[0.427 S_o - 0.004429 h - 0.3905 \left(\frac{1}{\mu_o} \right)^{0.25} \right] X, \quad \ldots\ldots\ldots\ldots\ldots\ldots (64)$$

where

$$X = \frac{i_{at} E_{O_2}}{[N_{sp}/(\phi S_o)](1-\phi)}.$$

$$F_{so} \text{ (in m}^3/\text{m}^3) = 1/\left(-0.011253 + 0.00009117 D + 0.0005180 h - 0.07775 \Theta + 0.007232 \mu_o + 0.00003467 \frac{kh}{\mu_o} + 0.5120 \phi S_o \right). \quad \ldots\ldots\ldots\ldots\ldots\ldots (67)$$

$$F_{so} \text{ (in m}^3/\text{m}^3) = 18.744 + 0.004767 D - 0.16693 h - 0.89814 k - 0.5915 \mu_o - 14.79 S_o - 0.0009767 \frac{kh}{\mu_o}. \quad \ldots\ldots\ldots\ldots\ldots\ldots (68)$$

$$C_m \text{ (in kg/m}^3) = -1.9222 + 0.137695 h + 1.85029 k + 35.72 S_o + 0.012887 \frac{kh}{\mu_o} - 0.00993 D - 1.0444 \mu_o. \quad \ldots\ldots\ldots\ldots\ldots\ldots (69)$$

$$a = \frac{\left(\frac{2F_{cc}+1}{F_{cc}+1} + \frac{F_{HC}}{2} \right) C_m}{0.01776(12 + F_{HC}) E_{O_2}}. \quad \ldots\ldots\ldots\ldots\ldots\ldots (70)$$

$$a \text{ (in std m}^3/\text{m}^3) = 108.356 + 2.75367 h + 229.477 S_o + 16.073 k. \quad \ldots\ldots\ldots\ldots\ldots\ldots (71)$$

$$F_{ao} = \frac{a}{\left[\left(\phi S_o - \frac{C_m}{1{,}000} \right) E_{vb} + \phi S_o (1 - E_{vb}) E_{Ru} \right]}. \quad \ldots\ldots\ldots\ldots\ldots\ldots (72)$$

$$F_{ao} \text{ (in std m}^3/\text{m}^3) = 3820.4 + 12.97 h + 192.20 k + 471.1 \mu_o - 13671.5 \phi S_o, \quad \ldots\ldots\ldots\ldots\ldots\ldots (73)$$

where
a is in std m^3/m^3,
A is in m^2,
C_m is in kg/m^3,
D is in m,
F_{ao} is in std m^3/m^3,
F_{so} is in m^3/m^3,
F_{so}^* is in m^3/m^3,
h is in kJ/m^2·h·K (Eqs. 2 through 4),
h is in m,
i_{at} is in std m^3,
k is in μm^2,
N_{sp} is in m^3,
p's are in kPa,
q_{oc} is in m^3/d,
Q_s is in m^3/h,
r_{in} is in m,
r_{ti} is in m,
t is in h,
v_t is in m^3/kg,
v_w is in kg/h,
w_s is in kg/h,
μ_o is in Pa·s, and
μ_{oc} is in Pa·s.

References

1. Farouq Ali, S.M.: "Steam Injection," *Secondary and Tertiary Oil Recovery Processes*, Interstate Oil Compact Commission, Oklahoma City (Sept. 1974) Chap. 4.
2. McNeil, J.S. and Moss, J.T.: "Oil Recovery by In-Situ Combustion," *Pet. Eng.* (July 1958) B-29–B-42.
3. Berry, V.J. Jr. and Parrish, D.R.: "A Theoretical Analysis of Heat Flow in Reverse Combustion," *Trans.*, AIME (1960) **219**, 124–31.
4. Dietz, D.N. and Weijdema, J.: "Reverse Combustion Seldom Feasible," *Producers Monthly* (May 1968) 10.
5. Smith, F.W. and Perkins, T.K.: "Experimental and Numerical Simulation Studies of the Wet Combustion Recovery Process," *J. Cdn. Pet. Tech.* (July-Sept. 1973) 44–54.
6. Stovall, S.L.: "Recovery of Oil from Depleted Sands by Means of Dry Steam," *Oil Weekly* (Aug. 13, 1934) 17–24.
7. Grant, B.R. and Szasz, S.E.: "Development of Underground Heat Wave for Oil Recovery," *Trans.*, AIME (1954) **201**, 108–18.
8. Kuhn, C.S. and Koch, R.L.: "In-Situ Combustion—Newest Method of Increasing Oil Recovery," *Oil and Gas J.* (Aug. 10, 1953) **52**, 92–96, 113, 114.
9. Trantham, J.C. and Marx, J.W.: "Bellamy Field Tests: Oil from Tar by Counterflow Underground Burning," *J. Pet. Tech.* (Jan. 1966) 109–15; *Trans.*, AIME, **237**.
10. Giusti, L.E.: "CSV Makes Steam Soak Work in Venezuela Field," *Oil and Gas J.* (Nov. 4, 1974) 88–93.
11. Stokes, D.D. and Doscher, T.M.: "Shell Makes a Success of Steam Flood at Yorba Linda," *Oil and Gas J.* (Sept. 2, 1974) 71–76.
12. Dietz, D.N.: "Wet Underground Combustion, State-of-the-Art," *J. Pet. Tech.* (May 1970) 605–17; *Trans.*, AIME, **249**.
13. "Steam Dominates Enhanced Oil Recovery," *Oil and Gas J.* (April 5, 1982) 139–59.
14. "Experts Assess Status and Outlook for Thermal, Chemical, and CO_2 Miscible Flooding Processes," *J. Pet. Tech.* (July 1983) 1279–92.
15. Johnson, L.A. Jr. *et al.*: "An Echoing In-Situ Combustion Oil Recovery Project in the Utah Tar Sand," *J. Pet. Tech.* (Feb. 1980) 295–304.
16. *Enhanced Oil Recovery Potential in the United States*, Report by Lewin and Assocs. for Office of Technology Assessment (Jan. 1978) 40–41.
17. Willman, B.T. *et al.*: "Laboratory Studies of Oil Recovery by Steam Injection," *Trans.*, AIME (1961) **222**, 681–90.
18. McAdams, W.H.: *Heat Transmission*, third edition, McGraw-Hill Book Co. Inc., New York City (1954) 261.
19. Ramey, H.J. Jr.: "Wellbore Heat Transmission," *J. Pet. Tech.* (April 1962) 427–35.
20. Satter, A.: "Heat Losses During Flow of Steam Down a Wellbore," *J. Pet. Tech.* (July 1965) 845–51.
21. Willhite, G.P.: "Overall-All Heat Transfer Coefficients in Steam and Hot Water Injection Wells," *J. Pet. Tech.* (May 1967) 607–15.
22. Earlougher, R.C. Jr.: "Some Practical Considerations in the Design of Steam Injection Wells," *J. Pet. Tech.* (Jan. 1969) 79–86.
23. Beggs, H.D. and Brill, T.P.: "A Study of Two-Phase Flow in Inclined Pipes," *J. Pet. Tech.* (May 1973) 607–14.
24. Farouq Ali, S.M.: "A Comprehensive Wellbore Steam/Water Flow Model or Steam Injection and Geothermal Applications," *Soc. Pet. Eng. J.* (Oct. 1981) 527–34.
25. Marx, J.W. and Langenheim, R.N.: "Reservoir Heating by Hot Fluid Injection," *Trans.*, AIME (1959) **216**, 312–15.
26. Evans, J.G.: "Heat Loss During the Injection of Steam Into a 5-Spot," paper presented as term project in PNG 515, Pennsylvania State U., University Park (June 1960).
27. Ramey, H.J. Jr.: "Discussion of Reservoir Heating of Hot Fluid Injection," *Trans.*, AIME (1959) **216**, 364–65.
28. Mandl, G. and Volek, C.W.: "Heat and Mass Transport in Steam-Drive Processes," *Soc. Pet. Eng. J.* (March 1969) 59–79.
29. Myhill, N.A. and Stegemeier, G.L.: "Steam Drive Correlations and Prediction," *J. Pet. Tech.* (Feb. 1978) 173–82.
30. Neuman, C.H.: "A Gravity Override Model of Steamdrive," *J. Pet. Tech.* (Jan. 1985) 163–69.
31. Doscher, T.M. and Ghassemi, F.: "The Influence of Oil Viscosity and Thickness on the Steam Drive," *J. Pet. Tech.* (Feb. 1983) 291–98.
32. Vogel, J.V.: "Simplified Heat Calculations for Steamfloods," *J. Pet. Tech.* (July 1984) 1127–36.
33. Boberg, T.C. and Lantz, R.B.: "Calculation of the Production Rate of a Thermally Stimulated Well," *J. Pet. Tech.* (Dec. 1966) 1613–23.
34. Boberg, T.C. and West, R.C.C.: "Correlation of Steam Stimulation Performance," *J. Pet. Tech.* (Nov. 1972) 1367–68.
35. Coats, K.H. *et al.*: "Three-Dimensional Simulation of Steamflooding," *Soc. Pet. Eng. J.* (Dec. 1974) 573–92.
36. Coats, K.H.: "Simulation of Steamflooding with Distillation and Solution Gas," *Soc. Pet. Eng. J.* (Oct. 1976) 235–47.
37. Coats, K.H.: "A Highly Implicit Steamflood Model," *Soc. Pet. Eng. J.* (Oct. 1978) 369–83.
38. Crookston, R.B., Culham, W.E., and Chen, W.H.: "Numerical Simulation Model for Thermal Recovery Processes," *Soc. Pet. Eng. J.* (Feb. 1979) 37–58.
39. Youngren, G.K.: "Development and Applications of an In-Situ Combustion Reservoir Simulator," *Soc. Pet. Eng. J.* (Feb. 1980) 39–51.
40. Coats, K.H.: "In-Situ Combustion Model," *Soc. Pet. Eng. J.* (Dec. 1980) 533–54.
41. Grabowski, J.W. *et al.*: "A Fully Implicit General Purpose Finite-Difference Thermal Model for In-Situ Combustion and Steam," paper SPE 8396 presented at the 1979 SPE Annual Technical Conference and Exhibition, Las Vegas, Sept. 23–26.
42. Alexander, J.D., Martin, W.L., and Dew, J.N.: "Factors Affecting Fuel Availability and Composition During In-Situ Combustion," *J. Pet. Tech.* (Oct. 1962) 1154–64.
43. Showalter, W.E.: "Combustion-Drive Tests," *Soc. Pet. Eng. J.* (March 1963) 53–58.
44. Parrish, D.R. and Craig, F.F. Jr.: "Laboratory Study of a Combination of Forward Combustion and Waterflooding—The COFCAW Process," *J. Pet. Tech.* (June 1969) 753–61.
45. Burger, J.G. and Sahuquet, B.C.: "Laboratory Research on Wet Combustion," *J. Pet. Tech.* (Oct. 1973) 1137–46.
46. Garon, A.M. and Wygal, R.J. Jr.: "A Laboratory Investigation of Firewater Flooding," *Soc. Pet. Eng. J.* (Dec. 1974) 537–44.
47. Moss, J.T. and Cady, G.V.: "Laboratory Investigation of the Oxygen Combustion Process for Heavy Oil Recovery," paper SPE 10706 presented at the 1982 SPE California Regional Meeting, San Francisco, March 24–26.
48. Pursley, S.A.: "Experimental Simulation of Thermal Recovery Processes," *Proc.*, Heavy Oil Symposium, Maracaibo, Venezuela (1974).
49. Huygen, H.H.A.: "Laboratory Steamfloods in Half of a Five-Spot," paper SPE 6171 presented at the 1976 Annual Technical Conference and Exhibition, New Orleans, Oct. 3–6.
50. Ehrlich, R.: "Laboratory Investigation of Steam Displacement in the Wabasca Grand Rapids 'A' Sand," *Oil Sands of Canada-Venezuela 1977*, CIM (1978) Special Vol.
51. Prats, M.: "Peace River Steam Drive Scaled Model Experiments," *Oil Sands of Canada-Venzuela 1977*, CIM (1978) Special Vol.
52. Doscher, T.M. and Huang, W.: "Steam-Drive Performance Judged Quickly from Use of Physical Models," *Oil and Gas J.* (Oct. 22, 1979) 52–57.
53. Singhal, A.K.: "Physical Model Study of Inverted Seven-Spot Steamfloods in a Pool Containing Conventional Heavy Oil," *J. Cdn. Pet. Tech.* (July-Sept. 1980) 123–34.
54. Binder, G.G. *et al.*: "Scaled-Model Tests of In-Situ Combustion in Massive Unconsolidated Sands," *Proc.*, 7th World Pet. Cong., Mexico City (1967).
55. Pujol, L. and Boberg, T.C.: "Scaling Accuracy of Laboratory Steamflooding Models," paper SPE 4191 presented at the 1972 SPE California Regional Meeting, Bakersfield, Nov. 8–10.
56. Stegemeier, G.L., Laumbach, D.D., and Volek, C.W.: "Representing Steam Processes with Vacuum Models," *Soc. Pet. Eng. J.* (June 1980) 151–74.
57. Farouq Ali, S.M.: "Current Status of Steam Injection as a Heavy Oil Recovery Method," *J. Cdn. Pet. Tech.* (Jan.-March 1974) 1–15.
58. Geffen, T.M.: "Oil Production to Expect from Known Technology," *Oil and Gas J.* (May 7, 1973) 66–76.
59. Lewin and Assocs. Inc.: *The Potentials and Economics of Enhanced Oil Recovery*, Federal Energy Administration (April 1976) Report B76/221, 2–6.
60. Iyoho, A.W.: "Selecting Enhanced Oil Recovery Processes," *World Oil* (Nov. 1978) 61–64.
61. Chu, C.: "State-of-the-Art Review of Steamflood Field Projects," paper SPE 11733 presented at the 1983 SPE California Regional Meeting, Ventura, March 23–25.

62. Chu, C.: "A Study of Fireflood Field Projects," *J. Pet. Tech.* (Feb. 1977) 171-79.
63. Chu, C.: "State-of-the-Art Review of Fireflood Field Projects," *J. Pet. Tech.* (Jan. 1982) 19-36.
64. Poettmann, F.H.: "In-Situ Combustion: A Current Appraisal," *World Oil*, Part 1 (April 1964), 124-28; Part 2 (May 1964) 95-98.
65. Blevins, T.R., Aseltine, R.J., and Kirk, R.S.: "Analysis of a Steam Drive Project, Inglewood Field, California," *J. Pet. Tech.* (Sept. 1969) 1141-50.
66. Blevins, T.R. and Billingsley, R.H.: "The Ten-Pattern Steamflood, Kern River Field, California," *J. Pet. Tech.* (Dec. 1975), 1505-14; *Trans.*, AIME, **259**.
67. Oglesby, K.D. *et al.*: "Status of the Ten-Pattern Kern River Field, California," *J. Pet. Tech.* (Oct. 1982) 2251-57.
68. Bursell, C.G.: "Steam Displacement—Kern River Field," *J. Pet. Tech.* (Oct. 1970) 1225-31.
69. Bursell, C.G. and Pittman, G.M.: "Performance of Steam Displacement in the Kern River Field," *J. Pet. Tech.* (Aug. 1975) 977-1004.
70. Greaser, G.R. and Shore, R.A.: "Steamflood Performance in the Kern River Field," paper SPE 8834 presented at the 1980 SPE/DOE Symposium on Enhanced Oil Recovery, Tulsa, April 20-23.
71. McBean, W.N.: "Attic Oil Recovery by Steam Displacement," paper SPE 4170 presented at the 1972 SPE California Regional Meeting, Bakersfield, Nov. 8-10.
72. Rehkopf, B.L.: "Metson Attic Steam Drive," paper SPE 5855 presented at the 1976 SPE California Regional Meeting, Long Beach, April 8-9.
73. Hearn, C.L.: "The El Dorado Steam Drive—A Pilot Tertiary Recovery Test," *J. Pet. Tech.* (Nov. 1972) 1377-84.
74. Valleroy, V.V. *et al.*: "Deerfield Pilot Test of Oil Recovery by Steam Drive," *J. Pet. Tech.* (July 1967) 956-64.
75. van Dijk, C.: "Steam-Drive Project in the Schoonebeek Field, The Netherlands," *J. Pet. Tech.* (March 1968) 295-302.
76. Gates, C.F. and Ramey, H.J. Jr.: "Field Results of South Belridge Thermal Recovery Experiment," *Trans.*, AIME (1958) **213**, 236-44.
77. Parrish, D.R. *et al.*: "A Tertiary COFCAW Pilot Test in the Sloss Field, Nebraska," *J. Pet. Tech.* (June 1974) 667-75; *Trans.*, AIME, **257**.
78. Parrish, D.R., Pollock, C.B., and Craig, F.F. Jr.: "Evaluation of COFCAW as a Tertiary Recovery Method, Sloss Field, Nebraska," *J. Pet. Tech.* (June 1974) 676-86; *Trans.*, AIME, **257**.
79. Buxton, T.S. and Pollock, C.B.: "The Sloss COFCAW Project—Further Evaluation of Performance During and After Air Injection," *J. Pet. Tech.* (Dec. 1974) 1439-48; *Trans.*, AIME, **257**.
80. Moss, J.T., White, P.D., and McNeil, J.S.: "In-Situ Combustion Process—Results of a Five-Well Field Experiment in Southern Oklahoma," *Trans.*, AIME (1959) **216**, 55-64.
81. Parrish, D.R. *et al.*: "Underground Combustion in the Shannon Pool, Wyoming," *J. Pet. Tech.* (Feb. 1962) 197-205; *Trans.*, AIME, **225**.
82. Smith, R.V. *et al.*: "Recovery of Oil by Steam Injection in the Smackover Field, Arkansas," *J. Pet. Tech.* (Aug. 1973) 833-89.
83. "Smackover Field," *Improved Oil Recovery Field Reports* (1975) **1**, No. 1, 135-43; *Enhanced Oil Recovery Field Reports*, SPE, Richardson, TX (1982) **8**, No. 1, 685-88.
84. "Kern River Field, Standard Oil Company of California," *Improved Oil Recovery Field Reports*, SPE, Richardson, TX (1975) **1**, No. 1, 83-92; *Enhanced Oil Recovery Field Reports*, SPE, Richardson, TX (1980) **6**, No. 1, 23-24.
85. "Midway-Sunset Field, Chanslor-Western Oil and Development Company," *Improved Oil Recovery Field Reports*, SPE, Richardson, TX (1976) **2**, No. 3, 445-54; *Enhanced Oil Recovery Field Reports*, SPE, Richardson, TX (1982) **8**, No. 1, 729-32.
86. Stokes, D.D. *et al.*: "Steam Drive as a Supplemental Recovery Process in an Intermediate Viscosity Reservoir, Mount Poso Field, California," *J. Pet. Tech.* (Jan. 1978) 125-31.
87. "Mount Poso Field," *Improved Oil Recovery Field Reports*, SPE, Richardson, TX (1975) **1**, No. 2, 277-86; *Enhanced Oil Recovery Field Reports*, SPE, Richardson, TX (1982) **8**, No. 1, 701-03.
88. Traverse, E.F., Deibert, A.D., and Sustek, A.J.: "San Ardo—A Case History of a Successful Steamflood," paper SPE 11737 presented at the 1983 SPE California Regional Meeting, Ventura, March 23-25.
89. Hall, A.L. and Bowman, R.W.: "Operation and Performance of a Slocum Thermal Recovery Project," *J. Pet. Tech.* (April 1973) 402-08.
90. "Slocum Field," *Improved Oil Recovery Field Reports*, SPE, Richardson, TX (1976) **2**, No. 1, 119-28; *Enhanced Oil Recovery Field Reports*, SPE, Richardson, TX (1979) **5**, No. 2, 291-97.
91. Pollock, C.B. and Buxton, T.S.: "Performance of a Forward Steamdrive Project—Nugget Reservoir, Winkleman Dome Field, Wyoming," *J. Pet. Tech.* (Jan. 1969) 35-40.
92. "Winkleman Dome Field," *Improved Oil Recovery Field Reports*, SPE, Richardson, TX (1975) **1**, No. 1, 155-62; *Enhanced Oil Recovery Field Reports*, SPE, Richardson, TX (1980) **6**, No. 1, 41-44.
93. Herrera, A.J.: "The M6 Steam Drive Project Design and Implementation," *J. Cdn. Pet. Tech.* (July-Sept. 1977) 62-83.
94. Herrera, A.J.: "Steam-Drive Recovery Being Used on Lake Maracaibo Coastal Field," *Oil and Gas J.* (July 17, 1978) 74-80.
95. "Tia Juana Este Field, Maraven, S.A.," *Enhanced Oil Recovery Field Reports*, SPE, Richardson, TX (1978) **3**, No. 4, 751-62; *Enhanced Oil Recovery Field Reports*, SPE, Richardson, TX (1982) **8**, No. 1, 751-53.
96. Showalter, W.E. and MacLean, M.A.: "Fireflood at Brea-Olinda Field, Orange County, California," paper SPE 4763 presented at the 1974 SPE Symposium on Improved Oil Recovery, Tulsa, April 22-24.
97. "Brea Olinda Field," *Improved Oil Recovery Field Reports*, SPE, Richardson, TX (1975) **1**, No. 1, 15-18; *Enhanced Oil Recovery Field Reports*, SPE, Richardson, TX (1981) **7**, No. 1, 407-08.
98. Gates, C.F. and Sklar, I.: "Combustion as a Primary Recovery Process—Midway Sunset Field," *J. Pet. Tech.* (Aug. 1971) 981-86; *Trans.*, AIME, **251**.
99. Counihan, T.M.: "A Successful In-Situ Combustion Pilot in the Midway Sunset Field, California," paper SPE 6525 presented at the 1977 SPE California Regional Meeting, Bakersfield, April 13-15.
100. Gates, C.F., Jung, K.D., and Surface, R.A.: "In-Situ Combustion in the Tulare Formation, South Belridge Field, Kern County, CA," *J. Pet. Tech.* (May 1978) 798-806; *Trans.*, AIME, **265**.
101. Hewitt, C.H. and Morgan, J.T.: "The Fry In-Situ Combustion Test—Reservoir Characteristics," *J. Pet. Tech.* (March 1965) 337-42; *Trans.*, AIME, **234**.
102. Clark, G.A. *et al.*: "The Fry In-Situ Combustion Test—Field Operations," *J. Pet. Tech.* (March 1965) 343-47; *Trans.*, AIME, **234**.
103. Clark, G.A. *et al.*: "The Fry In-Situ Combustion Test—Field Operations and Performance," *J. Pet. Tech.* (March 1965) 348-53; *Trans.*, AIME, **234**.
104. Earlougher, R.C. Jr., Galloway, J.R., and Parsons, R.W.: "Performance of the Fry In-Situ Combustion Project," *J. Pet. Tech.* (May 1970) 551-57.
105. Bleakley, W.B.: "Fry Unit Fireflood Surviving Economic Pressures," *Oil and Gas J.* (May 3, 1971) 92-97.
106. Howell, J.C. and Peterson, M.E.: "The Fry In Situ Combustion Project Performance and Economic Status," paper SPE 8381 presented at the 1979 SPE Annual Technical Conference and Exhibition, Las Vegas, Sept. 23-26.
107. Little, T.P.: "Successful Firefloooding of the Bellevue Field," *Pet. Eng. Intl.* (Nov. 1975) 55-56.
108. "Bellevue Field, Cities Service Oil Co.," *Improved Oil Recovery Field Reports*, SPE, Richardson, TX (1975) **1**, No. 3, 471-80; *Enhanced Oil Recovery Field Reports*, SPE, Richardson, TX (1982) **8**, No. 1, 713-15.
109. Cato, R.W. and Frnka, W.A.: "Getty Oil Reports Fireflood Pilot is Successful Project," *Oil and Gas J.* (Feb. 12, 1968) 93-97.
110. "Getty Expands Bellevue Fire Flood," *Oil and Gas J.* (Jan. 13, 1975) 45-49.
111. Bleakley, W.B.: "Getty's Bellevue Field Still Going and Growing," *Pet. Eng. Intl.* (Nov. 1978) 54-68.
112. "Bellevue Field, Getty Oil Co.," *Improved Oil Recovery Field Reports*, SPE, Richardson, TX (1976) **2**, No. 2, 275-84; *Enhanced Oil Recovery Field Reports*, SPE, Richardson, TX (1982) **8**, No. 1, 717-19.
113. Hardy, W.C. *et al.*: "In-Situ Combustion Performance in a Thin Reservoir Containing High-Gravity Oil," *J. Pet. Tech.* (Feb. 1972) 199-208; *Trans.*, AIME, **253**.
114. Mace, C.: "Deepest Combustion Project Proceeding Successfully," *Oil and Gas J.* (Nov. 17, 1975) 74-81.
115. "West Heidelberg Field," *Improved Oil Recovery Field Reports*, SPE, Richardson, TX (1975) **1**, No. 2, 351-59; *Enhanced Oil Recovery Field Reports*, SPE, Richardson, TX (1980) **7**, No. 1, 451-54.

116. Buchwald, R.W. Jr., Hardy, W.C., and Neinast, G.S.: "Case Histories of Three In-Situ Combustion Projects," *J. Pet. Tech.* (July 1973) 784-86.
117. "Glen Hummel Field," *Improved Oil Recovery Field Reports*, SPE, Richardson, TX (1975) **1**, No. 1, 45-46; *Enhanced Oil Recovery Field Reports*, SPE, Richardson, TX (1978) **4**, No. 1, 39-42.
118. "Gloriana Field," *Improved Oil Recovery Feld Reports*, SPE, Richardson, TX (1975) **1**, No. 1, 57-69; *Enhanced Oil Recovery Field Reports*, SPE, Richardson, TX (1978) **4**, No. 1, 43-46.
119. Martin, W.L. *et al.*: "Thermal Recovery at North Tisdale Field, Wyoming," *J. Pet. Tech.* (May 1972) 606-16.
120. Gadelle, C.P. *et al.*: "Heavy Oil Recovery by In-Situ Combustion—Two Field Cases in Romania," *J. Pet. Tech.* (Nov. 1981) 2057-66.
121. Terwilliger, P.L. *et al.*: "Fireflood of the P_{2-3} Sand Reservoir in the Miga Field of Eastern Venezuela," *J. Pet. Tech.* (Jan. 1975) 9-14.
122. Nelson, T.W. and McNeil, J.S.: "How to Engineer an In-Situ Combustion Project," *Oil and Gas J.* (June 5, 1961) **59**, No. 23, 58-65.
123. Satman, A., Brigham, W.E., and Ramey, H.J. Jr.: "In-Situ Combustion Models for the Steam Plateau and for Fieldwide Oil Recovery," DOE/ET/12056-11, U.S. DOE (June 1981).
124. Gates, C.F. and Ramey, H.J. Jr.: "A Method for Engineering In-Situ Combustion Oil Recovery Projects," *J. Pet. Tech.* (Feb. 1980) 285-94.
125. Volek, C.W. and Pryor, J.A.: "Steam Distillation Drive, Brea Field, California," *J. Pet. Tech.* (Aug. 1972) 899-906.
126. Burke, R.E.: "Combustion Project is Making a Profit," *Oil and Gas J.* (Jan. 18, 1965) 44-46.
127. Koch, R.L.: "Practical Use of Combustion Drive at West Newport Field," *Pet. Eng.* (Jan. 1965) 72-81.
128. Bowman, C.H.: "A Two-Spot Combustion Recovery Project," *J. Pet. Tech.* (Sept. 1965) 994-98.
129. Terwilliger, P.L.: "Fireflooding Shallow Tar Sands—A Case History," *J. Cdn. Pet. Tech.* (Oct.-Dec. 1976) 41-48.
130. Johnson, L.A. *et al.*: "An Echoing In-Situ Combustion Oil-Recovery Project in a Utah Tar Sand," *J. Pet. Tech.* (Feb. 1980) 295-305.
131. Perry, C.W., Hertzberg, R.H., and Stosur, J.J.: "The Status of Enhanced Oil Recovery in the United States," *Proc.*, Tenth World Pet. Congress, Bucharest (1980) **3**, 257-66.
132. Benham, A.L. and Poettmann, F.H.: "The Thermal Recovery Process—An Analysis of Laboratory Combustion Data," *Trans.*, AIME (1958) **213**, 83-85.
133. Caudle, B.H., Hickman, B.M., and Silberberg, I.H.: "Performance of the Skewed Four-Spot Injection Pattern," *J. Pet. Tech.* (Nov. 1968) 1315-19.
134. Cady, G.V., Hoffman, S.J., and Scarborough, R.M.: "Silverdale Combination Thermal Drive Project," paper SPE 8904 presented at the 1980 SPE California Regional Meeting, Los Angeles, April 9-11.
135. de Haan, M.J. and Schenk, L.: "Performance Analysis of a Major Steam Drive Project in the Tia Juana Field, Western Venezuela," *J. Pet. Tech.* (Jan. 1969) 111-19.
136. "Texas Fireflood Looks Like a Winner," *Oil and Gas J.* (Feb. 17, 1969) 52.
137. Afoeju, B.I.: "Conversion of Steam Injection to Waterflood, East Coalinga Field," *J. Pet. Tech.* (Nov. 1974) 1227-32.
138. Gates, C.F. and Brewer, S.W.: "Steam Injection into the D and E Zone, Tulare Formation, South Belridge Field, Kern County, California," *J. Pet. Tech.* (March 1975) 343-48.
139. Gomaa, E.E., Duerksen, J.H., and Woo, P.T.: "Designing a Steamflood Pilot in the Thick Monarch Sand of the Midway-Sunset Field," *J. Pet. Tech.* (Dec. 1977) 1559-68.
140. Chu, C. and Trimble, A.E: "Numerical Simulation of Steam Displacement—Field Performance Applications," *J. Pet. Tech.* (June 1975) 765-74.
141. Joseph, C. and Pusch, W.H.: "A Field Comparison of Wet and Dry Combustion," *J. Pet. Tech.* (Sept. 1980) 1523-28.
142. Gates, C.F. and Holmes, B.G.: "Thermal Well Completions and Operation," paper PD11 presented at the Seventh World Pet. Cong., Mexico City (1967).
143. Fox, R.L., Donaldson, A.B., and Mulac, A.J.: "Development of Technology for Downhole Steam Production," paper SPE 9776 presented at the 1981 SPE/DOE Joint Symposium on Enhanced Oil Recovery, Tulsa, April 5-8.
144. Carraway, P.M., Kloth, T.L., and Bull, A.D.: "Co-Generation: A New Energy System to Generate Both Steam and Electricity," paper SPE 9907, presented at the 1981 California Regional Meeting, Bakersfield, March 25-26.
145. Strange, L.K.: "Ignition: Key Phase in Combustion Recovery," *Pet. Eng.* (Nov.1964) 105-09; (Dec. 1964) 97-106.
146. Shore, R.A.: "The Kern River SCAN Automation System Sample, Control and Alarm Network," paper SPE 4173 presented at the 1972 SPE California Regional Meeting, Bakersfield, Nov. 8-10.
147. "Bodcau In-Situ Combustion Project," first annual report, DOE Publications SAN-1189-2, U.S. DOE (Sept. 1977).
148. Wagner, O.R.: "The Use of Tracers in Diagnosing Interwell Reservoir Heterogeneities—Field Results," *J. Pet. Tech.* (Nov. 1977) 1410-16.
149. Yoelin, S.D.: "The TM Sand System Stimulation Project," *J. Pet. Tech.* (Aug. 1971) 987-94.
150. Meldau, R.F., Shipley, R.G., and Coats, K.H.: "Cyclic Gas/Steam Stimulation of Heavy-Oil Wells," *J. Pet. Tech.* (Oct. 1981) 1990-98.
151. Britton, M.W. *et al.*: "The Street Ranch Pilot Test of Fracture-Assisted Steamflood Technology," *J. Pet. Tech.* (March 1983) 511-21.
152. Sahuquet, B.C. and Ferrier, J.J.: "Steam-Drive Pilot in a Fractured Carbonate Reservoir: Lacq Superieur Field," *J. Pet. Tech.* (April 1982) 873-80.
153. Hvizdos, L.J., Howard, J.V., and Roberts, G.W.: "Enhanced Oil Recovery Through Oxygen-Enriched In-Situ Combustion: Test Results from the Forest Hill Field in Texas," *J. Pet. Tech.* (June 1983) 1061-70.
154. Prats, M.: *Thermal Recovery*, Monograph Series, SPE, Richardson, TX (1983) 201-38.
155. Beal, C.: "The Viscosity of Air, Water, Natural Gas, Crude Oil and Its Associated Gases at Oil Field Temperatures and Pressures," *Trans.*, AIME (1946) **165**, 103.
156. *Petroleum Production Handbook*, T.C. Frick (ed.) Vol. II, McGraw-Hill Book Co. Inc., New York City (1962) 19-39.
157. Chew, J. and Connally, C.A. Jr.: "A Viscosity Correlation for Gas-Saturated Crude Oils," *Trans.*, AIME (1959) **216**, 23-25.
158. Beggs, H.D. and Robinson, J.R.: "Estimating the Viscosity of Crude Oil Systems," *J. Pet. Tech.* (Sept. 1975) 1140-41.
159. Brooks, R.H. and Corey, A.T.: "Properties of Porous Media Affecting Fluid Flow," *Proc.*, ASCE, Irrigation and Drainages Div. (1966) **92**, No. IR2.
160. Somerton, W.H. and Udell, K.S.: "Thermal and High Temperature Properties of Rock-Fluid Systems," paper presented at the 1981 OASTRA Workshop on Computer Modeling, Edmonton, Alta., Jan. 28-30.
161. Poston, S.W. *et al.*: "The Effect of Temperature on Irreducible Water Saturation and Relative Permeability of Unconsolidated Sands," *Soc. Pet. Eng. J.* (June 1970) 171-80.
162. Weinbrandt, R.M., Ramey, H.J. Jr., and Cassé, F.J.: "The Effect of Temperature on Relative and Absolute Permeability of Sandstones," *Soc. Pet. Eng. J.* (Oct. 1975) 376-84.
163. Sawabini, C.T., Chilingar, G.V., and Allen, D.R.: "Compressibility of Unconsolidated, Arkosic Oil Sands," *Soc. Pet. Eng. J.* (April 1974) 132-38.
164. Somerton, W.H., Keese, J.A., and Chu, S.L.: "Thermal Behavior of Unconsolidated Oil Sands," *Soc. Pet. Eng. J.* (Oct. 1974) 513-21.
165. Poettmann, F.H. and Mayland, B.J.: "Equilibrium Constants for High Boiling Hydrocarbon Fractions of Varying Characterization Factors," *Pet. Refiner* (July 1949) 101-12.
166. Lee, S.T. *et al.*: "Experimental and Theoretical Studies on the Fluid Properties Required for Simulation of Thermal Processes," *Soc. Pet. Eng. J.* (Oct. 1981) 535-50.
167. Fassihi, M.R., Brigham, W.E., and Ramey, H.J. Jr.: "The Reaction Kinetics of In-Situ Combustion," *Soc. Pet. Eng. J.* (Aug. 1984) 408-16.
168. "1967 ASTM Steam Tables," ASME, New York City (1967).

General References

"Bibliography of Thermal Methods of Oil Recovery," *J. Cdn. Pet. Tech.* (April-June 1975) 55-65.

Chu, C. and Crawford, P.B.: "In Situ Combustion," *Improved Oil Recovery*, Interstate Oil Compact Commission, Oklahoma City (1983) Chap. 6.

Crawford, P.B.: "In-Situ Combustion," *Secondary and Tertiary Oil Recovery Processes*, Interstate Oil Compact Commission, Oklahoma City (1974) Chap. 5.

Farouq Ali, S.M.: "Steam Injection," *Secondary and Tertiary Oil Recovery Processes*, Interstate Oil Compact Commission, Oklahoma City (1974) Chap. 6.

Farouq Ali, S.M. and Meldau, R.F.: "Steamflooding," *Improved Oil Recovery*, Interstate Oil Compact Commission, Oklahoma City (1983) Chap. 7.

Prats, M.: *Thermal Recovery*, Monograph Series, SPE, Richardson, TX (1982) **7**.

Thermal Recovery Processes, Reprint Series, SPE, Richardson, TX (1965, 1985) **7**.

Thermal Recovery Techniques, Reprint Series, SPE, Richardson, TX (1972) **10**.